

Dissertation
Submitted to the
Combined Faculties for the Natural Sciences and for
Mathematics
of the Ruperto-Carola University of Heidelberg, Germany,
for the Degree of
Doctor of Natural Sciences

presented by
Diploma Biologist Stephanie Geiger
born in Stuttgart

Oral examination:
22.10.2007

**Influence of the expression of mutated
B-type lamins on
nuclear architecture and function**

Referees: Prof. Dr. Harald Herrmann-Lerdon
Prof. Dr. Peter Lichter

Publications:

S.K.Geiger, H. Bär, P. Ehlermann, S. Wälde, D. Rutschow, R. Zeller, B.T. Ivandic, H. Zentgraf, H.A. Katus, H. Herrmann, D. Weichenhan (2008) Incomplete nonsense-mediated decay of mutant lamin A/C mRNA provokes dilated cardiomyopathy and ventricular tachycardia. *Journal of molecular medicine* 86: 281-289

Oral presentations at conferences:

DKFZ PhD Retreat, 2004, Weil-der-Stadt:

Assembly mechanisms of lamina-associated structural components.

Workshop on Cell Biology and Microscopy, 2005, Altleiningen:

Investigating nuclear morphology in human cancer cell lines and mouse embryonic stem cells.

Posters:

Tagung der Deutschen Gesellschaft für Zellbiologie (DGZ), 2004, Berlin:

M. Reichenzeller, **S.K. Geiger**, K. Richter, P. Lichter & H. Herrmann. Expression of XFP-chimeras of lamin A and lamins B1/B2 in human cultured cells.

Tagung der Deutschen Gesellschaft für Zellbiologie (DGZ), 2005, Heidelberg:

S.K. Geiger, M. Reichenzeller & H. Herrmann. Expression of XFP-chimeras of truncated lamin B2 constructs in human cultured cells and embryonic stem cells.

Workshop on Cell Biology and Microscopy, 2005, Altleiningen:

S.K. Geiger & H. Herrmann. Investigation of the assembly mechanism of lamina-associated structural components in human cultured cell lines and mouse embryonic stem cells.

DKFZ Doktoranden-Posterwettbewerb, 2005:

S.K. Geiger & H. Herrmann. Investigation of the assembly mechanism of lamina-associated structural components in human cultured cell lines and mouse embryonic stem cells.

Dynamic Organization of Nuclear Function, 2006, Cold Spring Harbor Laboratory, New York:

S.K. Geiger, H. Herrmann. Mutation of lamin cdk1 phosphoacceptor sites from serine to aspartic acid leads to drastic changes in nuclear morphology.

DKFZ Doktoranden-Posterwettbewerb, 2006:

S.K. Geiger, H. Herrmann. Mutation of lamin cdk1 phosphoacceptor sites from serine to aspartic acid leads to drastic changes in nuclear morphology.

EUROSTELLS Workshop "Exploring Chromatin in Stem Cells", 2007, Montpellier:

K. Rippe, T. Jegou, **S.K. Geiger**, M. Caudron, and H. Herrmann. Changes of chromatin organization and dynamics during stem cell differentiation and cell proliferation.

Acknowledgements

Bei Herrn Prof. Dr. Harald Herrmann möchte ich mich für die Überlassung des spannenden Themas, das angenehme Arbeitsklima und das in mich gesetzte Vertrauen bedanken.

Herrn Prof. Dr. Peter Lichter danke ich für das Interesse an meiner Arbeit und die Übernahme des Gutachtens.

Ich danke Herrn PD Dr. Karsten Rippe für seine Unterstützung und das Interesse an meiner Arbeit.

Dr. Harald Bär möchte ich für die lustige Unterhaltung im Laboralltag und die gute Zusammenarbeit zu unserem Paper danken.

Ich danke dem Team aus der Abteilung für Innere Medizin III, Universitätsklinikum Heidelberg für die erfolgreiche und gelungene Kooperation bei der Bearbeitung der Laminopathiestudie. Ein ganz besonderes Dankeschön an PD Dr. Dieter Weichenhan.

Ein ganz großes Dankeschön an die gesamte Arbeitsgruppe Herrmann: Tatjana, Doro, Nadine, Helga, Sarika, Thorsten, Julia. Ohne Euch hätte die Arbeit nur halb so viel Spaß gemacht. Ganz besonders möchte ich mich bei Michi für ihre große Diskussionsbereitschaft, die vielen nützlichen Tipps, ihre Freundschaft und die vielen lustigen Frauenabende bedanken. Ein extra großes Danke auch an Moni.

Van möchte ich für ihre große Unterstützung bei den Kotransfektions-Experimenten danken.

Heidi, Birgit, Markus, und Sylvia möchte ich für ihre Freundschaft und die vielen schönen Abende und Tage danken. Ohne Euch hätte ich das alles nicht geschafft.

Ein ganz besonderer Dank gilt meiner Familie, besonders meiner Schwester Molly, die immer für mich da waren und mich immer in jeder erdenklichen Art unterstützt haben.

Summary

The work presented here demonstrates new insights into the assembly mechanisms of the nuclear lamina. By generation and expression of several lamin mutants in mammalian cells it was possible to analyze the influence of distinct lamin domains on cellular localization and their assembly properties. Both partial and complete head deleted lamin B2 localized to the nuclear rim but highly impaired nuclear shape indicating that the head domain is dispensable for nuclear envelope localization and however, important for efficient lamin assembly. In contrast, tail deleted lamin B2 mutants did not incorporate into the nuclear rim and were distributed throughout the cytoplasm and the nucleoplasm. This suggests that the tail domain contains those elements that are necessary for effectively guiding these lamins to the nuclear envelope. However, tailless mutants did not impair the formation of a nuclear lamina. An exhaustive mutation trial of the individual mitotic phosphoacceptor sites flanking the central rod domain from serine to aspartic acid was performed in order to test if this would still allow the integration of these mutants into the nuclear lamina and if this would lead to the disassembly of the nuclear lamina. Notably, the mutant proteins were not incorporated into the lamina at all but instead they formed intranuclear aggregates when expressed in U2OS cells. Interestingly, the effect of nuclear aggregate formation was independent of both the position of the mutated site and the number of sites mutated. Live cell imaging experiments showed that the aggregates are rather dynamic structures that are able to fuse and occupy single large lamin territories. Co-transfection studies of "mitotic" lamin B1, "mitotic" lamin B2 and NLS-vimentin suggest that the aggregates are deposited in the interchromosomal domain compartment (ICD). However, intermingling of the proteins was not observed. Extraction experiments revealed that the aggregates were rather loosely connected to the nuclear matrix. Although the mechanism underlying aggregate formation of "mitotic" lamin B1, "mitotic" lamin B2, and NLS-vimentin remains elusive, our results strongly suggest the existence of nuclear "protein processing centers". Their functions may relate to the prevention of macromolecular crowding as well as to the organization and distribution of nuclear proteins in general.

Wild type and mutant lamins were also expressed in mouse embryonic stem (ES) cells. Their ability to differentiate into all specialized cell types found in the adult mouse and the exhibition and maintenance of a normal diploid complement of chromosomes make them a valuable tool for cell biological studies. As expected, both wild type lamin B1 and wild type lamin B2 localized to the nuclear rim. The stem cell status of the cells was not affected. Expression of lamin B2 deletion mutants in mouse ES cells showed similar effects as those observed in U2OS cells suggesting that lamin proteins are similarly processed and assembled into the nuclear lamina in both differentiated and ES cells.

Additionally, a novel nonsense mutation in the lamin A gene (pR321X) cosegregating with dilated cardiomyopathy and cardiac rhythm disturbances was analyzed in both cultivated cells and cardiac tissue of affected patients. Neither nuclear abnormalities nor reduced

expression of the wild type protein was observed. In line with a strong nonsense-mediated mRNA decay (NMD), i.e. the NMD-dependent reduction in the relative amount of mutant mRNA, the truncated protein was not found. The potential transient presence of this mutant protein could be uncovered, however, by inhibition of the proteasomal system. It is therefore suggested that NMD is not sufficient to completely prevent the expression of truncated lamin A and that even trace amounts of it may negatively interfere with structural and/or regulatory functions of lamin A/C eventually leading to the development of cardiomyopathy.

Zusammenfassung

Die Ergebnisse der vorgelegten Arbeit liefern neue Einblicke in die Assembly-Mechanismen der Kernlamina. Die Herstellung und Expression verschiedener Lamin-Mutanten in Kulturzellen ermöglichte es, den Einfluss bestimmter Lamin-Domänen auf Assembly-Eigenschaften und zelluläre Lokalisation der Proteine zu untersuchen.

Lamin B2 mit teilweise oder komplett deletierter Kopfdomäne lokalisierte an der Kernhülle. Dennoch ließ die veränderte Kernmorphologie in diesen Zellen vermuten, dass die Kopfdomäne zwar für eine Lokalisation an der Kernhülle entbehrlich, jedoch für ein intaktes Lamina-Assembly notwendig ist. Schwanz-deletierte Lamin B2 Mutanten hingegen wurden nicht in die Kernhülle eingebaut und verteilten sich sowohl über Zytoplasma als auch Nukleoplasma. Diese Schwanz-Domäne enthält also vermutlich jene Sequenzen, die wichtig sind für den Transport des Proteins an die Kernhülle. Die Schwanz-deletierten Mutanten beeinflussten jedoch nicht die Bildung der Lamina.

Wir vermuteten, dass Mutationen der Phosphoakzeptor-Stellen vor und hinter der „Rod“-Domäne von Serin nach Aspartat (die die mitosespezifischen Phospho-Serin-Gruppen imitieren) entweder die Integration der Mutanten in die Kernlamina verhindern oder zu deren Auflösung führen würden. Tatsächlich konnten diese Mutanten nicht in die Kernlamina eingebaut werden, und bildeten anstatt dessen intranukleäre Aggregate in U2OS Zellen aus. Erstaunlicherweise war diese Aggregatbildung unabhängig sowohl von der Position der Mutation als auch von der Anzahl mutierter Phosphoakzeptor-Stellen.

Mit Lebendbeobachtung konnte gezeigt werden, dass diese Aggregate sehr dynamische Strukturen darstellen, die fusionierten und große Lamin-Territorien bildeten. Kotransfektionen dieser „Mitose“-Lamine B2 und B1 mit NLS-Vimentin ließen darauf schließen, dass die Aggregate im Interchromatin-Kompartiment abgelagert werden. Dennoch konnten wir keine Vermischung der transfizierten „Mitose“-Lamine mit NLS-Vimentin beobachten. Zwar sind die Mechanismen, die zur Aggregation und getrennten „Deponierung“ dieser Proteine führen, unbekannt, unsere Ergebnisse lassen aber auf die Existenz nukleärer „Protein-Prozessierungs-Zentren“ schließen. Diese könnten das lokale Entstehen zu hoher Proteindichten (aufgrund der starken Überexpression) verhindern, oder auch generell mit der Organisation und Verteilung von Kernproteinen in Beziehung stehen.

Sowohl Wildtyp als auch mutierte Lamine wurden ebenfalls in embryonalen Stammzellen der Maus exprimiert. Die Fähigkeit zur Differenzierung in alle möglichen Zelltypen und ihr intakter diploider Karyotyp machen diese Zellen für zellbiologische Studien sehr wertvoll. Wie erwartet lokalisierten Wildtyp Lamin B1 und Lamin B2 an der Kernhülle, und der Stammzellcharakter der Zellen wurde durch ihre Expression nicht beeinflusst. Die Expression von Lamin B2 Deletionsmutanten in Mausstammzellen zeigte sehr ähnliche Ergebnisse wie in U2OS Zellen. Vermutlich liegen daher in Stammzellen wie in differenzierten Zellen die gleichen Prozessierungs- und Assembly-Mechanismen für die Kernlamina vor.

Des Weiteren wurde eine neu charakterisierte Mutation des Lamin A/C Gens (pR321X) untersucht, die mit dilatierter Kardiomyopathie und Herzrhythmusstörungen einhergeht. Kulturzellen und Herzgewebe betroffener Patienten zeigten weder Veränderungen der Zellkerne, noch eine verminderte Expression des Wildtyp-Lamin A Proteins. In Übereinstimmung mit der Theorie des „Nonsense-mediated decay“ (NMD) wurde kein mutiertes Protein nachgewiesen. Dennoch konnte mit Hilfe von Proteasomen-Inhibitoren gezeigt werden, dass das mutierte Protein kurzzeitig angereichert wurde. Wir vermuten, dass der NMD nicht effizient genug ist, um die trunkierte Lamin A-Mutante vollständig abzubauen. Vermutlich sind auch Spuren dieser Mutante ausreichend, um strukturelle und/oder regulatorische Funktionen von Lamin A/C zu beeinträchtigen, was letztlich zur Ausbildung der Kardiomyopathie führt.

Table of contents

1 INTRODUCTION	1
1.1 The nucleus	1
1.2 Lamins	4
1.2.1 Functions of nuclear lamins	5
1.2.2 Laminopathies	7
1.2.3 Structure of nuclear lamins	8
1.2.4 Lamin filament assembly	9
1.2.5 Modifications of nuclear lamins	10
1.2.6 Lamins in the nuclear interior	11
1.3 Aim of the thesis	12
2 MATERIAL	13
2.1 Biological material	13
2.1.1 Bacterial strains	13
2.1.2 Cultured cell lines	13
2.1.3 Stably transfected culture cell lines	13
2.2 Expression vectors	14
2.3 Expression plasmids	14
2.4 Antibodies	15
2.4.1 Primary antibodies	15
2.4.2 Secondary antibodies	15
2.5 Size markers	15
2.5.1 DNA size markers	15
2.5.2 Protein size markers	16
2.6 DNA oligonucleotides	16
2.7 Chemicals and enzymes	16
2.8 Cell culture material	16
2.9 Media and solutions	17
2.10 Kits	19

2.11 Instruments	19
3 METHODS	21
3.1 DNA techniques	21
3.1.1 Preparation of competent bacteria	21
3.1.2 Transformation of competent bacteria	21
3.1.3 Isolation of plasmid DNA ('Miniprep', 'Maxiprep')	21
3.1.4 Agarose gel electrophoresis	22
3.1.5 Determination of DNA concentration	22
3.1.6 Restriction digestion	23
3.1.6.1 Analytical restriction digestion	23
3.1.6.2 Preparative restriction digestion	23
3.1.6.3 Partial restriction digestion	23
3.1.7 PCR	24
3.1.8 Purification of PCR products	24
3.1.9 Site-directed Mutagenesis	25
3.1.10 Removal of 5'-phosphate residues from DNA fragments	25
3.1.11 Phosphorylation and annealing of DNA oligomers	25
3.1.12 Ligation	26
3.1.13 DNA sequencing	26
3.2 Generation of expression plasmids	26
3.2.1 Human lamin B2	26
3.2.2 Human lamin B2 deletion mutants	27
3.2.2.1 Human lamin B2 Δ 32head	28
3.2.2.2 Human lamin B2 headless	28
3.2.2.3 Human lamin B2 tailless	28
3.2.2.4 Human lamin B2 Δ 32head/tailless	28
3.2.2.5 Human lamin B2 rod	29
3.2.3 Human lamin B2 S→D mutants	29
3.2.3.1 Human lamin B2 S37D	29
3.2.3.2 Human lamin B2 S405D	29
3.2.3.3 Human lamin B2 S407D	30
3.2.3.4 Human lamin B2 S37+405D	30
3.2.3.5 Human lamin B2 S37+407D	30

3.2.3.6	Human lamin B2 S405+407D	30
3.2.3.7	Human lamin B2 S37+405+407D	31
3.2.4	Human Lamin B1	31
3.2.5	Human lamin B1 S→D mutants	31
3.2.5.1	Human lamin B1 S23D	31
3.2.5.2	Human lamin B1 S391D	32
3.2.5.3	Human lamin B1 S393D	32
3.2.6	Human lamin A p.R321X	32
3.3	Cell culture techniques	33
3.3.1	Cultivation of culture cell lines	33
3.3.2	Cultivation of embryonic stem cells	33
3.3.3	Freezing of cells	34
3.3.4	Thawing of cells	34
3.3.5	Transfection of cells	34
3.3.5.1	Transient transfection of cells	34
3.3.5.2	Stable transfection of cells	35
3.4	Fixation of cells	35
3.4.1	Methanol / Acetone fixation	35
3.4.2	Formaldehyde fixation	35
3.5	Indirect immunofluorescence	36
3.5.1	Double immunolocalization	36
3.6	Confocal laser scanning microscopy	36
3.7	Protein techniques	37
3.7.1	Protein extraction of heart muscle tissue	37
3.7.2	Differential protein extraction	37
3.7.3	Western blot	38
3.7.3.1	Discontinuous polyacrylamide gel electrophoresis (SDS-PAGE)	38
3.7.3.2	Transfer of proteins to PVDF membranes and detection	39
3.7.4	Immunoprecipitation	39

4	RESULTS	41
4.1	Influence of lamin B2 deletion mutants	41
4.1.1	Lamin B2 head deletions	42
4.1.2	Lamin B2 tail deletions	44
4.1.3	Effects of lamin B2 deletion mutants on the endogenous lamina	46
4.1.4	Effect of lamin B2 deletion mutants on endogenous NE proteins	48
4.1.5	Biochemical characterization of lamin B2 deletion mutants	50
4.1.6	Expression of lamins in mouse embryonic stem (ES) cells	51
4.1.7	Effects of lamin B2 head and/or tail deletion on their cellular localization and nuclear morphology in ES cells	53
4.2	The effect of mutations at the phosphoacceptor sites of lamins	54
4.2.1	Influence of mitotic lamin B2 mutants on nuclear localization and morphology	55
4.2.2	Generation of stable cell lines	57
4.2.3	Influence of "mitotic" lamin B1 mutants on nuclear localization and morphology	58
4.2.4	Effect of "mitotic" lamin expression on the endogenous lamina	59
4.2.5	Effect of "mitotic" lamin expression on endogenous NE proteins	60
4.2.6	<i>In vivo</i> dynamics of aggregate formation	61
4.2.7	Aggregate formation leads to drastic chromatin reorganization	62
4.2.8	Co-transfection of lamin B1 and lamin B2	63
4.2.9	Co-transfection of "mitotic" lamins with NLS-vimentin	64
4.2.10	Effects of mitotic lamin expression on PCNA localization	65
4.2.11	Biochemical analysis of cells expressing mitotic lamin mutants	66
4.2.12	Identification of interaction partners of soluble lamins	68
4.3	Characterization of a laminopathy causing lamin A mutant	70
4.3.1	Downregulation of the mutant <i>LMNA</i> allele by nonsense-mediated decay (NMD)	70
4.3.2	Biochemical characterization of cardiac tissue and skin fibroblasts	71
4.3.3	Inhibition of the proteasome uncovers the truncated <i>LMNA</i> R321X protein	73
4.3.4	Nuclear morphology, chromatin distribution and localization of nuclear proteins in patient tissues	74
4.3.5	Transfection of the lamin A p.R321X mutant	76

5	DISCUSSION	77
5.1	Topogenesis of lamins/lamina	77
5.1.1	Role of the lamin head and tail domains in cellular localization	77
5.1.2	“Mitotic” lamins	79
5.2	Influence of lamin B mutants on the endogenous lamina and lamina assembly	82
5.3	Organization of the nuclear envelope	85
5.4	The role of lamins in DNA replication	86
5.5	Role of lamins in chromatin organization	87
5.6	Lamins in ES cells	88
5.7	Identification of novel putative lamin interaction partners	90
5.8	Laminopathy	91
6	REFERENCES	95
7	ABBREVIATIONS	107
8	APPENDIX	109

1 Introduction

1.1 The nucleus

The cell nucleus was first described in the 17th century by A. van Leeuwenhoek. In 1831 R. Brown made the first detailed morphological description of the nucleus, and the "cell doctrine" of Matthias J. Schleiden und Theodor Schwann in 1839 claiming that all tissues are aggregates of individual cells marked the beginning of cell biology (described in Franke, 1988). Since these early days a lot more is known about the composition and the structure of the nucleus, but understanding the principles of the functional organization is still one of the major goals in cell biology.

The eukaryotic nucleus is a complex organelle that contains the chromosomes and is the site of DNA replication, RNA transcription and processing, and ribosome assembly. It is about 10 μm in diameter and is surrounded by a double membrane layer punctured in intervals by nuclear pore complexes (NPCs). Many activities are concentrated in subnuclear foci called nuclear bodies. In contrast to the cytoplasmic compartments the nuclear compartments are not surrounded by membranes and are usually characterized by specific antigens that are generally in rapid exchange with non-bound species. The most prominent nuclear compartment is the nucleolus. It is the site of RNA polymerase I-mediated rDNA transcription and ribosome subunit assembly. Other nuclear substructures include nuclear speckles, Cajal bodies, and PML bodies (Lamond & Sleeman, 2003; Spector, 2003).

The nucleus contains the chromosomes, consisting of highly condensed chromatin in mitosis and being organized into large scale domains called chromosome territories. Each chromosome territory occupies a predominantly distinct space in the nucleoplasm, even in interphase when they are in their most decondensed state. According to the level of compaction, one can distinguish between most condensed heterochromatin and less condensed euchromatin. In general, condensed heterochromatin domains tend to cluster preferentially at the nuclear periphery and around nucleoli, whereas the less condensed euchromatin is located within the nuclear interior (Lamond & Sleeman, 2003).

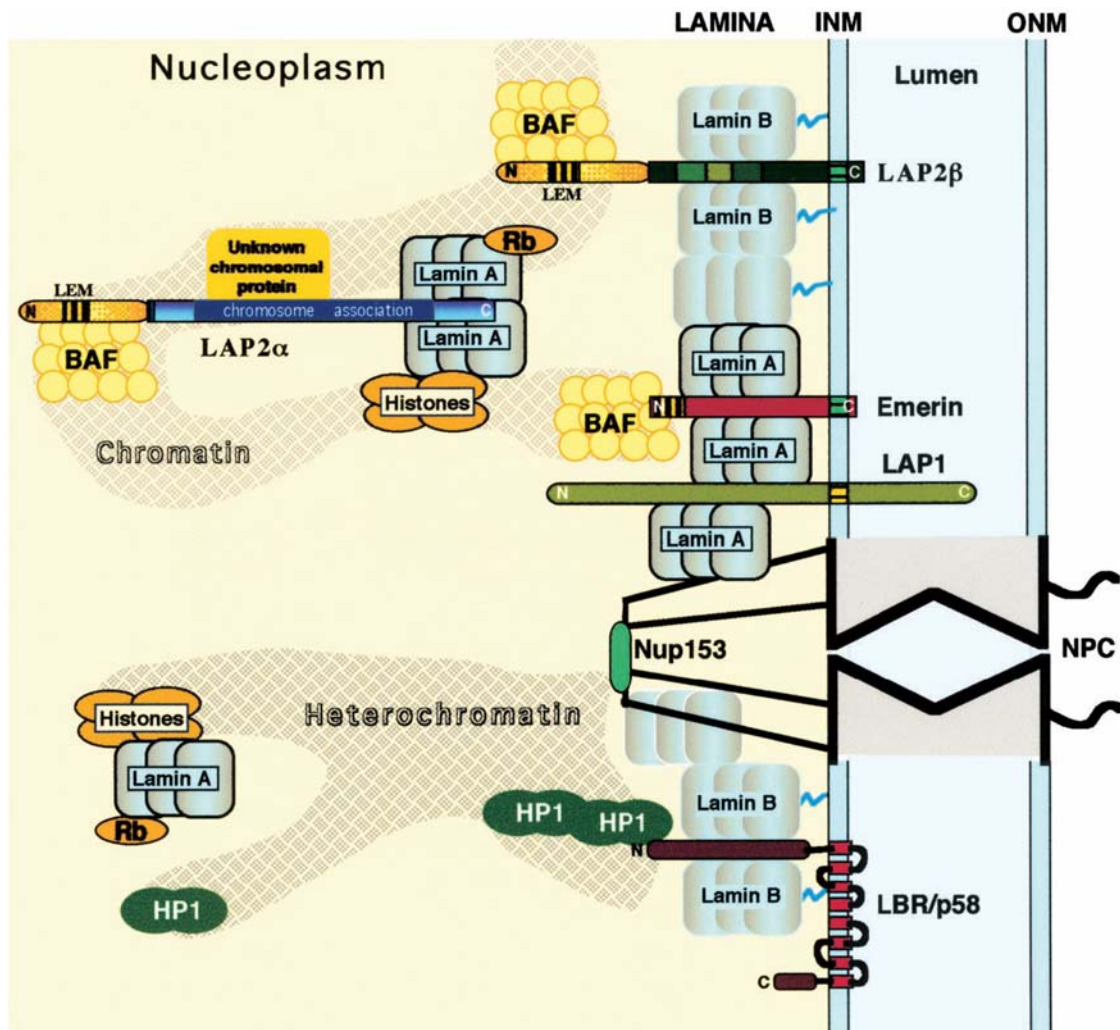


Figure 1: Proposed molecular interactions between components of the peripheral lamina, the nucleoskeleton and chromatin. INM, inner nuclear membrane; ONM, outer nuclear membrane; NPC, nuclear pore complex. Figure modified from Vlcek et al, 2001.

The existence of a biochemically distinct nuclear compartment depends on the presence of a selective barrier, the nuclear envelope (NE), which separates nuclear and cytoplasmic cellular activities. The NE is a double membrane layer composed of two concentric bilayers, the outer nuclear membrane (ONM) which is continuous with the endoplasmic reticulum (ER) and the inner nuclear membrane (INM). Outer and inner membranes are separated by a luminal space and are joined at sites, where nuclear pore complexes (NPCs) are inserted into the double membrane system. NPCs are large macromolecular assemblies that form aqueous gated channels across the NE and mediate the transport of macromolecules. The ONM has ribosomes attached to its outer surface and is biochemically and functionally similar to the ER. The INM, by contrast, is enriched in a distinctive set of membrane proteins. Associated is the

underlying lamina, consisting of lamin proteins, and chromatin (Aebi et al, 1986; Gerace & Burke, 1988). A proteomics analysis has suggested that as many as 80 transmembrane proteins are localized to the INM in mammalian interphase cells (Schirmer et al, 2003). To date, only few of these proteins are characterized in detail. The lamina associated polypeptide (LAP) 2 family members, emerin and MAN1 belong to a family of proteins that is defined by the presence of a so-called LEM domain. The LEM domain is exposed to the nucleoplasm and interacts with BAF (barrier-to-autointegration-factor), an abundant chromatin-associated protein (Shumaker et al, 2001). In this way, BAF might function as a link between certain INM proteins and chromatin. In addition, emerin, LAP1 and LAP2 family members and lamin B receptor (Holbrook et al) also interact with lamins.

Metazoans contain another NE structural element called the nuclear lamina. In mammalian cells, this appears as a thin protein meshwork underlying the INM (Fawcett, 1966). The most prominent proteins in the nuclear lamina are lamins and associated proteins (Aaronson & Blobel, 1975; Gerace et al, 1978). Currently there is no molecular proof of a nuclear lamina outside the metazoa (Erber et al, 1999). The nuclear lamins are largely resistant to extraction, when cells are treated with high concentrations of non-ionic detergents and ionic strength (Aebi et al, 1986; Gerace & Burke, 1988; Goldman et al, 1986). Electron microscopic images of cells extracted in this way show an electron dense layer at the nuclear periphery which is in close association with the NPCs (Schneider et al, 1995).

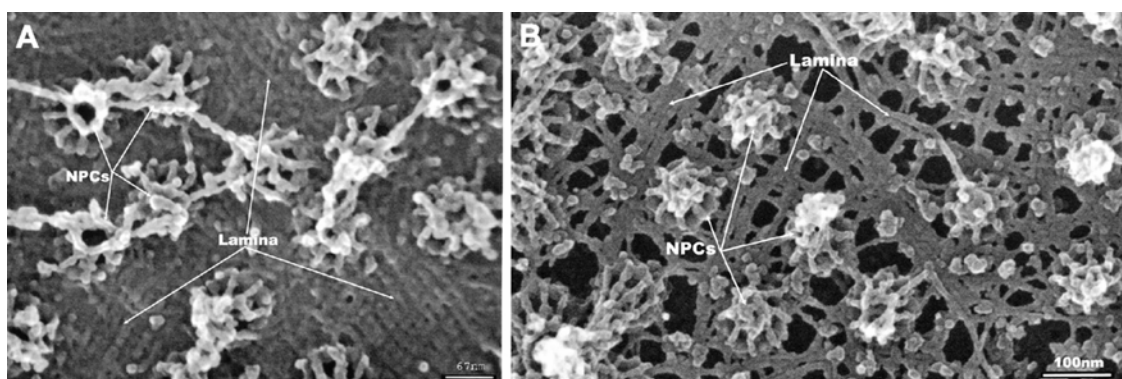


Figure 2: Field emission scanning electron micrographs showing lamina organization in *Xenopus* oocyte germinal vesicle. Manually isolated oocyte germinal vesicle envelopes were spread on silicon chips and either extracted with Triton X-100 (A) or fixed directly (B). Figure adapted from Broers et al, 2006.

It is still little known about the higher order structure of lamins in situ. In *Xenopus* oocytes and *Necturus*, both amphibian species, the lamina was shown to consist of a near-tetragonal meshwork of 10-nm-diameter lamin filaments (Aebi et al, 1986; Akey, 1989; Stuurman et al, 1998). These filaments attach directly to the NPCs, most likely to the spoke ring complex of nuclear pores (Aaronson & Blobel, 1975; Dwyer & Blobel, 1976; Goldberg & Allen, 1996; Scheer et al, 1976). Although the appearance of lamin filaments in other cell types is similar, a near-tetragonal meshwork of lamin filaments has not been visualized in other cells than the above mentioned (Goldberg et al, 1995).

1.2 Lamins

Nuclear lamins were initially identified as the major components of the nuclear lamina. In lesser amounts, lamins are also located throughout the nucleoplasm (Bridger et al, 1993; Goldman et al, 1992; Moir et al, 1994; Sasseville & Raymond, 1995). Sequencing of lamin cDNA clones from different species revealed that nuclear lamins belong to the intermediate filament (Lenz-Bohme et al) protein family (McKeon et al, 1986). Lamins have been identified in numerous eukaryotic species, including *Hydra*, *Caenorhabditis elegans*, *Drosophila melanogaster*, and all vertebrates (Erber et al, 1999). Analysis of the complete genome sequence of both, yeast and *Arabidopsis* has revealed that these species do not have nuclear lamins. This suggests that these proteins may have evolved in animal cells during the transition from a closed to an open mitosis (Cohen et al, 2001). The number and complexity of lamins has increased during metazoan evolution. While *Caenorhabditis elegans* has only one lamin gene and protein, vertebrates have three lamin genes (*LMNA*, *LMNB1*, *LMNB2*) encoding at least seven distinct isoforms (Cohen et al, 2001). In humans the *LMNA* gene is localized on chromosome 1q21.2 (Wydner et al, 1996) and encodes the A-type lamins. It gives rise to four splice variants, lamin A, AΔ10, C, and C2 (Fisher et al, 1986; Furukawa et al, 1994; Machiels et al, 1996; McKeon et al, 1986). Three B-type lamins have been reported in humans so far. Lamin B1 is the unique product of the *LMNB1* gene located on chromosome 5q23.3 (Lin & Worman, 1995). *LMNB2*, localized at chromosome 19p13.3, has two alternatively spliced products, lamin B2 and B3 (Biamonti et al, 1992; Furukawa &

Hotta, 1993). B-type lamins are constitutively expressed in somatic cells throughout development and all vertebrates express at least one B-type lamin. In contrast, lamins A, C, and AΔ10 are developmentally regulated and are expressed primarily in differentiated cells (Machiels et al, 1996; Rober et al, 1989). Expression of lamin C2 and lamin B3 is restricted to male germ-line cells (Furukawa & Hotta, 1993; Furukawa et al, 1994). Expression of B-type lamins is essential for nuclear integrity, cell survival and normal development. In contrast to B-type lamins, A-type lamins are dispensable for development. Despite the differences in the expression pattern of A- and B-type lamins, lamin isoforms are classified based on biochemical and structural criteria. A-type lamins are characterized by a neutral isoelectric point, while B-type lamins are more acidic (Gerace & Burke, 1988; Nigg, 1989; Peter et al, 1989). During mitosis when the lamina transiently disassembles, A-type lamins are completely solubilized and dispersed, whereas B-type lamins remain associated with remnants of nuclear membranes (Stuurman et al, 1998). Analyses of lamin and cytoplasmic IF genomic sequences indicate that nuclear lamins are the progenitors of all IF, with cytoplasmic IF arising through gene duplication (Riemer et al, 2000).

1.2.1 Functions of nuclear lamins

Since its discovery, the nuclear lamina has been thought to play primarily a structural role, supporting the nuclear membranes and the NPCs. It has been shown that mouse cells lacking lamin B1 have severely abnormal nuclear morphology (Vergnes et al, 2004). Depletion of A-type lamins leads to abnormalities in nuclear architecture and mislocalization of integral membrane proteins of the inner nuclear membrane (Harborth et al, 2001; Muchir et al, 2003; Nikolova et al, 2004; Sullivan et al, 1999). Such cells also have increased nuclear deformability, decreased mechanical stiffness, and decreased viability when subjected to mechanical strain (Broers et al, 2004; Lammerding et al, 2004). The lamina also plays a role in the spatial arrangement of nuclear pore complexes in the nuclear envelope (Aaronson & Blobel, 1975; Dwyer & Blobel, 1976; Smythe et al, 2000). Nuclear lamins may also be involved in the biogenesis or maintenance of the nuclear envelope membranes, as overexpression of prenylated lamins in cells induces excessive nuclear membrane formation and growth (Prufert et al, 2004; Ralle et al, 2004). The complex interactions of lamins and lamin-

binding proteins with whole chromatin, DNA, and histones suggest functions of these proteins in higher order chromatin organization by providing specific chromatin docking sites at the NE and by structurally organizing chromatin fibers in the 3-dimensional nuclear space (Glass et al, 1993; Goldberg et al, 1999; Luderus et al, 1992; Stierle et al, 2003; Taniura et al, 1995). However, there may be much more to lamins than just a scaffolding function. Since higher order chromatin organization is ultimately linked to control of gene expression, lamina proteins might also be involved in this process. In addition, lamins may directly influence transcription by interacting with transcription factors and/or chromatin remodeling complexes (Mattout-Drubezki & Gruenbaum, 2003). There is significant amount of evidence that lamins play a role in DNA replication. Nuclei assembled *in vitro* in *Xenopus* egg extracts lacking a functional lamina fail to replicate DNA (Ellis et al, 1997; Moir et al, 2000; Newport et al, 1990; Spann et al, 1997). Lamins have also been implicated in DNA replication at the cellular level by the finding that DNA replication sites or replication foci co-localize with nuclear lamins (Kennedy et al, 2000; Moir et al, 1994). However, the precise spatial coincidence between the intranuclear pool of lamins and DNA replication sites is a matter of debate (Barbie et al, 2004; Dimitrova & Berezney, 2002; Kennedy et al, 2000). Recent studies provided direct evidence for nuclear lamin involvement in RNA polymerase II (Pol II)-dependent transcription (Kumaran et al, 2002; Spann et al, 2002). Some studies have also implicated lamins in RNA splicing (Jagatheesan et al, 1999; Kumaran et al, 2002). However, recent evidence indicates that formation of nuclear splicing compartments is independent of lamins A and C (Vecerova et al, 2004). Since lamins or domains of lamins have not been studied in *in vitro* assays of DNA replication, DNA transcription, and RNA splicing, their roles in these processes may be indirect, resulting from secondary effects of the pleiotropic functions of lamins. Finally, there is strong evidence now that lamina proteins are also involved in apoptosis, since inhibition of lamin cleavage delays apoptosis (Rao et al, 1996; Ruchaud et al, 2002), and conversely, inhibition or downregulation of lamin B triggers apoptosis (Harborth et al, 2001; Steen & Collas, 2001).

1.2.2 Laminopathies

Mutations in genes encoding the nuclear lamins and associated proteins cause a wide spectrum of diseases commonly designated laminopathies. These diseases comprise a group of heterogeneous genetic disorders that have been associated with mutations in *LMNA* and, most recently, *LMNB1* and *LMNB2*. More than 230 different mutations in the lamin A/C gene alone have been associated with at least twelve different heritable disease phenotypes (Mattout et al, 2006). These include diseases affecting muscle tissues (autosomal and recessive Emery-Dreifuss muscular dystrophy (EDMD), autosomal dominant limb girdle muscular dystrophy and dilated cardiomyopathy, all of which include cardiac conduction defects), adipose tissues (autosomal dominant Dunnigan-type familial partial lipodystrophy), and axonal neurons (recessive Charcot-Marie-Tooth disorder type 2) (Capell & Collins, 2006; Worman & Courvalin, 2005). Recently, the premature aging diseases Hutchinson-Gilford progeria syndrome (HGPS), atypical Werner's syndrome and mandibuloacral dysplasia have also been linked to mutations in *LMNA* (Broers et al, 2006; Worman & Courvalin, 2005).

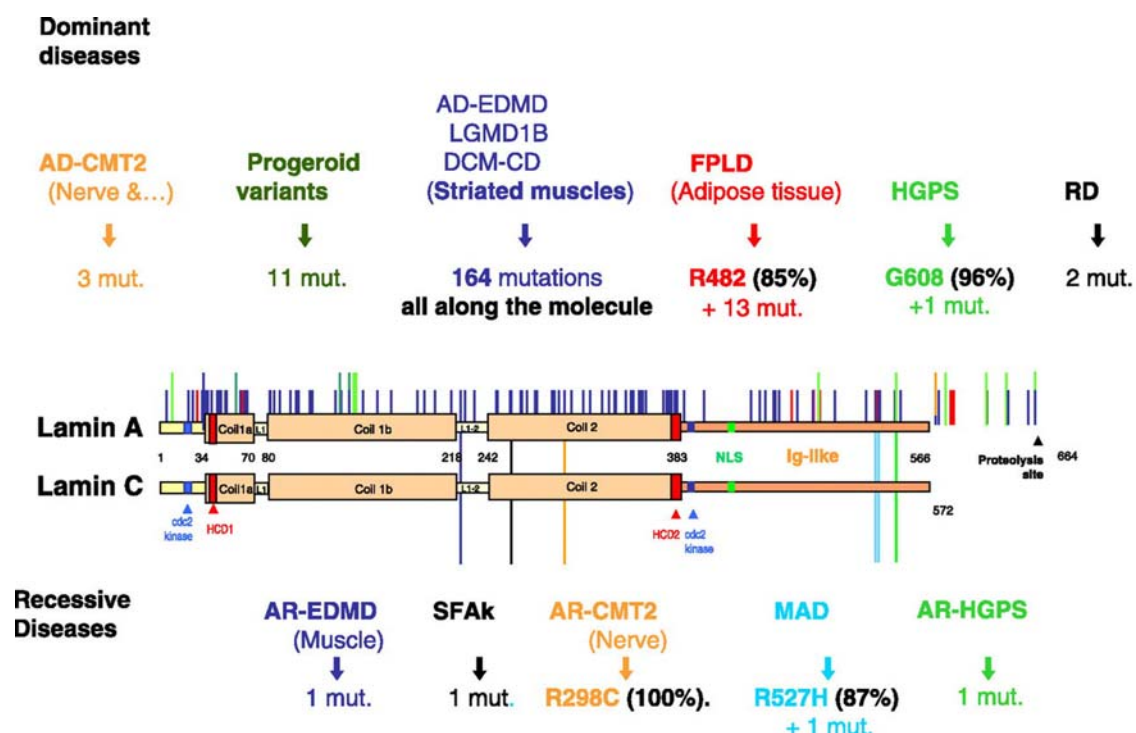


Figure 3: Schematic representation of LMNA mutations identified in the various types of laminopathies. Dominant disorders due to heterozygous LMNA mutations are depicted on the top of the protein scheme, whereas recessive disorders due to homozygous mutations are presented below. Figure adapted from Broers et al, 2006.

Heritable disease-causing mutations, including missense and nonsense mutations, frameshifts and splice site mutations, are distributed over almost the entire *LMNA* gene (Figure 3). Different patients carrying a single mutation may suffer multiple laminopathies, and the phenotype of any given *LMNA* mutation can vary between individuals and between siblings (Mattout et al, 2006). However, despite the knowledge of both type and position of these gene defects, the cellular mechanisms underlying the development of the various disease phenotypes are still largely unknown. There are three, not mutually exclusive models that try to explain laminopathic diseases. The structural model suggests that mutations in lamina proteins cause defects in lamin assembly and lamina structure leading to nuclear fragility or loss of nuclear organization. The gene expression model suggests that lamin complexes are important control elements of gene expression such that their absence is fatal. Finally, the cell fate model suggests that their mutation is linked to early apoptosis or premature aging (Herrmann & Foisner, 2003).

1.2.3 Structure of nuclear lamins

Nuclear lamins are type V intermediate filaments. Analyses of lamin and cytoplasmic IF genomic sequences indicate that nuclear lamins are the progenitors of all IF, with cytoplasmic IF arising through gene duplication (Riemer et al, 2000).

Similar to cytoplasmic IFs, lamins have a characteristic tripartite organization consisting of a short N-terminal head domain, a central α -helical rod domain and a long C-terminal globular tail domain (Figure 4). The rod domain comprises four coiled-coil forming domains (1A, 1B, 2A, 2B) separated by more or less flexible linker regions (L1, L12, and L2). The hydrophobic residues in the first and fourth position of a heptad in a α -helical subdomain drive the interaction between two lamin protein chains, to form a parallel, in register coiled-coil dimer, the basic structural unit of lamin assembly (Stuurman et al, 1998). The α -helical rod domain is flanked by highly conserved phosphoacceptor sites which are phosphorylated with the onset of mitosis and thereby causing morphological changes involving the disassembly of the lamina meshwork (Heald & McKeon, 1990; Peter et al, 1990).

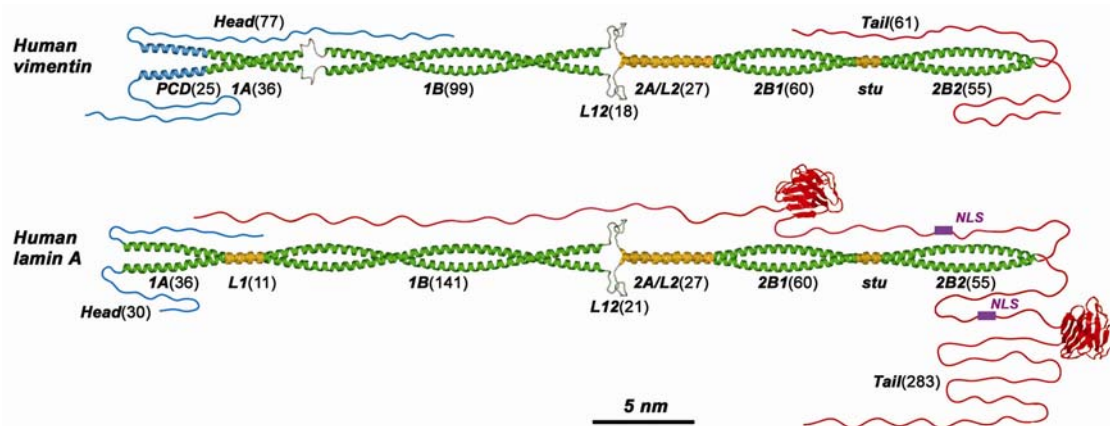


Figure 4: Structural model of cytoplasmic and nuclear intermediate filament protein dimers (Herrmann et al, 2007).

The non α -helical head and tail domains play an important role in lamin assembly (Moir et al, 1991). The C-terminal tail domain contains a nuclear localization sequence (NLS) which is necessary for nuclear import of lamins (Loewinger & McKeon, 1988). Mammalian lamins, except for lamin C and C2, possess at the very C-terminus a CAAX box motif.

1.2.4 Lamin filament assembly

Studies of nuclear lamin assembly *in vitro* have revealed interesting differences relative to cytoskeletal IFs. Lamins are obligate dimers, although it is still not clear whether lamins form homodimers or heterodimers (Gruenbaum et al, 2005). Dimerization occurs through in register parallel associations within the coiled coil domains of the central rod region (Aebi et al, 1986). At their next level of structural organization, lamin dimers associate longitudinally to form polar head to tail polymers. In a further step, lamin head to tail polymers associate laterally, probably in an antiparallel, approximately half-staggered fashion. However, at least *in vitro* these protofilaments are not stable over time and, instead, further associate laterally into large paracrystalline structures (Stuurman et al, 1998). These paracrystals do not exist *in vivo* under normal circumstances. Elimination of the head, and to a lesser extent, tail domains inhibits the formation of head-to-tail polymers (Heitlinger et al, 1992).

1.2.5 Modifications of nuclear lamins

The CAAX box motif (a cysteine (C), two aliphatic residues (AA), and any residue (X)) at the very C-terminus of lamins is the target for a sequence of posttranslational modifications. Initially, the cysteine is farnesylated followed by proteolytic cleavage of the last three amino acids (AAX). After this cleavage the cysteine undergoes methyl esterification (Moir et al, 1995). The farnesylated modification is important but not sufficient for targeting and anchoring the protein to the INM (Moir et al, 1995). While B-type lamins remain farnesylated throughout their lifespan, prelamin A undergoes another maturation step in which the 15 C-terminal amino acids, including the farnesyl group, are cleaved off by the ZMPSTE24 zinc metalloproteinase (Corrigan et al, 2005; Weber et al, 1989). Therefore, B-type lamins are more tightly associated with membrane structures than A-type lamins in mitosis and interphase and are less stably incorporated into the lamina (Gerace & Burke, 1988; Izumi et al, 2000).

Lamins contain a great number of putative phosphorylation sites (serine/threonine). Highly conserved serine residues flanking the rod domain are phosphorylated with the onset of mitosis by a cdc2 kinase (Heald & McKeon, 1990; Nigg, 1992; Peter et al, 1990). This hyperphosphorylation leads to the depolymerization of the lamina *in vivo* concomitant with NE breakdown. *In vitro* studies showed that phosphorylation of lamin dimers inhibited the formation of higher order assemblies such as polar head-to-tail polymers (Nigg, 1992; Peter et al, 1991). These findings have led to the conclusion that lamina disassembly follows a similar principle *in vivo* and that the formation of head-to-tail polymers is influenced by the degree of phosphorylation at sites flanking the rod domain. Mitotic A-type lamins solubilize and are dispersed throughout the cytoplasm, while B-type lamins remain associated with nuclear membrane structures due to their C-terminal farnesyl modification (Nigg et al, 1992). Following mitosis, lamins are dephosphorylated by phosphatase PP1 (Steen et al, 2000) and bind on the periphery of decondensing chromosomes. B-type lamins are suggested to be incorporated into the reforming NE in earlier stages whereas A-type lamins are incorporated only after the nuclear membranes and pores are formed.

1.2.6 Lamins in the nuclear interior

Lamins were traditionally regarded as the major building blocks of the peripheral nuclear lamina underneath the inner nuclear membrane. After many years of debate, the idea that lamins exist also in the nuclear interior is mostly accepted (Dechat et al, 2000; Moir et al, 2000). Since the nuclear membrane forms extensive tubular invaginations extending into the nucleoplasm (Fricker et al, 1997) it is likely that at least some of the intranuclear foci observed are still in direct contact with the nuclear envelope. Two different manifestations of intranuclear lamins have been reported: 1.) intranuclear spots (Bridger et al, 1993; Goldman et al, 1992; Moir et al, 1994) that contain either A- or B-type lamins; and 2.) lamins distributed in a diffuse fashion throughout the nucleus (Hozak et al, 1995). It remains unclear whether intranuclear lamins form filaments as detected in some electron microscopic preparations (Hozak et al, 1995). However, free vimentin-type 10-nm filaments within the nucleus, as observed upon ectopic expression of NLS-modified vimentin (Goldman et al, 1992; Herrmann et al, 1993), have not been described for intranuclear lamins (Herrmann & Foisner, 2003). It is also unclear whether lamins in the nucleoplasm represent transient structures during lamina assembly (Bridger et al, 1993; Goldman et al, 1992) mediating their posttranslational processing, or whether they fulfill specific functions in the nucleus. Nucleoplasmic lamin A/C has been shown to interact with lamina-associated polypeptide 2 α (LAP2 α), a LAP2 isoform exclusively located throughout the nucleoplasm (Dechat et al, 2000; Markiewicz et al, 2002). LAP2 α -lamin A/C complexes have further been shown to interact with the tumor suppressor retinoblastoma protein pRB (Markiewicz et al, 2002), implicating a function in transcriptional control. As lamins are often associated with nuclear bodies (Jagatheesan et al, 1999; Moir et al, 1994) they may represent nucleoplasmic functional units involved in DNA replication, transcription, chromatin organization and gene expression (Moir et al, 2000; Spann et al, 2002).

1.3 Aim of the thesis

The aim of this thesis was to investigate basic steps in the mechanism of lamin *in vivo* assembly and the “cross-talk” of lamin assembly processes with nuclear morphology. For this reason, we wanted to follow a dominant negative type approach by use of different lamin mutants.

In the first part of the project, the impact of distinct domains of the lamin protein on lamin assembly was analyzed. Human lamin B2 is the least studied lamin and therefore, several human lamin B2 mutants fused to YFP were generated carrying head and/or tail deletions. In a next step, we generated lamin B1 and lamin B2 mutants, in place of the highly conserved mitotic serine residues exhibiting aspartic acids. All mutants should be expressed in different cancer cell lines and their cellular localization and influence on the lamina and on inner nuclear membrane proteins should be analyzed by confocal microscopy. In addition, we wanted to analyze all mutants biochemically with regard to their solubility properties. Beside the use of different cancer cell lines, we aimed to analyze wild type lamins and lamin mutants both fused to YFP in mouse embryonic stem (ES) cells. Their ability to differentiate into all specialized cell types found in the adult mouse and the exhibition and maintenance of a normal diploid complement of chromosomes make them a valuable tool for cell biological studies. Therefore, we wanted to establish ES cell culture in our laboratory and establish the conditions for transfection of these cells and further processing for microscopy.

2 Material

2.1 Biological material

2.1.1 Bacterial strains

E. coli TG-1, sure, and XL10 gold (Stratagene, Germany) strains were used for amplification and preparation of plasmid DNA.

2.1.2 Cultured cell lines

Table 1: Cell lines used in this thesis.

designation.	ATCC no.	organism/tissue	characteristics
HeLa	ACC 57	human cervix carcinoma	adherent monolayer
SW13-F8	CCL-105	human primary small cell carcinoma adrenal gland; cortex	adherent monolayer
U2OS	HTB-96	human osteosarcoma	adherent monolayer
HM1 ES	Magin et al., 1992	mouse embryonic stem cells	adherent

2.1.3 Stably transfected culture cell lines

Table 2: Properties of the used stably transfected cell lines.

designation	origin	stably transfected expression plasmid	eukaryotic resistance
U2OS H2A-CFP	U2OS cells	human histone H2A-CFP	Neomycin
U2OS LB2 S407D-YFP	U2OS cells	human lamin B2 S407D-pEYFP-C1	Neomycin
U2OS LB2 S37+407D-YFP	U2OS cells	human lamin B2 S37+407D-pEYFP-C1	Neomycin
ES LB2-YFP	HM1 ES cells	human lamin B2-pEYFP-C1	Neomycin
ES LB1-YFP	HM1 ES cells	human lamin B1-pEYFP-C1	Neomycin

2.2 Expression vectors

Table 3: Expression vectors used for transfection of cell cultures.

plasmid vector	size in bp	resistance		reference
		prokaryotic	eukaryotic	
pEGFP-C1	4700	kanamycin	neomycin	Clontech, Germany
pEYFP-C1	4700	kanamycin	neomycin	Clontech, Germany
pECFP-C1	4700	kanamycin	neomycin	Clontech, Germany
mCherry-C1	4700	kanamycin	neomycin	Tsien et al., 2004

2.3 Expression plasmids

Table 4: Origin of the used expression constructs.

construct	reference
Human Lamin B2-pEYFP-C1	this study
Human Lamin B2 Δ 32head-pEYFP-C1	this study
Human Lamin B2 headless-pEYFP-C1	this study
Human Lamin B2 tailless-pEYFP-C1	this study
Human Lamin B2 Δ 32head/tailless-pEYFP-C1	this study
Human Lamin B2 rod-pEYFP-C1	this study
Human Lamin B2 S37D-pEYFP-C1	this study
Human Lamin B2 S405D-pEYFP-C1	this study
Human Lamin B2 S407D-pEYFP-C1/-pEGFP-C1/-mCherry	this study
Human Lamin B2 S37+405D-pEYFP-C1	this study
Human Lamin B2 S37+407D-pEYFP-C1	this study
Human Lamin B2 S405+407D-pEYFP-C1	this study
Human Lamin B2 S37+405+407D-pEYFP-C1	this study
Human Lamin B1-pEYFP-C1	this study
Human Lamin B1 S23D-pEYFP-C1	this study
Human Lamin B1 S391D-pEYFP-C1	this study
Human Lamin B1 S393D- pEYFP-C1/-pEGFP-C1/-mCherry	this study
Human PCNA-CFP	(Leonhardt et al, 2000)
Human histone H2A-CFP	T. A. Knoch
Human lamin A p.R321X-pEGFP-C1	this study
<i>Xenopus laevis</i> NLS-vimentin-pEGFP	(Reichenzeller et al, 2000)

2.4 Antibodies

2.4.1 Primary antibodies

Table 5: Origin, properties and dilution of the used primary antibodies.

antibody	antigen	type	origin	IF	WB	reference
X223	lamin B2	monoclonal	mouse	undiluted	1:5	(Hoger et al, 1991)
X167	lamin A	monoclonal	mouse	undiluted	1:5	(Hoger et al, 1991)
LA-Z1	lamin A	monoclonal	mouse	undiluted	1:5	(Geiger et al, 2008)
5-1-3	LBR	monoclonal	rabbit	undiluted	-	Epitomics INC
EM-N-term	Emerin	polyclonal	guinea pig	1:300	-	(Dreger et al, 2002)

2.4.2 Secondary antibodies

Species specific antibodies conjugated with Alexa 488, Alexa 568 (Molecular Probes, Netherlands) or Cy5 (Dianova, Germany) were used for immunofluorescence.

Membrane bound antigen-antibody complexes were detected by use of horseradish peroxidase coupled antibodies raised against mouse, rabbit or guinea pig immunoglobulins (Dianova, Germany).

2.5 Size markers

2.5.1 DNA size markers

As DNA size markers EcoRI and HindIII digested λ -DNA (λ /E/H marker) or HinfI digested pBluescribe DNA (BsHinf marker) were used. Digestion yields the following discrete fragments (in base pairs):

λ /E/H marker: 24.700, 5148, 4973, 4268, 3480, 2027, 1904, 1584, 1375, 947, 831, 564, 125

BsHinf marker 1400, 517, 396, 356, 247, 75

2.5.2 Protein size markers

As protein size marker the Broad Range P7702L marker (New England Biolabs, Germany) was used. It comprises the following fragments (in kDa):

Broad Range P7702L marker 212, 158, 116, 97.2, 66.4, 55.6, 42.7, 34.6, 27, 20, 14.3, 6.5, 3.4, 2.3

2.6 DNA oligonucleotides

All oligonucleotides used for PCR amplification, cloning, and DNA sequencing were synthesized by Dr. Wolfgang Weinig (DKFZ, Heidelberg). Primers used for mutagenesis were bought in HPLC grade from MWG Biotech (Germany).

2.7 Chemicals and enzymes

The used chemicals and reagents were purchased in analytical quality from the following companies: Invitrogen (Germany), Fluka (Germany), Merck (Germany), Pharmacia (Germany), Roche (Germany), Roth (Germany), Serva (Germany), Sigma (Germany), Qiagen (Germany).

Enzymes were purchased from Roche (Germany), Stratagene (Germany), and New England Biolabs (Germany).

2.8 Cell culture material

1-thioglycerol	Sigma-Aldrich, Germany
BMP-2 (bone morphogenic protein)	kindly provided by T. Magin, Bonn
Bovine albumin fraction V	Invitrogen, Germany
DMEM (High Glucose)	Invitrogen, Germany
DMEM-F12	Invitrogen, Germany
DMSO	Sigma-Aldrich, Germany
Epoxomicin	Sigma-Aldrich, Germany
Fetal calf serum	Biochrom, Germany

Gelatine swine skin type I	Sigma-Aldrich, Germany
Genitacin	Sigma-Aldrich, Germany
Insulin, human recombinant, zinc	Invitrogen, Germany
L-glutamine	Invitrogen, Germany
LIF (leukemia inhibitory factor)	kindly provided by T. Magin, Bonn
Neurobasal medium	Invitrogen, Germany
Penicillin and Streptomycin	Invitrogen, Germany
Progesteron	Sigma-Aldrich, Germany
Putrescin	Sigma-Aldrich, Germany
Sodium selenite	Sigma-Aldrich, Germany
Supplement B27	Invitrogen, Germany
Transferrin, bovine (APO form)	Invitrogen, Germany
Trypsin inhibitor	Sigma-Aldrich, Germany
Trypsin solution	Invitrogen, Germany

2.9 Media and solutions

LB-medium (pH 7.2)

1%	Bacto tryptone (w/v)
0.5%	yeast extract (w/v)
86 mM	NaCl
10 mM	MgSO ₄

LB-media with antibiotics

Appropriate antibiotics were added after autoclaving of LB-medium. The concentration of ampicillin was 100 µg/ml and of kanamycin 50 µg/ml.

LB-agarplates with antibiotics

15 g agar was added to 1000 ml LB-medium and autoclaved. Antibiotics were added to the cooled, autoclaved medium.

TAE (pH 8.0)

40 mM	Tris/HCl
0.12%	acetic acid
1 mM	EDTA

6x DNA loading dye	200 mM	EDTA
	100 mM	Tris/HCl (pH 7.5)
	0.01%	bromophenol blue (w/v)
	0.01%	xylencyanol
	30%	ficoll (w/v)
PBS (pH 7.4)	2.7 mM	KCl
	1.7 mM	KH ₂ PO ₄
	137 mM	NaCl
	10 mM	Na ₂ HPO ₄
TE	10 mM	Tris/HCl (pH 7.5)
	1 mM	EDTA
Laemmli electrophoresis buffer	25 mM	Tris/HCl
	192 mM	glycine
	0.1%	SDS (w/v)
Lower Tris	1.5 M	Tris/HCl (pH 8.8)
	0.4%	SDS (w/v)
Upper Tris	0.5 M	Tris/HCl (pH 6.8)
	0.4%	SDS (w/v)
3x Laemmli sample buffer	30%	glycerine
	0.2%	bromophenol blue (w/v)
	9%	SDS (w/v)
	187.5 mM	Tris/HCl
	150 mM	DTT
Coomassie stain	40%	isopropanol
	7%	acetic acid
	0.2%	Coomassie Brilliant Blue R-50
Coomassie destain	20%	isopropanol
	7.5%	acetic acid

Borate transfer buffer (pH 8.8)	20 mM	boric acid
	1 mM	Na ₂ -EDTA
	4 mM	DTT
TBST (pH 8.0)	10 mM	Tris/HCl
	150 mM	NaCl
	0.05%	Tween 20

2.10 Kits

ECL Kit	PerkinElmer Life Sciences, USA
FuGene6 Transfection Reagent	Roche, Germany
Lipofectamine 2000 Transfection Reagent	Invitrogen, Germany
Qiaquick PCR-Purification Kit	Qiagen, Germany
QIAprep spin Miniprep Kit	Qiagen, Germany
Qiaex Agarose Gel Extraction Kit	Qiagen, Germany
Qiagen Plasmid Maxi Kit	Qiagen, Germany
QuikChange II XL Site-Directed Mutagenesis Kit	Stratagene, Germany

2.11 Instruments

Agarose gel electrophoresis apparatus	Cti-GmbH, Germany
Centrifuges	Heraeus, Germany
	Beckmann, Germany
CO ₂ incubator	Thermo Life Sciences, Germany
Fluorescence microscope	Zeiss, Germany
Gel documentation system	DNR Bio-imaging systems
Gel electrophoresis power supply	Biotech Fischer, Germany
Laser scanning microscope Leica TCS SP2	Leica Microsystems, Mannheim
NanoDrop spectrophotometer	NanoDrop Technologies, USA
PCR cycler	MJ Research, Biozym, Germany
pH-meter	Schott, Germany

Refrigerated centrifuge	Eppendorf, Germany
SDS-PAGE gel apparatus	Cti-GmbH, Germany
Vortex mixer	Neolab Migge, Germany
Water baths	Julabo, Germany
Western blot apparatus	Bio Rad, Germany

3 Methods

3.1 DNA techniques

3.1.1 Preparation of competent bacteria

The treatment of *E.coli* cells with calcium chloride solution leads to an increased uptake of DNA from the solution into the bacteria.

An over night culture (5 ml) of *E.coli* was diluted 1:100 to a final volume of 400 ml LB-medium and grown in a shaker at 37°C to an optical density of $OD_{600} = 0.5-0.6$. Subsequently, the culture was centrifuged for 5 minutes at 0°C at 5000 rpm (Beckmann J2-HS-centrifuge, rotor JA-14). The cell pellet was resuspended in 100 ml ice cold sterile 0.1 M $CaCl_2$ solution and incubated on ice for 30 minutes. Cells were again centrifuged as described above. The pellet was resuspended in 2 ml freezing solution (0.1 M $CaCl_2$, 15% glycerine (v/v)) and stored at -80°C.

3.1.2 Transformation of competent bacteria

The term transformation describes the uptake of plasmid DNA into competent bacteria using a heat shock.

Competent *E. coli* cells were thawed on ice. 4-10 ng plasmid-DNA was added, followed by incubation for 20-30 minutes on ice. Depending on the bacterial strain heat shock temperature was adapted (42°C for XL gold and 37°C for TG-1 and sure). The heat shock duration was 3 minutes. Cells were immediately cooled on ice for 1 minute. After addition of 400 μ l LB-medium, cells were incubated at 37°C for 60 minutes. According to the antibiotic resistance of the transformed plasmid DNA, cells were plated on agar plates with the respective selection marker and incubated over night at 37°C.

3.1.3 Isolation of plasmid DNA (Miniprep, Maxiprep)

E. coli containing the plasmid of interest were grown on agar plates. Colonies were picked from the plates and grown for minipreps in 2 ml LB-medium containing the appropriate antibiotic in a shaking incubator at 37°C over night. For maxipreps a 5

ml preculture in LB-medium was grown for 6 hours and transferred to an overnight culture (100 ml for low-copy and 500 ml for high-copy plasmids). Isolation of plasmid DNA was performed according to the manufacturers protocol (QIAprep Spin Miniprep Kit and Qiagen Plasmid Maxi Kit; Qiagen, Germany).

3.1.4 Agarose gel electrophoresis

DNA fragments can be separated in an electric field according to their size by agarose gel electrophoresis. The used concentration of the agarose is dependent on the size of the DNA fragments.

Table 6: Agarose concentration and separation range in kb for DNA fragments

agarose concentration	separation range in kilo bases (kb)
0.5%	1-30
1%	0.5-10
1.5%	0.2-3
2%	0.05-2

The agarose was melted by boiling in 1x TAE buffer. After cooling to 60°C, ethidium bromide was added to a final concentration of 1 µg/ml. The solution was poured into a horizontal casting tray and was allowed to harden. For electrophoresis, the gel was placed in a gel chamber and was covered with 1x TAE buffer. The samples mixed with 6x DNA loading buffer and a DNA size marker (see 2.5.1) were loaded onto the gel. Electrophoresis was run at 70-90 V. After the run, the separated DNA bands were visualized with a transilluminator at 280 nm.

3.1.5 Determination of DNA concentration

The concentration of DNA was measured in a spectrophotometer (NanoDrop Technologies, USA). The absorbance of the nucleic acid solution was measured with a wavelength of $\lambda = 260$ nm.

3.1.6 Restriction digestion

3.1.6.1 Analytical restriction digestion

Analytical restriction digestion was used to check for the correct orientation and length of the inserted DNA fragment into the plasmid vector.

1-2 µg of plasmid DNA was digested with 5 units of restriction enzyme. Buffer was used as recommended by the manufacturer. Digests were normally incubated for 1 hour at 37°C. The DNA fragments were analyzed by agarose gel electrophoresis (see 3.1.4).

3.1.6.2 Preparative restriction digestion

The preparative restriction digestion was used to isolate specific DNA fragments. 2-4 µg of plasmid DNA was digested with 5-10 units of restriction enzyme in the appropriate buffer for 1-2 hours at 37°C. The DNA was separated by agarose gel electrophoresis (see 3.1.4) on a low melting agarose gel. The DNA bands were cut out with a disposable scalpel as precise as possible on a transilluminator at 366 nm and put into a reaction tube. Gel slices were washed for 5 minutes in 500 µl band washing buffer. After removal of the washing buffer, the reaction tube was incubated for 3-5 minutes at 70°C. The melted gel slice was directly used for ligation or was stored at -20°C until use. Alternatively, DNA was extracted from the gel with a gel extraction kit (Qiaex Agarose Gel Extraction Kit; Qiagen, Hilden) according to the manufacturer's instruction.

3.1.6.3 Partial restriction digestion

4-5 µg of plasmid DNA was digested with 5-10 units of the single cutting enzyme at 37°C in a final volume of 40 µl. After 1-2 hours, 5-10 units of the multi cutting enzyme were added and the final volume was adjusted to 85 µl. Digests were incubated at 37°C. 10 µl samples were taken after 2, 5, 10, 15, 20, 25, 30, and 40 minutes and mixed with 2 µl of 6x DNA loading buffer with 100 mM EDTA and kept on ice. Subsequently, 2 µl of each sample were subjected to agarose gel electrophoresis (see 3.1.4). Samples containing the desired DNA fragment were

pooled and loaded onto a low melting agarose gel. The DNA band of interest was cut out with a scalpel and processed as described in section 3.1.6.2.

3.1.7 PCR

In order to amplify a specific DNA target sequence, a forward and reverse primer were designed. They contained ~20 bases complementary to the target sequence and recognition sites for restriction enzymes at the 5' and 3' end. The target sequences were amplified with Pfu DNA polymerase (Stratagene, Germany).

A standard PCR reaction contained: 5 ng template DNA, 170 ng of each primer, 5 µl dNTP mix, 5 µl 10x polymerase buffer, 1 µl DNA polymerase and was adjusted with ddH₂O to a final volume of 50 µl. In some cases 3, 6, or 9% DMSO were added to the reaction in order to lower the DNA melting temperature.

The following PCR cycling program was used:

1 cycle	initial denaturation	3 minutes	94°C
35 cycles	denaturation	20 seconds	92°C
	annealing	30 seconds	58°C
	extension	1 minute	72°C
1 cycle	final extension	10 minutes	72°C

The annealing temperature was modified according to the used primer pairs. PCR products were then analyzed on a 1% agarose gel.

3.1.8 Purification of PCR products

The PCR products were purified from primers and nucleotides before restriction digestion. Purification was performed according to the protocol of a PCR purification kit (Qiaquick PCR Purification Kit; Qiagen, Hilden). The purified fragments were finally dissolved in 30 µl TE buffer.

3.1.9 Site-directed Mutagenesis

In order to replace single amino acids the QuikChange II XL Site-Directed Mutagenesis kit (Stratagene, Germany) was used according to the manufacturer's instructions. The site-directed mutagenesis method is performed using a high-fidelity DNA polymerase for mutagenic primer-directed replication of both plasmid strands. The basic procedure utilizes a supercoiled double-stranded DNA vector with an insert of interest and two synthetic oligonucleotide primers, both containing the desired mutation. The primers used were between 25 and 40 bases in length and were designed so that they annealed to the same sequence on opposite strands of the plasmid. Both mutagenic primers contained the desired mutation in the middle of the primer flanked by sequences complementary to the template sequence.

The primers are extended during temperature cycling by the DNA polymerase, without primer displacement. Extension of the primers generates a mutated plasmid containing staggered nicks. Following temperature cycling, the product is treated with DpnI endonuclease, which is specific for methylated and hemimethylated DNA and is used to digest the parental DNA template and to select for mutation-containing synthesized DNA. The nicked vector DNA incorporating the desired mutation is then transformed into *E. coli* XL10 Gold cells.

3.1.10 Removal of 5'-phosphate residues from DNA fragments

In order to prevent re-ligation of a linearized vector, the phosphate groups which deliver the reactive phosphor required for the sugar-phosphate bonds of the DNA, were removed by an alkaline phosphatase (Shrimp alkaline phosphatase, SAP).

The digested vector DNA was dephosphorylated for 1 hour with 1 unit SAP at 37°C and subsequently inactivated for 15 minutes at 70°C.

3.1.11 Phosphorylation and annealing of DNA oligomers

In order to insert DNA oligomers into plasmids by ligation, the complementary oligomers have to be phosphorylated at the 5' end and have to be annealed.

For phosphorylation, 0.5 nM oligomers were incubated in 2 µl 10x polynucleotide kinase buffer in a final volume of 18 µl for 10 minutes at 70°C. After denaturation,

1 μ l 10 mM ATP and 1 μ l (=10 units) polynucleotide kinase were added and incubated for 30 minutes at 37°C. The reaction was stopped by incubation for 10 minutes at 70°C. 100 ng of each oligomer were used for the annealing reaction and incubated in 50 μ l TE with 50 mM NaCl for 10 minutes at 70°C and for 30 minutes at 37°C. For ligation, 4, 10, and 20 ng were used.

3.1.12 Ligation

For ligation and the following transformation into *E. coli* cells, the ratio of insert to vector was ranging from 5:1 to 10:1. Either purified PCR products or DNA fragments isolated from low melting agarose gels were ligated. The reaction was carried out in a final volume of 20-30 μ l by addition of 10x ligase buffer and 1 μ l (=1 unit) T4 DNA ligase and was either incubated for 2 hours at 16-18°C or over night at 4°C.

3.1.13 DNA sequencing

All cloned expression plasmids were sequenced by Andreas Hunziker (DKFZ, Heidelberg) to verify the DNA sequence.

3.2 Generation of expression plasmids

The full-length human lamin B2 cDNA clone BC006551 (NCBI data bank) in pOTB was obtained from the RZPD (Germany). The full-length human lamin B1 cDNA in pBluescript was provided by E. Tan (The Scripps Research Institute, La Jolla, USA).

3.2.1 Human lamin B2

The coding sequence of the human lamin B2 cDNA in pOTB was partially amplified by PCR. A fragment encoding amino acid 1-77 was amplified using a forward primer (SG96: 5'-GAGAGATCCGGAATGAGCCCGCCGAGCCCG-3') inserting a BspEI restriction site and a reverse primer (SG97: 5'-CTTCTCTGAGATCTTGAGCAGGAGCCGGTCG-3'). The PCR product was digested with BspEI/BglII and was inserted into the multiple cloning site of pEYFP-C1. Human lamin B2 headless cDNA in pEYFP-C1 (see below)

was digested with BglII/EcoRI and was ligated into cloned lamin B2 [1-77] in pEYFP-C1 digested with the same enzymes. The resulting cDNA construct was validated by sequencing.

3.2.2 Human lamin B2 deletion mutants

For generation of human lamin B2 deletion mutants the coding sequence of the human lamin B2 cDNA in pOTB was partially amplified by PCR and cloned comprising the following fragments:

a) LB2[33-309]

Amplified with a forward primer (SG8: 5'-GAGAGAGGATCCATGGCCACGCCGCTGTCCGCCACG-3') introducing a start codon and a NcoI restriction site and a reverse primer (SG4: 5'-CTCCCCGGCCATGGCCTCCTCCAGCTCCCGAATGC-3'). The PCR product was digested with NcoI and ligated into the multiple cloning site of a modified pBluescript cut with the same enzyme. The construct was validated by sequencing.

b) LB2[46-309]

Amplified with a forward primer (SG3: 5'-GAGAGAGGATCCATGGAGAAGGAGGAGCTGCGGAGC-3') introducing a start codon and a NcoI restriction site and a reverse primer (SG4: 5'-CTCCCCGGCCATGGCCTCCTCCAGCTCCCGAATGC-3'). The PCR product was digested with NcoI and ligated into the multiple cloning site of a modified pBluescript cut with the same enzyme. The construct was validated by sequencing.

c) LB2[310-402]

Amplified with a forward primer (SG5: 5'-CGGGAGCTGGAGGACGCCATGGCCGGGGAGC-3') and a reverse primer (SG6: 5'-GAATTCTTACAGCCTCTCCTCCTCGCC-3') introducing a stop codon and a EcoRI restriction site. The PCR product was digested with NcoI/EcoRI and ligated into the multiple cloning site of a modified pBluescript cut with the same enzymes. The construct was validated by sequencing.

d) LB2[310-620]

Amplified with a forward primer (SG5: 5'-CGGGAGCTGGAGGACGCCATGGCCGGGG AGC-3') and a reverse primer (SG7: 5'-GAGAGAGAATTCTTACATCACGTAGCAGCCTC TTG-3') introducing a EcoRI restriction site. The PCR product was digested with NcoI/EcoRI and ligated into the multiple cloning site of a modified pBluescript cut with the same enzymes. The construct was validated by sequencing.

3.2.2.1 Human lamin B2 Δ 32head

Cloned LB2[33-309] cDNA in pBluescript was digested with NcoI and ligated into LB2[310-620] in pBluescript cut with the same enzymes. The resulting LB2 Δ 32head cDNA in pBluescript was then cut out by partial restriction digestion with BspEI/EcoRI and was ligated into the multiple cloning site of pEYFP-C1. The construct was validated by sequencing.

3.2.2.2 Human lamin B2 headless

Cloned LB2[46-309] cDNA in pBluescript was digested with NcoI and ligated into LB2[310-620] in pBluescript cut with the same enzymes. The resulting LB2 headless cDNA in pBluescript was then cut out by partial restriction digestion with BspEI/EcoRI and was ligated into the multiple cloning site of pEYFP-C1. The construct was validated by sequencing.

3.2.2.3 Human lamin B2 tailless

Cloned LB2 rod cDNA in pEYFP-C1 (see below) was digested with BglII/EcoRI and ligated into full-length lamin B2 cDNA in pEYFP-C1 cut with the same enzymes. The construct was validated by sequencing.

3.2.2.4 Human lamin B2 Δ 32head/tailless

Cloned LB2[33-309] cDNA in pBluescript was digested with NcoI and ligated into LB2[310-402] in pBluescript cut with the same enzymes. The resulting LB2 Δ 32head/tailless cDNA in pBluescript was then cut out by partial restriction digestion

with BspEI/EcoRI and was ligated into the multiple cloning site of pEYFP-C1. The construct was validated by sequencing.

3.2.2.5 Human lamin B2 rod

Cloned LB2[46-309] cDNA in pBluescript was digested with NcoI and ligated into LB2[310-402] in pBluescript cut with the same enzymes. The resulting LB2 rod cDNA in pBluescript was then cut out by partial restriction digestion with BspEI/EcoRI and was ligated into the multiple cloning site of pEYFP-C1. The construct was validated by sequencing.

3.2.3 Human lamin B2 S→D mutants

3.2.3.1 Human lamin B2 S37D

The human lamin B2 cDNA in pEYFP-C1 was used as a template for the mutagenesis reaction. The S37D (TCG>GAC) mutation was introduced by site-directed mutagenesis with the QuikChange II XL Site-Directed Mutagenesis kit (Stratagene, Germany) according to the manufacturer's protocol (forward primer SG41: 5'-GCC ACGCCGCTGGACCCCACGCGCCTG-3'; reverse primer SG42: 5'-CAGGCGCGTGGGGTC CAGCGGCGTGGC-3'). The resulting cDNA sequence was verified by sequencing.

3.2.3.2 Human lamin B2 S405D

The human lamin B2 headless cDNA in pBluescript was used as a template for the mutagenesis reaction. The S405D (TCC>GAC) mutation was introduced by site-directed mutagenesis with the QuikChange II XL Site-Directed Mutagenesis kit (Stratagene, Germany) according to the manufacturer's protocol (forward primer SG45: 5'-GAGGCTGAAGCTGGACCCCAGCCCATCC-3'; reverse primer SG46: 5'-GGA TGGGCTGGGGTCCAGCTTCAGCCTC-3'). The resulting cDNA construct was verified by sequencing. The human lamin B2 headless S405D cDNA was then digested with BglII/EcoRI and cloned into the human lamin B2-pEYFP-C1 plasmid cut with the same restriction enzymes.

3.2.3.3 Human lamin B2 S407D

The human lamin B2 headless cDNA in pBluescript was used as a template for the mutagenesis reaction. The S407D (AGC>GAC) mutation was introduced by site-directed mutagenesis with the QuikChange II XL Site-Directed Mutagenesis kit (Stratagene, Germany) according to the manufacturer's protocol (forward primer SG13: 5'-CTGAAGCTGTCCCCGACCCATCCTCGCGCGTC-3'; reverse primer SG14: 5'-GACGCGCGAGGATGGGTCGGGGACAGCTTCAG-3'). The resulting cDNA construct was verified by sequencing. The human lamin B2 headless S407D cDNA was then digested with BglII/EcoRI and cloned into the human lamin B2-pEYFP-C1 plasmid cut with the same restriction enzymes.

3.2.3.4 Human lamin B2 S37+405D

The human lamin B2 S405D cDNA in pEYFP-C1 was digested using BglII/EcoRI and cloned into the human lamin B2 S37D-pEYFP-C1 plasmid cut with the same restriction enzymes. The construct was validated by sequencing.

3.2.3.5 Human lamin B2 S37+407D

The human lamin B2 S407D cDNA in pEYFP-C1 was digested using BglII/EcoRI and cloned into the human lamin B2 S37D-pEYFP-C1 plasmid cut with the same restriction enzymes. The construct was validated by sequencing.

3.2.3.6 Human lamin B2 S405+407D

The human lamin B2 headless S407D cDNA in pBluescript was used as a template for the mutagenesis reaction. The S405D (TCC>GAC) mutation was introduced by site-directed mutagenesis with the QuikChange II XL Site-Directed Mutagenesis kit (Stratagene, Germany) according to the manufacturer's protocol (forward primer SG75: 5'-GAGGCTGAAGCTGGACCCCGACCCATCC-3'; reverse primer SG76: 5'-GGA TGGGTCGGGTCCAGCTTCAGCCTC-3'). The resulting cDNA construct was verified by sequencing. The human lamin B2 headless S405+407D cDNA was then digested with BglII/EcoRI and cloned into the human lamin B2-pEYFP-C1 plasmid cut with the same restriction enzymes.

3.2.3.7 Human lamin B2 S37+405+407D

The human lamin B2 S405+407D cDNA in pEYFP-C1 was digested with BglII/EcoRI and cloned into the human lamin B2 S37D-pEYFP-C1 plasmid cut with the same restriction enzymes. The construct was validated by sequencing.

3.2.4 Human Lamin B1

The human lamin B1 cDNA in pBluescript was amplified by PCR with a forward primer (SG73: 5'-GAGAGATCCGGAATGGCGACTGCGACCCC-3') introducing a BspEI restriction site and a reverse primer (SG74: 5'-GAGAGACTCGAGCATAATTGCACAGCTTC-3') introducing a XhoI restriction site. The PCR fragment was digested with BspEI and XhoI and inserted into the multiple cloning site of pEYFP-C1. The construct was validated by sequencing.

3.2.5 Human lamin B1 S→D mutants

3.2.5.1 Human lamin B1 S23D

The human lamin B1 cDNA in pBluescript was used as a template for the mutagenesis reaction. The S23D (AGC>GAC) mutation was introduced by site-directed mutagenesis with the QuikChange II XL Site-Directed Mutagenesis kit (Stratagene, Germany) according to the manufacturer's protocol (forward primer SG57: 5'-CACCACGCCGCTGGACCCACGCGCCTG-3'; reverse primer SG58: 5'-CAGGCGCGTGGGGTCCAGCGGCGTGGTG-3'). The resulting cDNA construct was verified by sequencing. The human lamin B1 S23D cDNA was then amplified by PCR with a forward primer (SG73: 5'-GAGAGATCCGGAATGGCGACTGCGACCCC-3') introducing a BspEI restriction site and a reverse primer (SG74: 5'-GAGAGACTCGAGCATAATTGCACAGCTTC-3') introducing a XhoI restriction site. The PCR fragment was digested with BspEI and XhoI and inserted into the multiple cloning site of pEYFP-C1. The construct was validated by sequencing.

3.2.5.2 Human lamin B1 S391D

The human lamin B1 cDNA in pBluescript was used as a template for the mutagenesis reaction. The S391D (TCT>GAT) mutation was introduced by site-directed mutagenesis with the QuikChange II XL Site-Directed Mutagenesis kit (Stratagene, Germany) according to the manufacturer's protocol (forward primer SG53: 5'-GAGGTTGAAGCTGGATCCAAGCCCTTCT-3'; reverse primer SG54: 5'-AGAAGGGCTTGGATCCAGCTTCAACCTC-3'). The resulting cDNA construct was verified by sequencing. The human lamin B1 S391D cDNA was then amplified by PCR with a forward primer (SG73: 5'-GAGAGATCCGGAATGGCGACTGCGACCCC-3') introducing a BspEI restriction site and a reverse primer (SG74: 5'-GAGAGACTCGAGCATAAT TGCACAGCTTC-3') introducing a XhoI restriction site. The PCR fragment was digested with BspEI and XhoI and inserted into the multiple cloning site of pEYFP-C1. The construct was validated by sequencing.

3.2.5.3 Human lamin B1 S393D

The human lamin B1 cDNA in pBluescript was used as a template for the mutagenesis reaction. The S393D (AGC>GAC) mutation was introduced by site-directed mutagenesis with the QuikChange II XL Site-Directed Mutagenesis kit (Stratagene, Germany) according to the manufacturer's protocol (forward primer SG49: 5'-GAAGCTGTCTCCAGACCCTTCTTCCCGTG-3'; reverse primer SG50: 5'-CAC GGAAGAAGGGTCTGGAGACAGCTTC-3'). The resulting cDNA construct was verified by sequencing. The human lamin B1 S391D cDNA was then amplified by PCR with a forward primer (SG73: 5'-GAGAGATCCGGAATGGCGACTGCGACCCC-3') introducing a BspEI restriction site and a reverse primer (SG74: 5'-GAGAGACTCGAGCATAAT TGCACAGCTTC-3') introducing a XhoI restriction site. The PCR fragment was digested with BspEI and XhoI and inserted into the multiple cloning site of pEYFP-C1. The construct was validated by sequencing.

3.2.6 Human lamin A p.R321X

The cloned full-length cDNA of human lamin A (McKeon et al, 1986) in pEYFP-C1 was used as a template for the mutagenesis reaction. The p.R321X (CGA>TGA) mutation was introduced by site-directed mutagenesis with the QuikChange II XL Site-Directed

Mutagenesis kit (Stratagene, Germany) according to the manufacturer's protocol (forward primer SG112: 5'-CACCACGCCGCTGGACCCACGCGCCTG-3'; reverse primer SG113: 5'-CAGGCGCGTGGGGTCCAGCGGCGTGGTG-3'). The resulting cDNA construct was verified by sequencing.

3.3 Cell culture techniques

3.3.1 Cultivation of culture cell lines

Adherent cultured cells were grown in cell culture flasks in an incubator with 95% relative air humidity and 5% CO₂ in DMEM medium supplemented with 10% FCS, 20 mM L-glutamine and 100 µg/ml antibiotics. According to their doubling time, cells were split every 3 – 5 days to keep them in the logarithmic growth phase. For splitting, the culture medium was removed and the cells were washed with 1 x PBS. Cells were detached from the culture flask surface by incubation at 37°C in trypsin solution for 3 – 5 minutes. Trypsinized cells were resuspended in fresh, pre-warmed medium and transferred into new flasks, thereby diluted 1:5 to 1:10.

3.3.2 Cultivation of embryonic stem cells

The murine embryonic stem cells were cultured in DMEM-F12/Neurobasal medium supplemented with 1x Supplement B27, 50 µg/ml BSA fraction V, 100 µg/ml APO-transferrin bovine, 25 µg/ml human recombinant insulin, 6 ng/ml progesterone, 16 µg/ml putrescin, 30 nM Na-selenite, 2 mM glutamine, 0.15 mM 1-thioglycerol, 10 ng/ml BMP-2 and LIF. Cells were routinely grown in an incubator with 95% relative air humidity and 5% CO₂ on gelatinized flasks. Culture medium was changed every other day as long as the culture was thin; later on it was changed daily. Cells were split twice a week between 1:6 and 1:12. For splitting, the culture medium was removed and the cells were washed once with ES trypsin solution (0.025% trypsin/1 mM EDTA) before they were incubated in ES trypsin solution at 37°C until they detached. Trypsin activity was stopped by adding a trypsin inhibitor and the cells were resuspended in fresh culture medium. Subsequently, cells were centrifuged for

2 minutes at 1200 rpm, the cell pellet was resuspended in fresh culture medium and the cells were transferred to new gelatinized flasks.

3.3.3 Freezing of cells

Cells were stored at -80°C or in liquid nitrogen.

After trypsinization, the cells were resuspended in DMEM and centrifuged at 1000 rpm for 5 minutes. The cell pellet was resuspended in 1.5 ml complete growth medium with 10% DMSO and transferred to 1.8 ml cryo tubes. After incubation for 20 minutes at -20°C , the tubes were transferred to -80°C or liquid nitrogen.

ES cells were trypsinized as usual. After centrifugation, the cell pellet was resuspended in culture medium and freezing medium (complete ES medium with 20% DMSO) was added drop wise. 0.5-1 ml aliquots with approximately 2-4 million cells per cryo vial were placed in a "Mr. Frosty" container filled with isopropanol and placed at -80°C over night. The following day, the cryo tubes were transferred to liquid nitrogen.

3.3.4 Thawing of cells

Cryo tubes were thawed in a 37°C water bath. Cells were immediately transferred into a 50 ml Falcon tube with 10 ml pre-warmed (37°C) culture medium and centrifuged at 1000 rpm for 5 minutes. The cell pellet was resuspended in culture medium and transferred into a 5 ml cell culture flask and placed in the incubator. The following day the medium was replaced to remove dead cells and cell debris.

3.3.5 Transfection of cells

3.3.5.1 Transient transfection of cells

Transient transfection of cultured cells was performed with FuGene6 transfection reagent (Roche, Germany). After transfection, cells were incubated under the normal growth conditions.

For transient transfection of embryonic stem cells, Lipofectamine2000 (Invitrogen, Germany) was used according to the manufacturers instructions.

3.3.5.2 Stable transfection of cells

Culture cell lines were transfected with FuGene6 transfection reagent (Roche, Germany) in 60 mm cell culture dishes. Cells were further incubated under normal growth conditions. After 2 days, cells were split onto two 10 cm cell culture dishes. For selection for stably integrated neomycin resistance genes, G418 was added to the culture medium the next day in a concentration of 0.5 mg/ml for SW13 cells and 1 mg/ml for U2OS cells.

ES cells were transfected with Lipofectamine2000 (Invitrogen, Germany) in 60 mm cell culture dishes. ES cells were further handled as described for culture cell lines. For selection for stably integrated neomycin resistance genes, G418 was added to the culture medium in a concentration of 350 µg/ml.

3.4 Fixation of cells

3.4.1 Methanol / Acetone fixation

Methanol and acetone were cooled down to -20°C. Cells grown on coverslips were washed twice in PBS with 2 mM MgCl₂ at room temperature and then fixed in ice cold methanol for 5 minutes. Cells were then transferred to acetone for 30 seconds and air dried.

3.4.2 Formaldehyde fixation

Fixation of cells with formaldehyde was used in order to better preserve the cell structure. Cells grown on coverslips were washed twice in PBS with 2 mM MgCl₂ at room temperature and then fixed for 7 minutes in ice cold 4% formaldehyde in PBS (pH 6.8). After fixation, cells were washed three times in PBS with 2 mM MgCl₂ and incubated in ice cold 0.1% Triton in PBS for 5 minutes. After permeabilization, cells were washed three times with PBS with 2 mM MgCl₂.

3.5 Indirect immunofluorescence

Coverslips with fixed cells were placed with the cell layer on the top side into a humid plastic chamber and incubated for 10 – 15 minutes with 10% goat serum in PBS to block unspecific antibody binding. After removal of the blocking solution, the cells were incubated with 20 μ l of the appropriate primary antibody adequately diluted in PBS for 30 – 60 minutes. Coverslips were rinsed in PBS with 2 mM $MgCl_2$ and afterwards put back into the humid incubation chamber. The secondary antibody was diluted in PBS. A total volume of 20 μ l was applied to the cells and incubated 30 – 60 minutes. Subsequently, DAPI stain was applied to the cells for 5 minutes. After rinsing three times in PBS with 2 mM $MgCl_2$, the coverslips were dipped briefly into ddH₂O and were either directly mounted or incubated for 1 minute in ethanol and air dried. Coverslips were mounted with Fluoromount G (SouthernBiotech, USA) on microscope slides. Slides were stored at 4°C.

3.5.1 Double immunolocalization

For simultaneous detection of two proteins in the same cell, the cells were prepared as described above. The two primary antibodies were selected to have no cross reactivity with each other, diluted and incubated together. The fluorescently labelled secondary antibodies were chosen in a way to have no overlapping emission spectra.

3.6 Confocal laser scanning microscopy

For a detailed 3D analysis, the cells were imaged with a LEICA TCS SPII confocal laser scanning microscope. The used fluorophores were excited using the respective laser in combination with the filter of the suitable wavelength. The fluorescence signal was detected using a photomultiplier (PMT). The detection range was adjusted manually. Before imaging, the offset of each PMT was controlled. During imaging the photomultiplier setting was constantly at 750 Volt and the laser excitation was minimized to keep photobleaching at a minimum and to avoid oversaturation of the images. The pinhole was constantly kept at 1 Airy. All images were made with the 63x/1.3 oil objective. The digital images were processed using Adobe Photoshop (Adobe, San Jose, CA), ImageJ software, or Leica LSM software, respectively.

Table 7: Laser lines of the Leica TSC SPII confocal microscope

laser type	wavelength (nm)	fluorochromes and respective excitation (nm)
diode laser	405	DAPI (405)
cadmium laser	443	CFP (443)
argon laser	458, 478, 488, 514	GFP (488), Alexa 488 (488), YFP (514)
helium neon laser	543	Cy 3 (543), Alexa 568 (543/561)
helium neon laser	633	Cy 5 (633)

3.7 Protein techniques

3.7.1 Protein extraction of heart muscle tissue

Frozen heart muscle tissue was disrupted and homogenized in ice cold lysis buffer (20 mM Tris/HCl, pH 7.4, 1% Triton X-100, 10% glycerol, 150 mM NaCl, 1 mM PMSF, 1 µg/ml leupeptin, 1 µg/ml antipain, 1 µg/ml chymostatin, 1 µg/ml pepstatinA) and subjected to SDS-PAGE.

3.7.2 Differential protein extraction

All volumes are adjusted for protein extraction from a 10 cm cell culture dish. Confluently grown cells were washed twice with PBS with 25 µM pefabloc and 76 mM PMSF. Subsequently, cells were incubated in 1 ml lysis low buffer (50 mM MOPS, 10 mM EGTA, 100 mM MgCl₂, 0.02% NP-40, 2.85 mM PMSF, 0.5 mM pefabloc in 0.5x PBS) at room temperature for 2 minutes. The supernatant was removed and a 200 µl sample of it was boiled in 100 µl 3x Laemmli sample buffer for 3 minutes (fraction 1: soluble and extractable cytoplasmic proteins). The remaining buffer was discarded. The cells were then incubated in 1 ml ice cold lysis high buffer (50 mM MOPS, 100 mM MgCl₂, 0.1% NP-40, 2.85 mM PMSF, 0.5 mM pefabloc, 0.25 mg/ml DNase in 0.5x PBS) on ice for 3 minutes and were carefully resuspended from time to time. 200 µl 5 M NaCl were added and incubated for another 3 minutes. The cells were scraped off the dishes with a rubber policeman and transferred to an eppendorf tube. A 100 µl sample was taken from the cell lysate and mixed with 100 µl ddH₂O and 100 µl 3x Laemmli sample buffer and was boiled for 3 minutes (fraction 2: cytoskeletal fraction). The remaining cell lysate was centrifuged at 13.000 rpm and 4°C for 15 minutes. Subsequently, 100 µl supernatant were removed and mixed with 100 µl

ddH₂O and 100 µl 3x Laemmli sample buffer (fraction 3: high-salt and high-detergent soluble cytoskeletal fraction). The sample was then boiled for 3 minutes. The cell pellet was resuspended in 200 µl 3x Laemmli sample buffer with 600 mg/ml urea and was boiled for 3 minutes (fraction 4: insoluble cytoskeleton proper).

3.7.3 Western blot

Western blotting is a method used for the qualitative and quantitative detection of proteins using specific antibodies. Proteins, e.g. from cell extracts, are first separated by SDS-PAGE, then transferred to a PVDF membrane, and the proteins are subsequently detected with specific antibodies.

3.7.3.1 Discontinuous polyacrylamide gel electrophoresis (SDS-PAGE)

For SDS-PAGE under reducing conditions, gel solutions with 10% acrylamide in the resolving part were prepared using an acrylamide/bis-acrylamide solution (37.5:1). Protein samples were boiled for 5 minutes in Laemmli sample buffer and were loaded onto the gel together with a protein size marker (Broad Range 7701S; New England Biolabs, Germany). Electrophoresis was run at 25 mA without restriction of the impressed voltage.

Table 8: Composition of 10% acrylamide gels (adequate volume for 5 minigels)

Stacking gel		Resolving gel	
acrylamide	1.32 ml	acrylamide	10 ml
ddH ₂ O	6.2 ml	ddH ₂ O	13 ml
upper Tris	2.5 ml	lower Tris	7.5 ml
10% APS	0.1 ml	10% APS	0.3 ml
10% TEMED	0.1 ml	10% TEMED	0.3 ml

After electrophoresis, the gel was either stained with Coomassie staining solution or was soaked in borate transfer buffer for Western blot analysis.

3.7.3.2 Transfer of proteins to PVDF membranes and detection

Electrophoretic transfer of proteins from polyacrylamide gels to a polyvinylidene fluoride (PVDF) membrane was performed by use of a wet blot apparatus. The membrane was briefly activated in 100% ethanol and soaked in borate transfer buffer for 10-15 minutes. Transfer was carried out for 2 hours at 500 mA at room temperature. After the transfer, the membrane was stained with Ponceau-S in order to verify the transfer efficiency and was subsequently dried or directly used for protein detection.

For protein detection with antibodies, the activated membrane was incubated in blocking solution (TBST, 5% non-fat milk powder) for 1 hour at room temperature or over night at 4°C on a rocking platform. The membrane was then incubated with the primary antibody (diluted in blocking solution according to Table 5) for 1 hour at room temperature. To remove unbound antibody, the membrane was washed three times in TBST and was subsequently incubated with the secondary antibody conjugated to horse radish peroxidase (HRP) for 1 hour at room temperature. After washing the membranes three times in TBST, the membrane was incubated in ECL (Enhanced Chemiluminescence) solution (NEN, Germany) according to the manufacturer's instructions. The solution was drained off the membrane and the membrane was exposed to an X-ray film (Kodak X-OMAT AR5) which was subsequently developed.

3.7.4 Immunoprecipitation

For immunoprecipitation, 50 µl protein G sepharose beads were washed three times in ice cold PBS. 50 µl beads were either incubated with 1 ml α-lamin B2 antibody (X223) or with 1 ml cell lysate in IP buffer (50 mM MOPS, 100 mM MgCl₂, 0.4% Triton X-100, 2.85 mM PMSF, 0.5 mM pefabloc, 0.25 mg/ml DNase in 0.5x PBS) for 1 hour. Antibody coated beads were washed twice with ice cold PBS and once with IP buffer and were subsequently incubated either with the precleared cell lysate or IP buffer in a final volume of 1 ml. Immunoprecipitation was carried out in an overhead rotator for 2 hours. Beads were washed three times with ice cold IP buffer and twice with ice cold PBS and were resuspended in 40 µl 3x Laemmli loading buffer. All steps were performed at 4°C.

Proteins were isolated from the beads and denatured by boiling for 5 minutes and separated by SDS-PAGE. After electrophoresis, the gel was either stained with Coomassie staining solution or was processed for Western blot analysis.

4 Results

4.1 Influence of lamin B2 deletion mutants

We wanted to investigate the mechanism of lamin *in vivo* assembly, its influences on nuclear morphology, and its behavior during mitosis. Therefore we generated a series of lamin B2 deletion mutants and tested the influence of the expression of these mutant proteins on nuclear morphology in several cell lines, including U2OS, HeLa, SW13 and mouse embryonic stem (ES) cells. In Figure 5 a schematic overview of the lamin B2 deletion mutants evaluated in this thesis is given.

By recombinant DNA technology we removed either a part of the head domain (first 32 amino acids, $\Delta 32$ head), the complete head domain (headless), or the tail domain (tailless). In one case both, the first 32 amino acids of the head domain and the tail domain have been removed ($\Delta 32$ head/tailless). Another mutant represents the rod domain (Walther et al). All protein coding sequences were constructed as N-terminal fusions with spectral variants of the green fluorescent protein (GFP). The detailed description of the cloning strategy of the expression plasmids is presented in section 3.2.

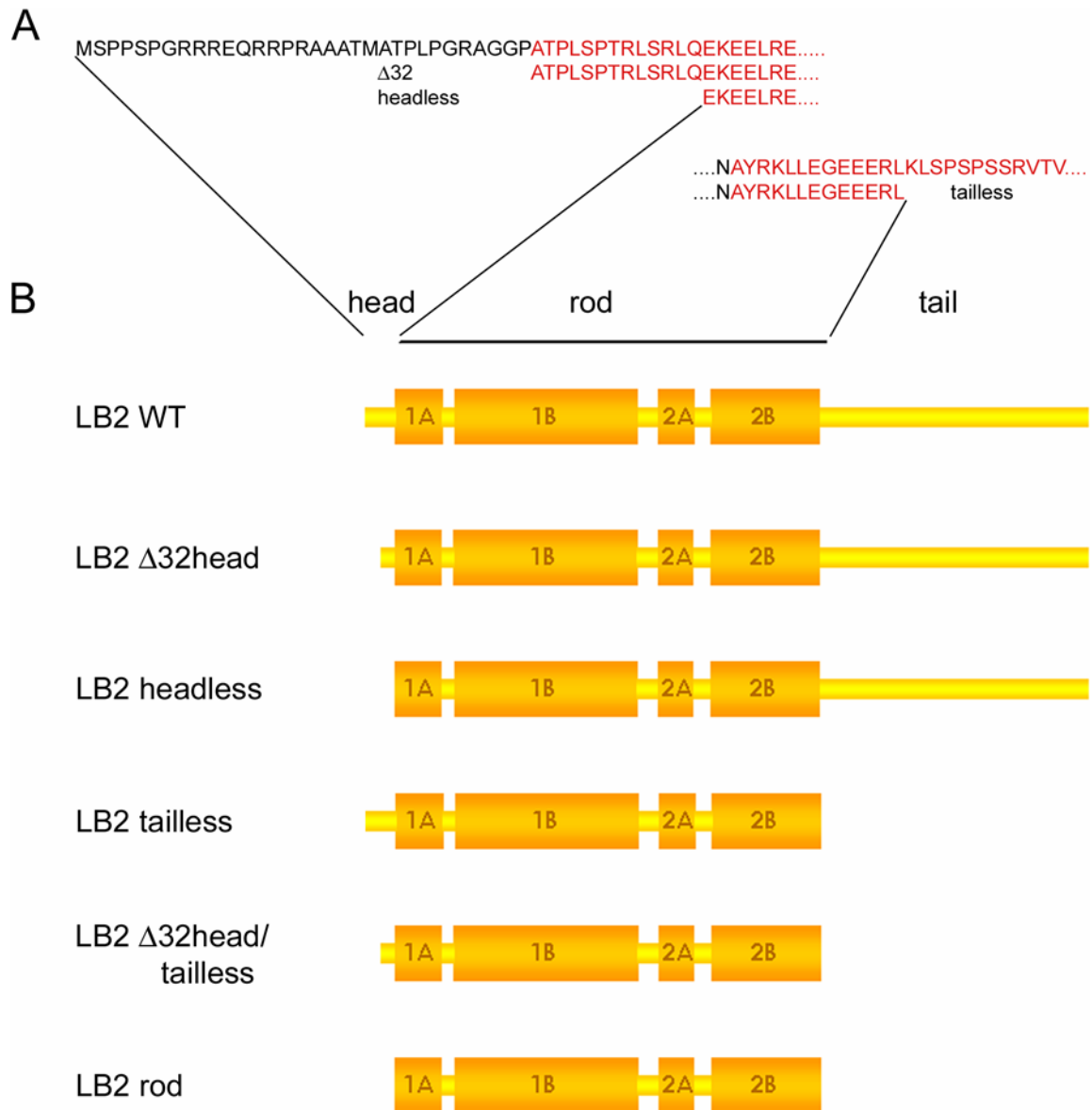


Figure 5: Diagram showing the domain structure of lamin B2 and the generated deletion mutants. (A) Amino acid sequences of the complete N-terminus and two progressively deleted mutants and of the C-terminal end of coil 2B with part of the tail domain and a tail deleted mutant. Conserved sequences are depicted in red. (B) Schematic overview of generated lamin B2 deletion mutants.

4.1.1 Lamin B2 head deletions

In order to investigate the influence of the lamin head domain on cellular localization and morphology, U2OS, HeLa and SW13 cells were transfected with YFP-tagged lamin B2 $\Delta 32$ head and lamin B2 headless expression plasmids, respectively. After 48 hours of incubation, cells were fixed and analyzed by confocal laser scanning microscopy (CLSM). Although lamin B2 headless is devoid of a conserved

sequencethat is still present in lamin B2 Δ 32head both mutants showed the same effects. In U2OS cells, both YFP-lamin B2 Δ 32head protein (Figure 6 A + A') and YFP-lamin B2 headless (Figure 6 B + B') became localized at the nuclear rim which was identified as the boundary of the DAPI staining region, but were also massively present in a dot-like distribution throughout the nucleoplasm (Figure 6). Furthermore, the nuclei were highly lobulated and irregularly shaped. Overall chromatin distribution was not altered (Figure 6 A' + B'). Expression of the mutant proteins did not interfere with cell cycle progression and mitosis (data not shown). Transfection of HeLa and SW13 cells showed similar results. These observations suggest that the lamin B2 head domain is dispensable for nuclear envelope localization of the lamin B2 protein. However, its incorporation into the nuclear lamina appears to be less efficient and if integrated interferes with proper lamina assembly.

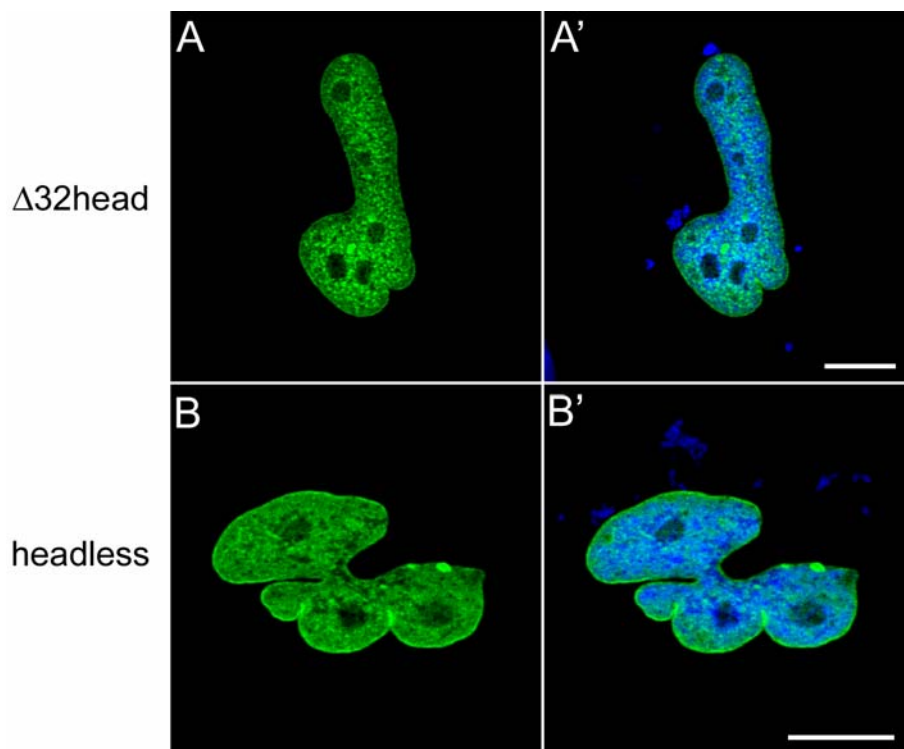


Figure 6: Patterns of YFP-lamin B2 Δ 32head and YFP-lamin B2 headless transiently transfected in U2OS cells. (A) U2OS cell expressing YFP-lamin B2 Δ 32head, (B) U2OS cell expressing YFP lamin B2 headless, (A', B') double staining with DAPI. Extranuclear DAPI staining represents DNA which was not taken up by the cells and is often observed upon transfection of cells with FuGene6. All images are confocal sections. Bars 10 μ m.

4.1.2 Lamin B2 tail deletions

The influence of the lamin tail domain on cellular localization and nuclear morphology of U2OS, HeLa and SW13 cells was studied by transient transfection with lamin B2 tailless, lamin B2 Δ 32head/tailless or lamin B2 rod YFP-expression plasmids. All constructs are devoid of the NLS, which is in the tail domain. Confocal microscopic analysis revealed that YFP-lamin B2 tailless protein was distributed throughout the nucleoplasm and the cytoplasm (Figure 7 A). The cytoplasmic signal appeared as a rather filamentous structure. Localization to the nuclear rim could not be observed. DAPI staining showed that nuclear shape was not impaired by the mutant protein, neither was chromatin distribution altered (Figure 7 A'). Mutants lacking either part of the head domain and the tail domain (LB2 Δ 32head/tailless) (Figure 7 B + B') or the complete head domain and the tail domain (LB2 rod) (Figure 7 C + C') displayed the same phenotype as the tail domain deletion alone. Both mutant proteins were distributed throughout the nucleoplasm and formed filament-like structures in the cytoplasm. Expression of YFP-lamin B2 tail deletion mutants in SW13 and HeLa cells exhibited the same effects as observed in U2OS cells. Although tailless mutants are devoid of the NLS, nucleoplasmic distribution could be observed. We explain this by the presence of a conserved sequence motif at the end of coil 2 of the α -helical rod domain mediating nuclear localization (Rogers et al, 1995). Hence, the tail domain was necessary to direct ectopic lamin B2 protein to the nuclear envelope. This experiment clearly demonstrates further that the endogenous wild type lamin B2 is not able to recruit the mutant proteins to the nuclear lamina.

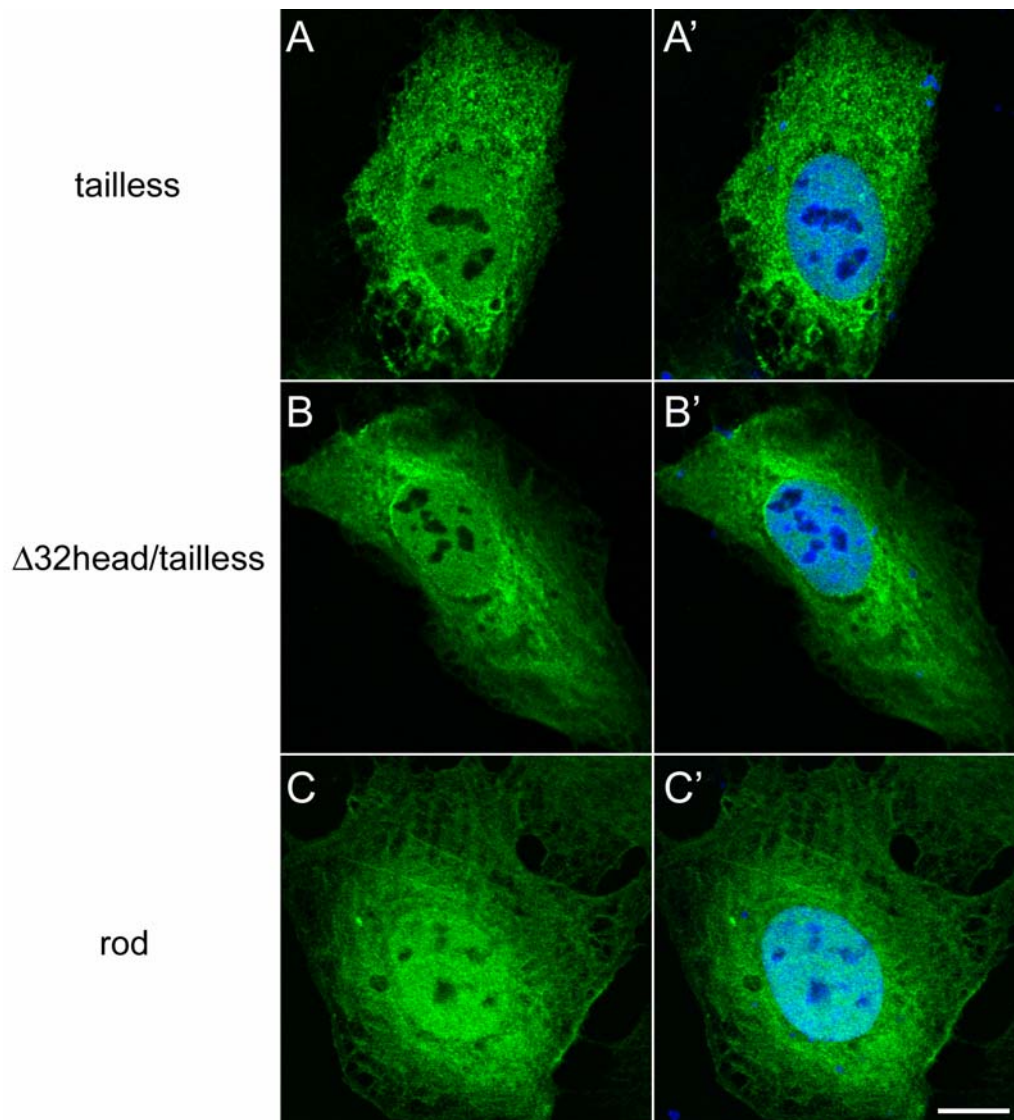


Figure 7: Patterns of YFP-lamin B2 tailless, YFP-lamin B2 $\Delta 32$ head/tailless and YFP-lamin B2 rod transiently transfected in U2OS cells. U2OS cells expressing (A) YFP-lamin B2 tailless, (B) YFP-lamin B2 $\Delta 32$ head/tailless, and (C) YFP-lamin B2 rod (all shown in green). (A', B', C') double staining with DAPI. All images are confocal sections. Bar 10 μ m.

4.1.3 Effects of lamin B2 deletion mutants on the endogenous lamina

To evaluate the effects of the head and/or tail deletions on the integrity of the nuclear lamina, U2OS cells were fixed 48 hours post transfection with the respective YFP-expression plasmids and were stained with antibodies specific for lamin B2 or lamin A/C. Immunofluorescence was analyzed by confocal microscopy. Lamin B2 antibody staining co-localized with the YFP-signal of all tailless mutants in the nucleoplasm and the cytoplasm but additionally showed the expected rim stain (Figure 8). With the lamin B2 antibody used it was not possible to distinguish between endogenous lamin B2 and exogenous mutant lamin B2. It can thus not be excluded that at least part of the endogenous lamin B2 also localized to the cytoplasm and the nucleoplasm.

Endogenous lamin A/C localization at the nuclear rim was not affected by any of the mutants except for YFP-lamin B2 tailless (Figure 9). In cells expressing this mutant, lamin A/C localized to the nuclear rim, but was also present in the cytoplasm (Figure 9 D, see insert). The cytoplasmic lamin A/C staining was rather weak and co-localized with the YFP signal of the tail deletion mutant. Since synthesis and posttranslational processing of lamins take place in the cytoplasm it is conceivable that newly synthesized lamin A forms heteropolymers with the mutant lamin B2 protein in the cytoplasm. This observation suggests that the lamin B2 head domain is necessary for the formation of heteropolymers with lamin A. This experiment clearly demonstrates further that a functional lamina can be built up in the presence of tailless lamin B2 mutants.

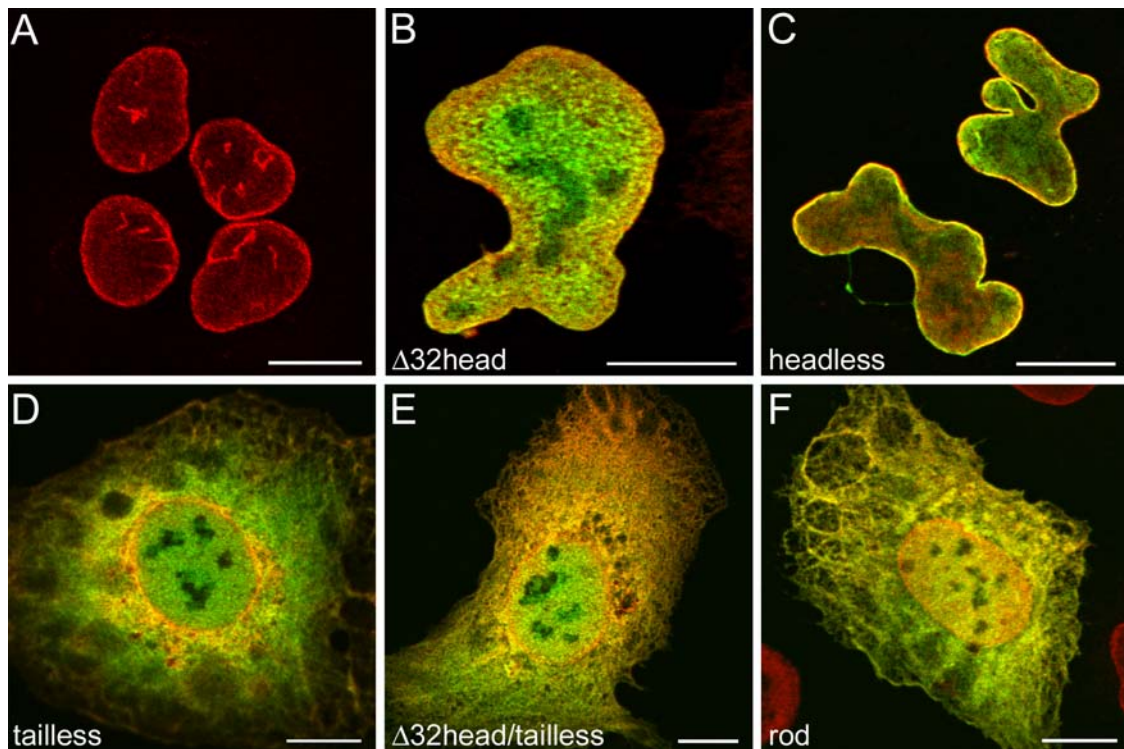


Figure 8: Double labeling of YFP-lamin B2 deletion mutants and lamin B2. Confocal sections of U2OS cells (A) untransfected, expressing (B) YFP-lamin B2 $\Delta 32$ head, (C) YFP-lamin B2 headless, (D) YFP-lamin B2 tailless, (E) YFP-lamin B2 $\Delta 32$ head/tailless, (F) YFP-lamin B2 rod (all shown in green), stained with an antibody specific for lamin B2 (red). Bars 10 μ m.

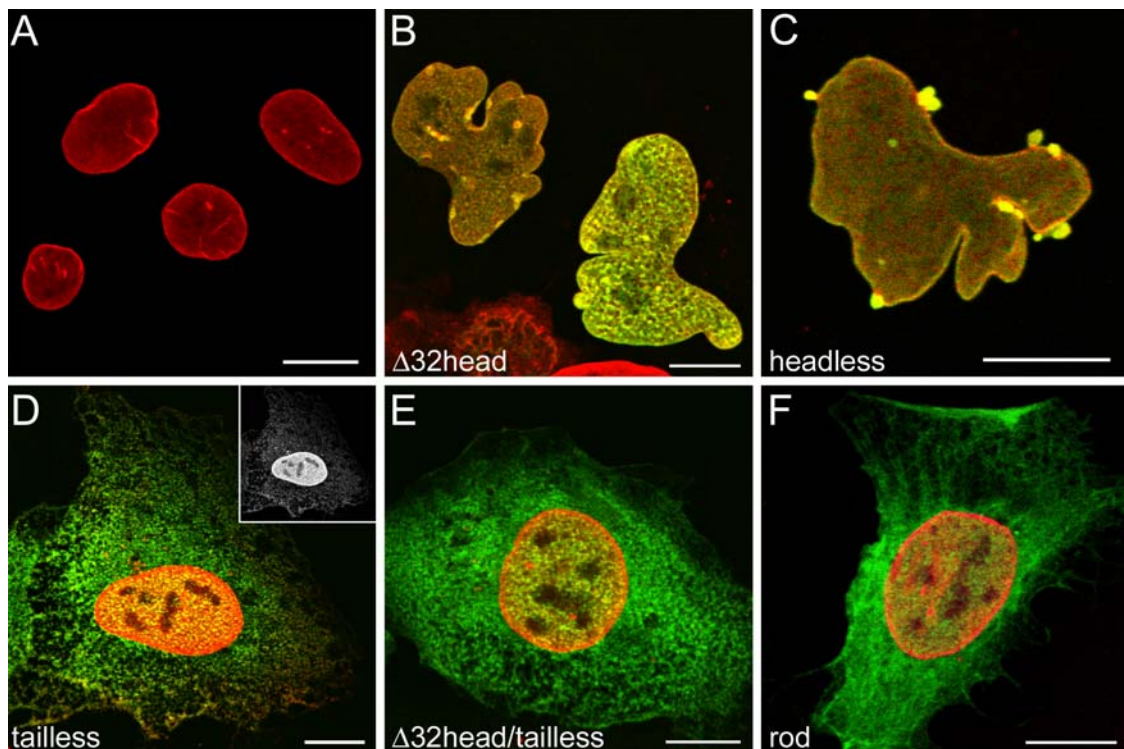


Figure 9: Double labeling of YFP-lamin B2 deletion mutants and lamin A/C. Confocal sections of U2OS cells (A) untransfected, expressing (B) YFP-lamin B2 $\Delta 32$ head, (C) YFP-lamin B2 headless, (D) YFP-lamin B2 tailless, (E) YFP-lamin B2 $\Delta 32$ head/tailless, (F) YFP-lamin B2 rod (all shown in green), stained with an antibody specific for lamin A/C (red). Bars 10 μ m.

4.1.4 Effect of lamin B2 deletion mutants on endogenous NE proteins

Lamins have been shown to interact with several integral membrane proteins of the inner nuclear membrane (Gruenbaum et al, 2003). To study the effects of the lamin head and/or tail deletions on the organization of inner nuclear membrane proteins in the nuclear envelope, U2OS cells were fixed 48 hours post transfection with the respective YFP-expression plasmids and were stained with antibodies specific for LBR (Figure 10) or emerin (Figure 11). LBR localization was not disturbed by any of the tailless lamin B2 mutants (Figure 10 D, E, F). However, in cells expressing YFP-lamin B2 Δ 32head and YFP-lamin B2 headless LBR was indeed mainly localized at the nuclear envelope but was in addition massively found at the ER (compare Figure 10 A to B + C). This suggests that incorporation of headless lamin B2 mutants into the nuclear envelope interferes with proper nuclear envelope organization and thus leads to a redistribution or retention after synthesis of LBR in the ER. In contrast, emerin distribution was not influenced neither by the presence of head deleted lamin mutants nor by tail deleted lamin mutants (Figure 11).

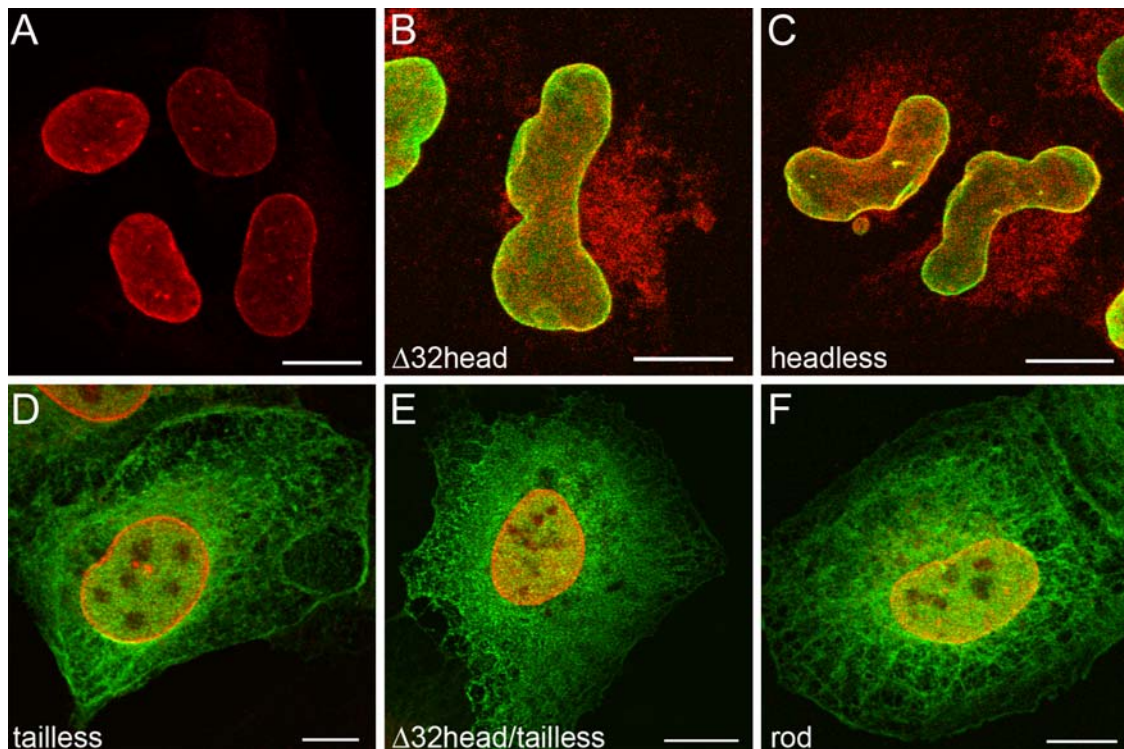


Figure 10: Double labeling of YFP-lamin B2 deletion mutants and LBR. Confocal sections of U2OS cells (A) untransfected, expressing (B) YFP-lamin B2 $\Delta 32$ head, (C) YFP-lamin B2 headless, (D) YFP-lamin B2 tailless, (E) YFP-lamin B2 $\Delta 32$ head/tailless, (F) YFP-lamin B2 rod (all shown in green), stained with an antibody specific for LBR (red). Bars 10 μ m.

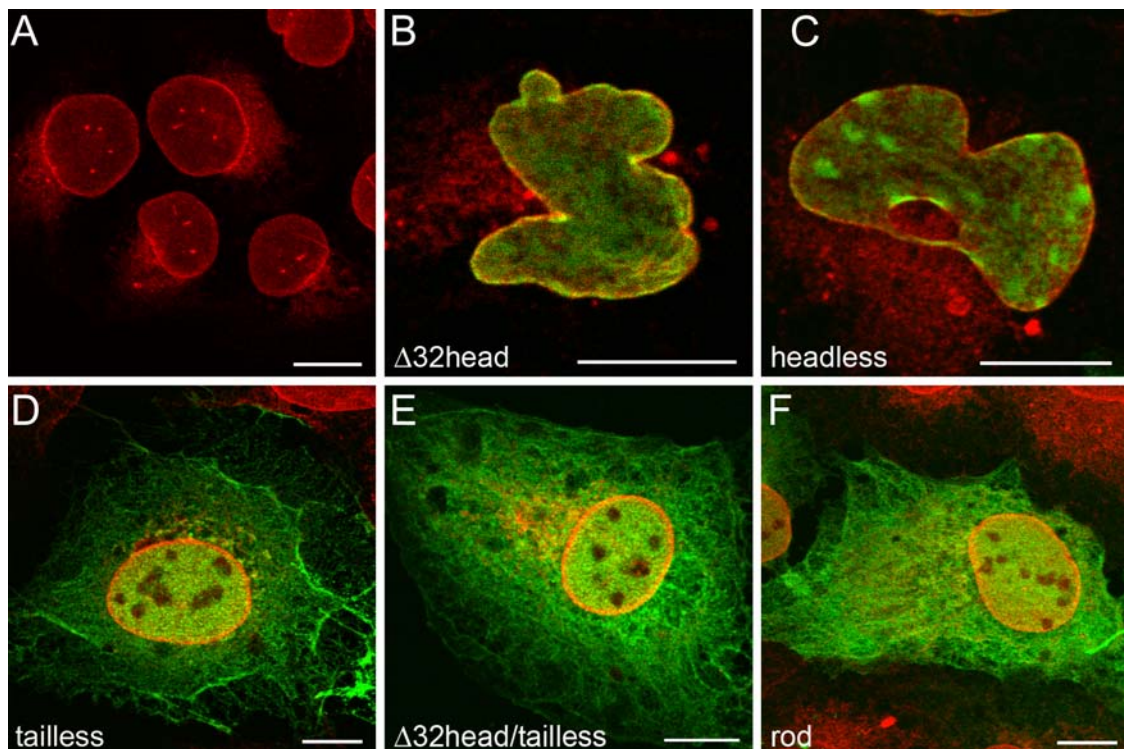


Figure 11: Double labeling of YFP-lamin B2 deletion mutants and emerin. Confocal sections of U2OS cells (A) untransfected, expressing (B) YFP-lamin B2 $\Delta 32$ head, (C) YFP-lamin B2 headless, (D) YFP-lamin B2 tailless, (E) YFP-lamin B2 $\Delta 32$ head/tailless, (F) YFP-lamin B2 rod (all shown in green), stained with an antibody specific for emerin (red). Bars 10 μ m.

4.1.5 Biochemical characterization of lamin B2 deletion mutants

U2OS cells were transfected 48 hours prior to differential protein extraction (see section 3.7.1). The transfection efficiency was estimated to be 70-90%. The gained fractions 1-4 were subjected to SDS-PAGE in aliquot amounts and were analyzed in a Western blot by using an antibody specific for lamin B2 (Figure 12). In extracts of cells expressing YFP-lamin B2 wild type (WT) both, YFP-lamin B2 WT and endogenous lamin B2 protein were detectable in cytoskeletal fractions 2 and 4 (Figure 12 A). In cell extracts of YFP-lamin B2 Δ 32head (Figure 12 B) and YFP-lamin B2 headless (Figure 12 C) expressing cells the mutant protein was primarily detectable in fractions 2-4. However, a weak signal could also be detected in fraction 1 indicating that a small amount of the mutant protein is cytoplasmic. It can be concluded that partial or complete deletion of the head domain of lamin B2 increases the solubility of the protein. Endogenous lamin B2 protein was primarily detectable in fractions 2 and 4 and to a smaller extent also in fraction 3 (Figure 12 B + C). Thus, expression of lamin B2 head deletion mutants increases the solubility of endogenous lamin B2 protein. The relative amount of the YFP-tagged fusion proteins was several folds higher than that observed for endogenous lamin B2 protein.

Western blot analysis of extracts of cells expressing YFP-lamin B2 tailless (Figure 12 D) and YFP-lamin B2 rod (Figure 12 E) revealed that the mutant proteins could not be separated from endogenous lamin B2 by the SDS-PAGE system used. It is thus not possible to make a statement about the solubility of tail deleted lamin B2 mutants and its influence on endogenous lamin B2 protein. The lower band detected in the Western blots most likely represents a degradation product as it was also detected by an antibody specific for GFP (data not shown).

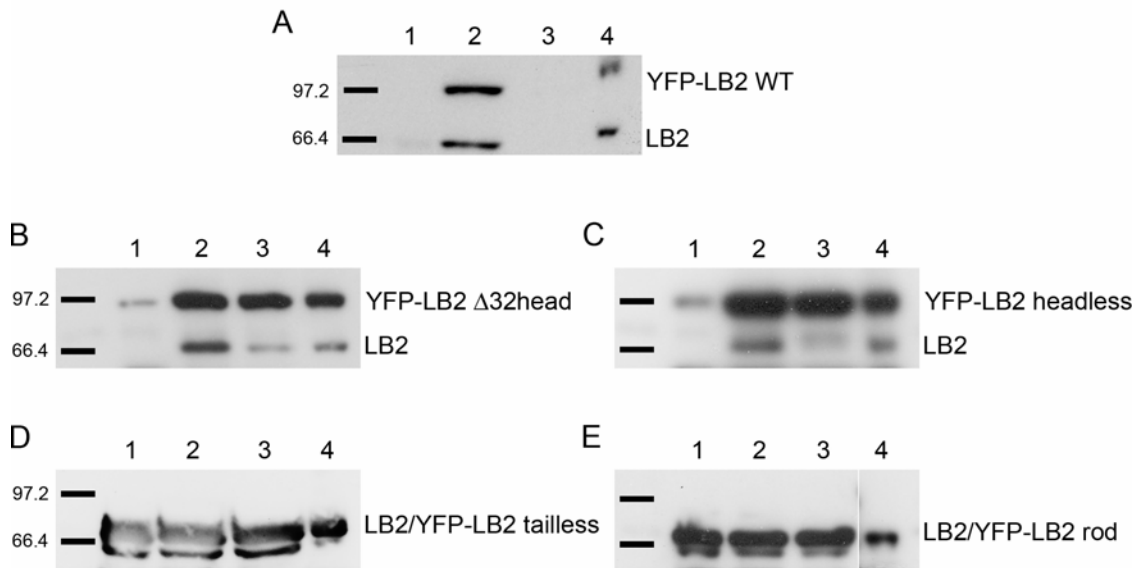


Figure 12: Western blot analysis of differentially extracted fractions from U2OS cells expressing YFP-lamin B2 deletion mutants using an antibody specific for lamin B2. Extracts of U2OS cells expressing (A) YFP-lamin B2 WT, (B) YFP-lamin B2 Δ 32head, (C) YFP-lamin B2 headless, (D) YFP-lamin B2 tailless, (E) YFP-lamin B2 rod. Lane 1, soluble and extractable cytoplasmic proteins, lane 2, total cytoskeletal fraction, lane 3, high-salt and high-detergent soluble cytoskeletal fraction, lane 4, insoluble cytoskeleton proper. It should be considered that the signal intensities of the different immunoblots can not be compared directly, since the exposure times of the X-ray film varied between cell preparations.

4.1.6 Expression of lamins in mouse embryonic stem (ES) cells

Mouse embryonic stem cells are derived from the inner cell mass of the blastocyst stage of the embryo. They possess a unique characteristic distinguishing them from other cells: They have the dual abilities to self-renew and give rise to new pluripotent ES cells, and to differentiate into all specialized cell types found in the adult mouse. A further feature of ES cells is their exhibition and maintenance of a full (diploid), normal complement of chromosomes. In order to study localization of YFP-tagged wild type lamin B1 or lamin B2 respectively, and their influences on nuclear morphology, ES cells were transiently transfected with the respective expression plasmids. Before fixation, cells were dissociated into single cells and transferred on matrigel-coated coverslips, and were allowed to settle. Confocal microscopic analysis showed that both YFP-lamin B2 (Figure 13 A) and YFP-lamin B1 (Figure 13 C) protein localized to the nuclear rim as expected. However, the thickness of the nuclear envelope varied between cells, in some cells appearing as a rather thick structure. Chromatin distribution as revealed by DAPI staining remained unaffected.

In order to study the fate of ES cells stably expressing YFP-lamin B1 or YFP-lamin B2, respectively, stable cell lines were generated as described in 3.3.5.2 and were analyzed by confocal microscopy. Both, lamin B2 (Figure 13 B) and lamin B1 (Figure 13 D) YFP fusion proteins localized to the nuclear rim as observed after transient transfection of the respective expression plasmid. Stably expressing cells showed no variation in the thickness of the nuclear envelope. Also chromatin distribution was not affected as revealed by DAPI staining. ES cells stably expressing YFP-lamin B2 or YFP-lamin B1 did not show a higher tendency to differentiate when compared to untransfected cells as analyzed by morphological criteria.

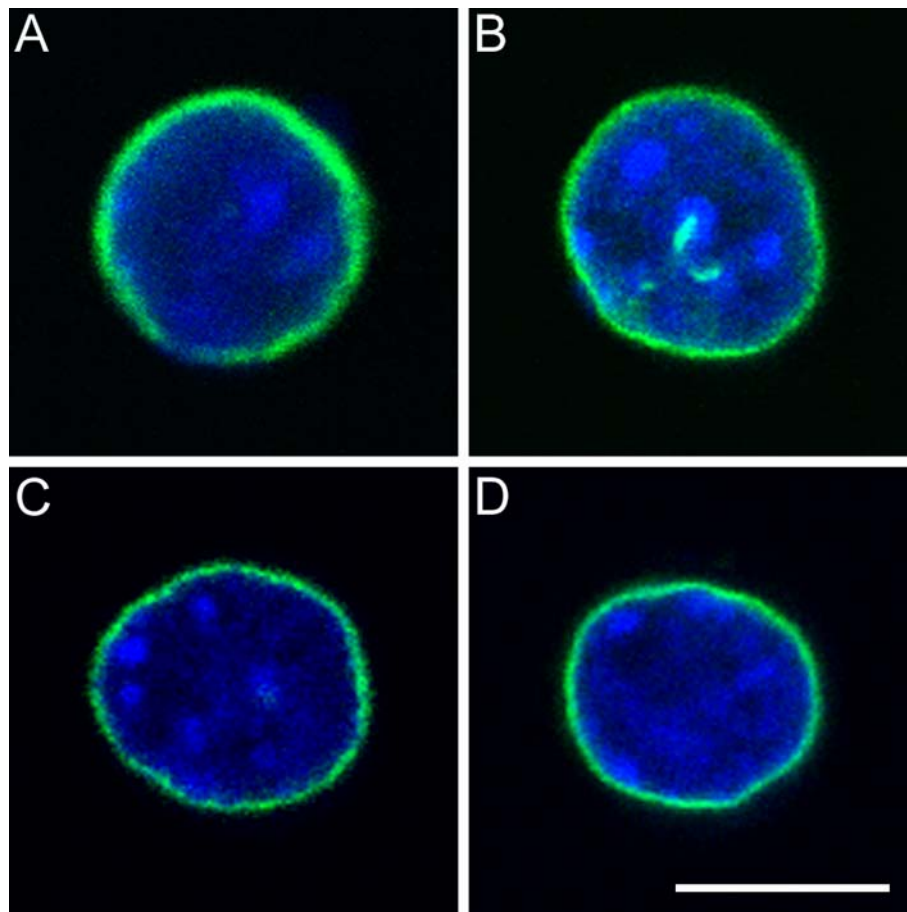


Figure 13: Patterns of YFP-lamin B2 and YFP-lamin B1 in mouse ES cells. (A+B) localization of YFP-lamin B2 in (A) transiently transfected and (B) stably expressing ES cells (shown in green). (C+D) localization of YFP-lamin B1 in (C) transiently transfected and (D) stably expressing ES cells (shown in green). DAPI staining is shown in blue. All images are confocal sections. Bar 5 μ m.

4.1.7 Effects of lamin B2 head and/or tail deletion on their cellular localization and nuclear morphology in ES cells

To evaluate the effects of lamin B2 head and/or tail deletions on their cellular localization and nuclear morphology in ES cells, cells were transfected with the respective expression plasmids and were transferred to matrigel-coated coverslips 44-48 hours thereafter.

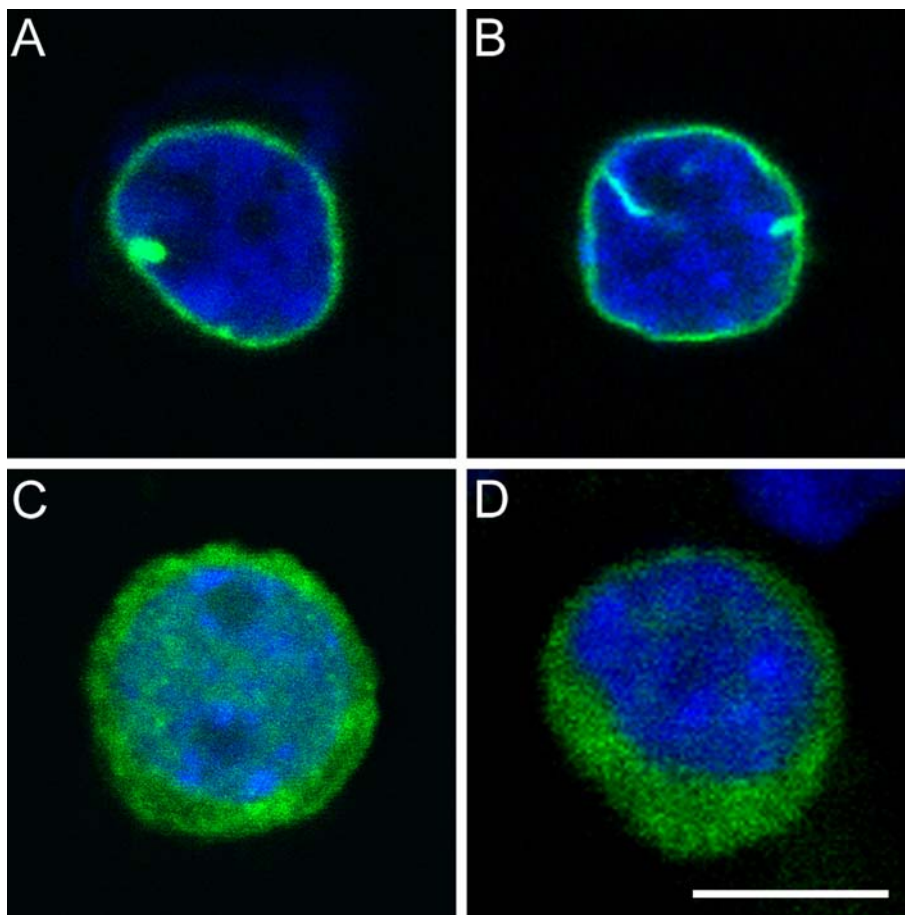


Figure 14: Patterns of YFP-lamin B2 deletion mutants in ES cells. (A) YFP-lamin B2 $\Delta 32$ head, (B) YFP-lamin B2 headless, (C) YFP-lamin B2 tailless, (D) YFP-lamin B2 rod (all shown in green). DAPI staining is shown in blue. All images are confocal sections. Bar 5 μ m.

The YFP-lamin B2 $\Delta 32$ head mutant localized to the nuclear rim, as seen in confocal mid-sections (Figure 14 A). In some cells the mutant protein formed single small aggregates along the nuclear lamina. Nuclear shape remained unaffected. ES cells transfected with the YFP-lamin B2 headless construct also showed a clear nuclear rim staining (Figure 14 B). Nuclei were slightly less regularly shaped and in some cells invaginations of the nuclear envelope were observed. The tailless lamin B2 mutants,

YFP-lamin B2 tailless (Figure 14 C) and YFP-lamin B2 rod (Figure 14 D), were both diffusely distributed throughout the nucleoplasm and the cytoplasm. Nuclear rim stain was not observed. All four lamin deletion mutants did not affect overall chromatin distribution as revealed by DAPI staining. These results demonstrate again that the head domain is dispensable for nuclear localization and integration of lamin B2 protein into the nuclear envelope of ES cells. In contrast, the tail domain is necessary for nuclear envelope localization and integration.

4.2 The effect of mutations at the phosphoacceptor sites of lamins

With the onset of mitosis, lamins become phosphorylated and the lamina disassembles. In order to study the fate of cells expressing lamin mutants permanently mimicking the mitotic phosphorylated state, several lamin B1 and lamin B2 mutants were generated. Thereby we aimed to study if a nuclear lamina can be built up in the presence of these lamin mutants. Here, the three mitotic Cdk1 phosphoacceptor sites flanking the rod domain in human lamin B1 and lamin B2 were changed from serine (S) to aspartic acid (D) by site-directed mutagenesis. In Figure 15 a schematic overview of the lamin B1 and lamin B2 S→D mutants evaluated in this thesis is given. All protein coding sequences were constructed as N-terminal fusions with spectral variants of the green fluorescent protein (GFP). For lamin B1 three different single mutants were generated, namely S23D, S391D, and S393D. For lamin B2 all single (S37D, S405D, S407D), double (S37+405D, S37+407D, S405+407D), and triple (S37+405+407D) mutants were generated. The detailed description of the cloning strategy of the expression plasmids is presented in section 3.2. In the following, lamin S→D mutants will be referred to as “mitotic” lamin mutants.

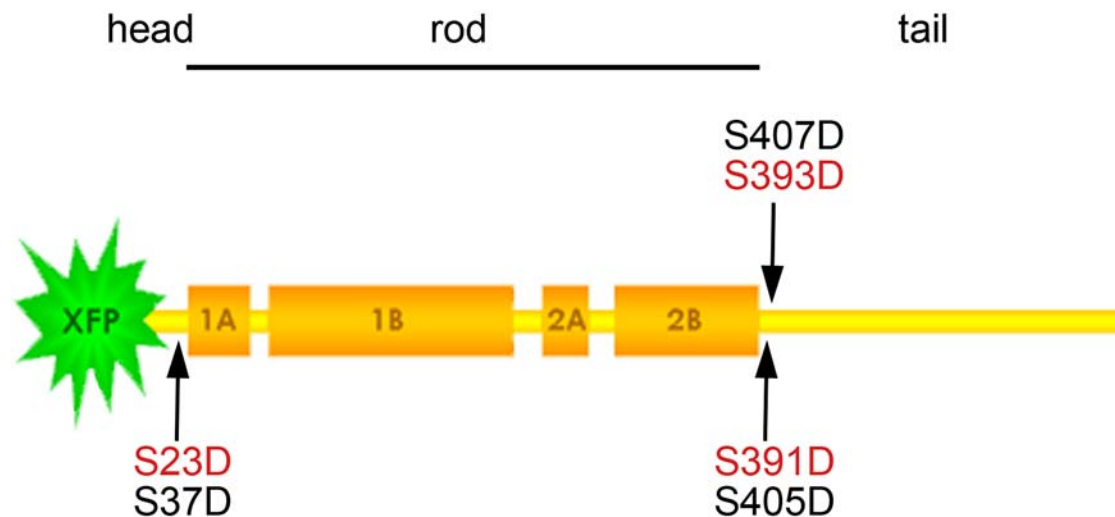


Figure 15: Schematic overview of mutated mitotic phosphoacceptor sites in lamins. Positions of amino acid exchanges are depicted in red for lamin B1 and in black for lamin B2, respectively.

4.2.1 Influence of mitotic lamin B2 mutants on nuclear localization and morphology

To evaluate the effects of lamin B2 mutants mimicking the phosphorylated state on localization and nuclear morphology, U2OS cells were transfected with the YFP-lamin B2 S407D expression plasmid and fixed 9 and 24 hours thereafter. In cells fixed after 9 hours, the mutant protein localized to intranuclear aggregates (Figure 16 A + B). In few cells, the mutant lamin protein localized to the nuclear rim, similar to wild type lamin B2 (Figure 16 C). In these cells, nuclear shape was impaired since nuclei were lobulated and showed invaginations of the nuclear lamina. After 24 hours, YFP-lamin B2 S407D also aggregated inside the nucleus, in most cells forming single large lamin territories (Figure 16 D – F). Some of these aggregations appeared to be attached to the nuclear envelope, whereas others were not as analyzed by confocal microscopy. Most of the aggregates were larger than those observed in cells fixed after 9 hours. Nuclear shape was not affected, neither after 9 hours nor after 24 hours.

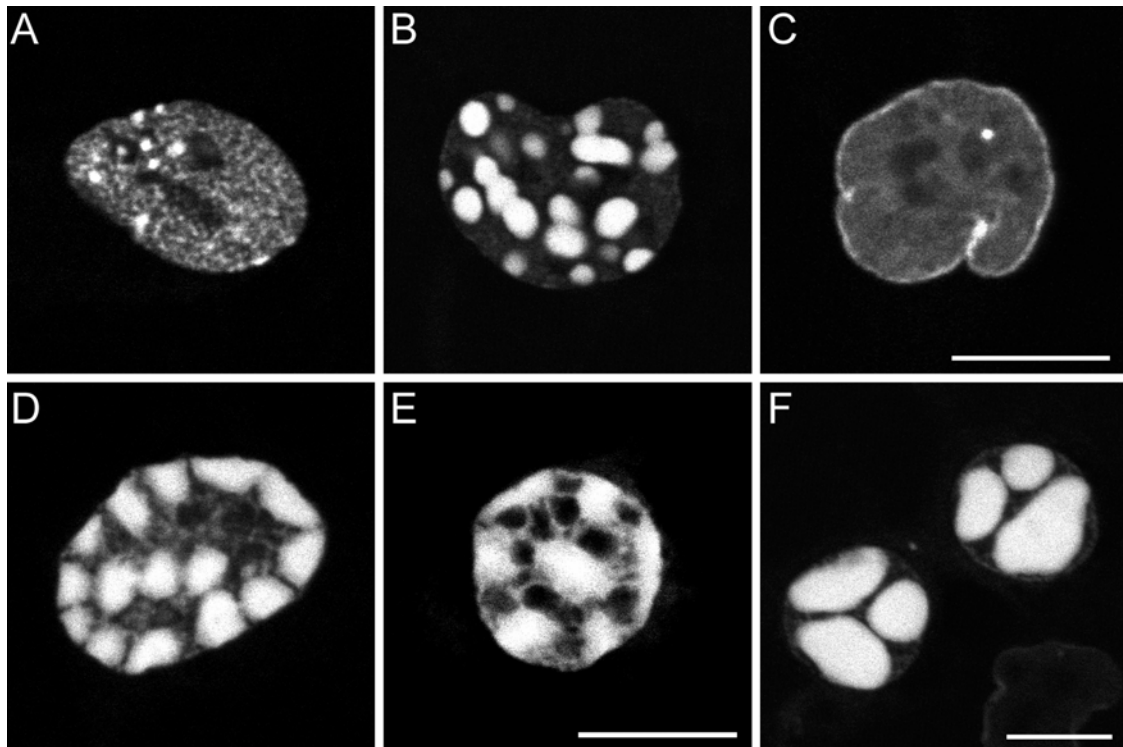


Figure 16: Pattern of YFP-lamin B2 S407D in U2OS cells. (A-C) cells fixed 9 hours post transfection, (D-F) cells fixed 24 hours post transfection. All images are confocal sections. Bars 10 μ m.

Cells transfected with YFP-lamin B2 S37D, S405D, S37+405D, S37+407D, S405+407D, or S37+405+407D expression plasmids were fixed 24 hours thereafter and analyzed by confocal microscopy (data not shown). Localization of all YFP-lamin B2 S \rightarrow D mutants was indistinguishable from the lamin S407D mutant. Thus, a single amino acid exchange on mitotic phosphorylation sites from serine to aspartic acid seems to be sufficient to cause intranuclear and membrane associated aggregation of the mutant protein. This effect was independent of both, the position of the mutated site and the number of mutated sites.

Long-term cultivation of transiently transfected cells under standard conditions showed that cells expressing "mitotic" lamin B2 mutants are viable and thus must be able to undergo mitosis (not shown).

4.2.2 Generation of stable cell lines

In order to characterize whether the large aggregations formed by lamin B2 proteins mutated from serine to aspartic acid in mitotic phosphoacceptor sites, are due to overexpression of the protein and if cells expressing these mutants are still able to undergo mitosis, stable U2OS cell lines were generated and analyzed by confocal microscopy (Figure 17). YFP-lamin B2 S37+407D protein localized to the nuclear rim, but also aggregated along the nuclear lamina and in the nucleoplasm (Figure 17 A + B). Aggregations varied in size, but were not as large as observed upon transient transfection. Due to the clone heterogeneity, in some cells localization of YFP-lamin B2 S37+407D was restricted to the nuclear rim (Figure 17 C + D). Nuclear shape was impaired by YFP-lamin B2 mimicking the phosphorylated state. Some nuclei were kidney-like shaped or were highly lobulated (Figure 17 A + B), whereas others showed large invaginations and had a donut-like shape (Figure 17 C + D).

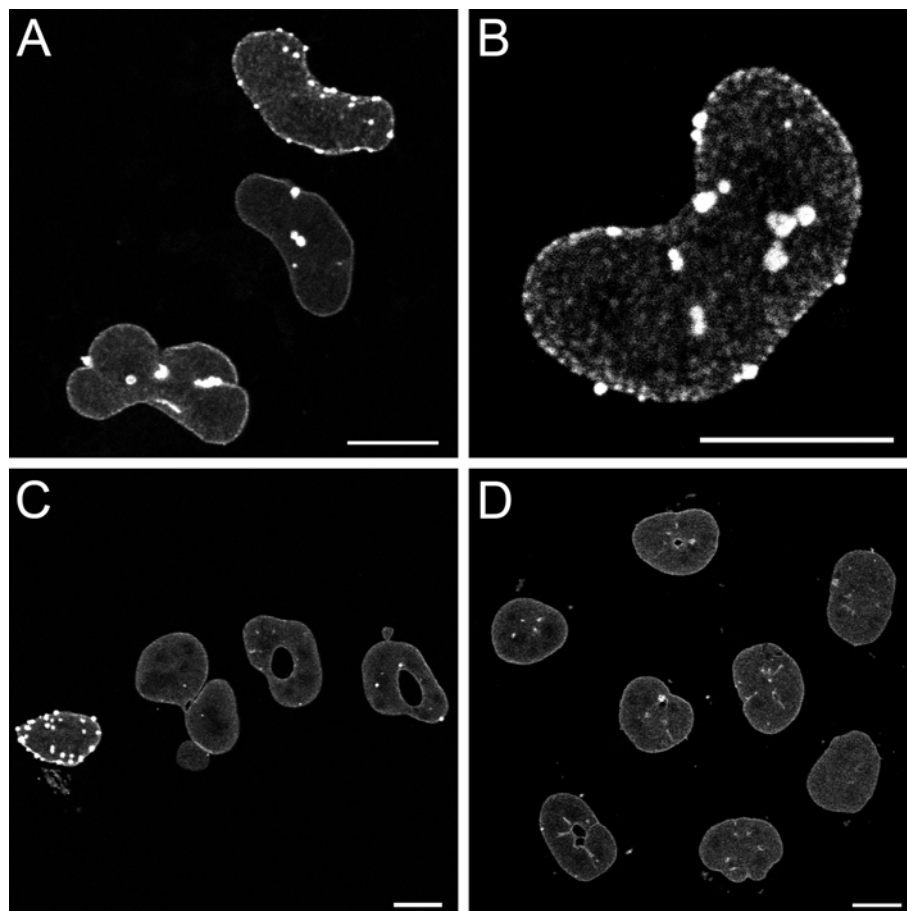


Figure 17: Confocal sections of U2OS cells stably expressing YFP-lamin B2 S37+407D. Bars 10 μ m.

4.2.3 Influence of “mitotic” lamin B1 mutants on nuclear localization and morphology

In man almost all cells express another B-type lamin besides lamin B2, namely lamin B1. To investigate the localization of transiently expressed lamin B1 mutated in mitotic phosphoacceptor sites from serine to aspartic acid, U2OS cells were transiently transfected with YFP-lamin B1 S23D, S391D, or S393D and were fixed 24 hours thereafter (Figure 18).

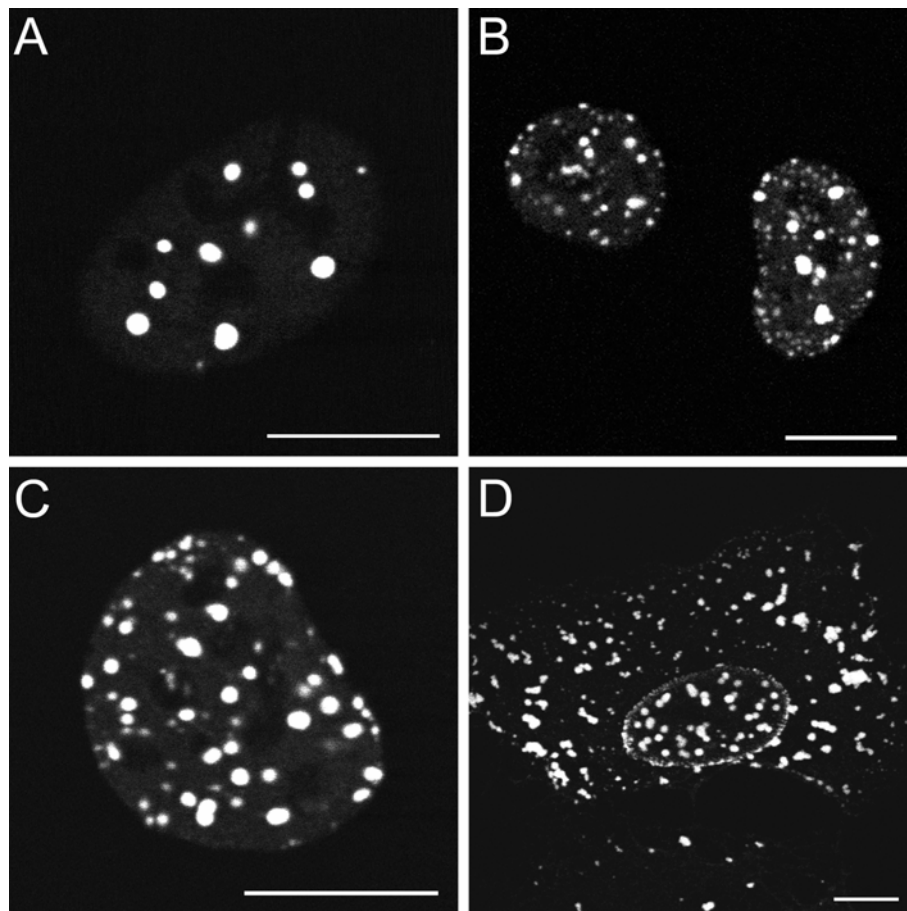


Figure 18: Patterns of YFP-lamin B1 mutated in mitotic phosphorylation sites from serine to aspartic acid in U2OS cells. Confocal sections of cells expressing (A) YFP-lamin B1 S37D, (B + D) YFP-lamin B1 S391D, (C) YFP-lamin B1 S393D. Bars 10 μm .

The YFP-lamin B1 S37D protein localized to intranuclear aggregates (Figure 18 A). These aggregates were generally smaller than those observed for lamin B2 mutated in the corresponding mitotic phosphoacceptor sites. YFP-lamin B1 S391D (Figure 18 B) and YFP-lamin B1 S393D (Figure 18 C) also localized to intranuclear aggregates. In some cells the YFP-lamin B1 S \rightarrow D protein accumulated and aggregated also in the

cytoplasm (Figure 18 D). The nuclear morphology was not affected. As observed for YFP-lamin B2 S→D mutants, localization of YFP-lamin B1 S→D protein was independent of the position of the mutated site.

4.2.4 Effect of “mitotic” lamin expression on the endogenous lamina

In order to study the effects of lamin B1 and lamin B2 mutated in mitotic phosphoacceptor sites on the integrity of the nuclear lamina, U2OS cells were fixed 16-18 hours post transfection with the respective expression plasmids and stained with antibodies specific for lamin B2 or lamin A/C (Figure 19). Since all “mitotic” lamin B2 mutants showed the same effects on nuclear localization and morphology representative examples will be shown in the following figures. “Mitotic” lamin B1 mutants will be proceeded the same way. In cells expressing YFP-lamin B2 S407D the endogenous lamin B2 was absent from the nuclear rim. Instead, it localized at the rim of the aggregates formed by the mutant protein (Figure 19 A). In contrast, endogenous lamin A/C was still present at the nuclear rim but was also, to some extent, recruited to the aggregates formed by the mutant lamin protein (Figure 19 B). In cells expressing YFP-lamin B1 S391D, nuclear rim localization of endogenous lamin B2 remained unaffected (Figure 19 C). The endogenous lamin A/C protein localized to the nuclear rim but also co-localized with the intranuclear aggregates formed by the mutant protein (Figure 19 D). The co-localization of lamin B2 and lamin B1 mutated in phosphoacceptor sites with lamin A/C suggests an interaction between these proteins that depends on the presence of the “mitotic” signal.

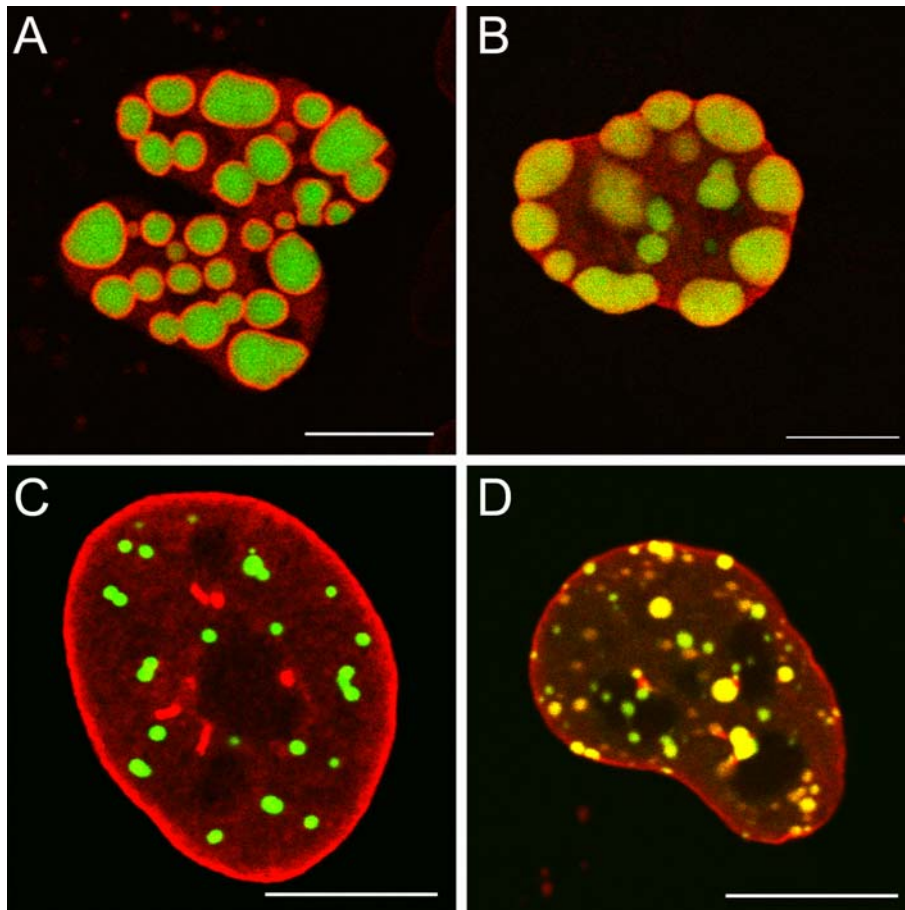


Figure 19: Double labeling of lamin B2 and lamin B1 phosphoacceptor mutants and nuclear lamins. Confocal sections of U2OS cells transfected with YFP-fusion proteins of lamin B2 S407D (A) or S37+405D (B) or lamin B1 S391D (C + D) (shown in green), and stained with antibodies specific for lamin B2 (A + C) or lamin A (B + D) (shown in red). Bars 10 μm .

4.2.5 Effect of “mitotic” lamin expression on endogenous NE proteins

In order to investigate if the distribution of inner nuclear membrane proteins was affected by the presence of “mitotic” lamin proteins, U2OS cells were fixed 16-18 hours post transfection with the respective expression plasmids and stained with antibodies specific for LBR, emerin, or Nup153 (Figure 20). In cells expressing YFP-lamin B2 S37+407D both, endogenous emerin and LBR were localized at the nuclear rim (Figure 20 A + B). However, rim staining was not homogeneously and was interrupted at sites of lamin aggregates that appeared to be attached to the nuclear envelope. Nup153 also localized to the nuclear rim as expected but in contrast to LBR and emerin was accumulated at sites of aggregates formed by the mutant protein (Figure 20 C).

Cells transfected with the YFP-lamin B1 S391D expression plasmid showed no alterations in LBR, emerlin, or Nup153 localization (Figure 20 E - F).

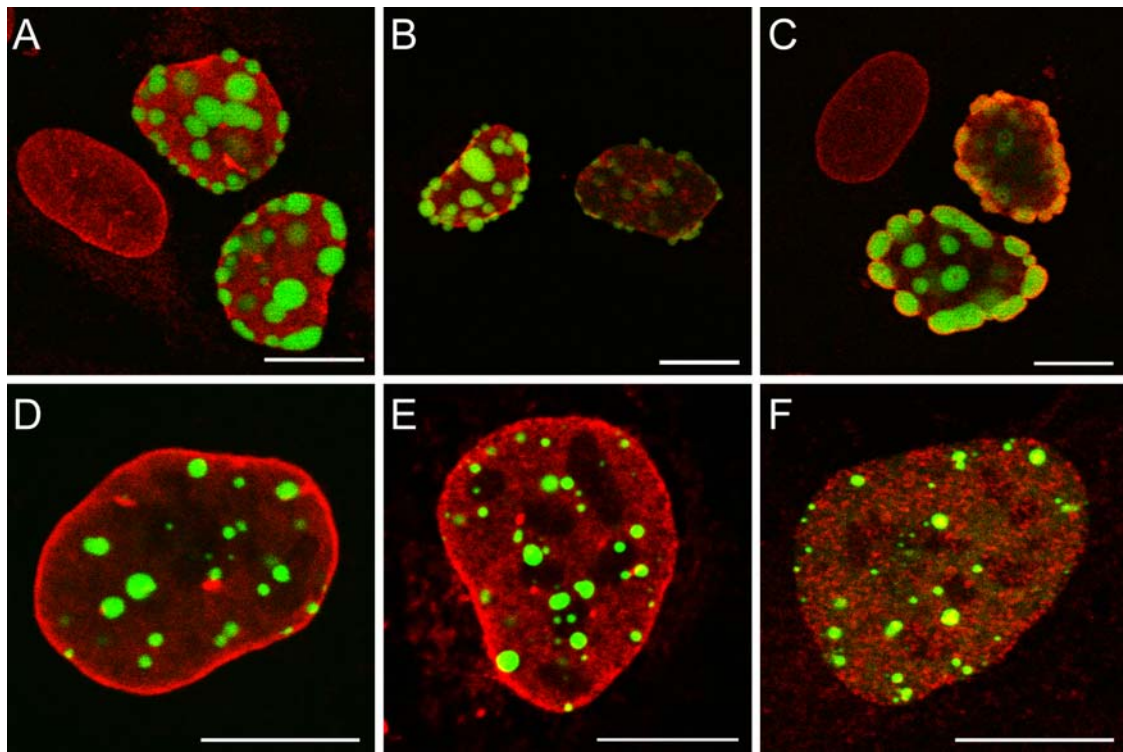


Figure 20: Double labeling of lamin B1 and lamin B2 phosphoacceptor mutants with NE proteins. Confocal sections of cells transfected with YFP-lamin B2 S37+407D (A – C, shown in green) or YFP-lamin B1 S391D (D – F, shown in green) respectively, and stained with antibodies specific for LBR (A + D), emerlin (B + E), Nup153 (C + F) (shown in red). Bars 10 μ m.

4.2.6 *In vivo* dynamics of aggregate formation

The investigation of “mitotic” lamin B2 mutants in U2OS cells showed that these mutants formed large aggregates in the nucleus after about 24 hours post transfection of the respective expression plasmids. In order to analyze the process of the formation and the mobility of these aggregates in more detail, U2OS cells were transiently transfected with the YFP-lamin B2 S407D expression plasmid and directly processed for live cell imaging. The cells were observed by confocal imaging in 3D with a time lapse of 30 minutes. Formation and mobility of nuclear aggregates was analyzed in maximum projections of the 3D stacks (Figure 21). From about 4-5 hours on post transfection the mutant protein was observed to be expressed in significant amounts. At 11 hours after transfection the formed aggregates varied in size but were still relatively small (Figure 21 A). However, the aggregates grew over time and

fused when in spatial proximity (Figure 21: B - F, aggregates about to fuse are indicated by arrows). The number of aggregates decreased, resulting in some of the cells in the formation of single large lamin territories (Figure 21: compare E (18 aggregates) to F (9 aggregates)). These reorganization events were very dynamic. The nuclei became very mobile and reversibly formed large lobulations (Figure 21 C).

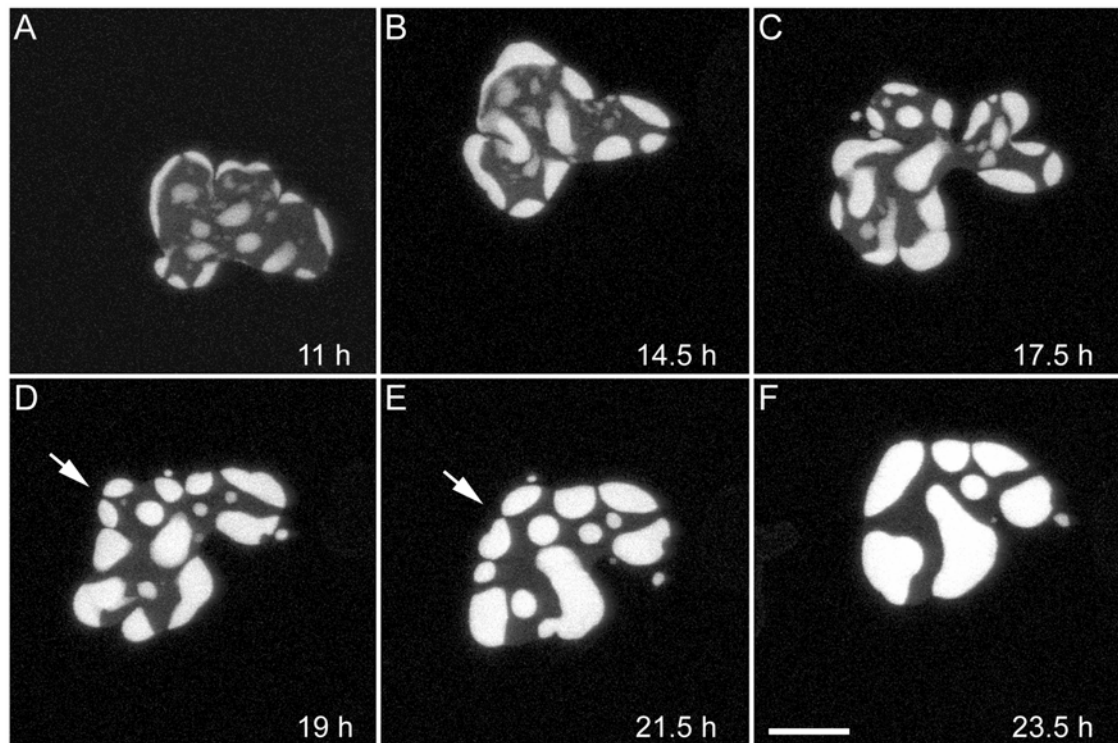


Figure 21: In vivo dynamics of YFP-lamin B2 S407D aggregate formation in U2OS cells. Maximum projections of 3D stacks. Time points indicated are post transfection. Arrows indicate aggregates about to fuse. Bar 10 μ m.

4.2.7 Aggregate formation leads to drastic chromatin reorganization

Lamins are thought to be involved in chromatin organization (Bridger et al, 2007). In order to study changes in chromatin distribution due to aggregate formation in U2OS cells expressing YFP-lamin B2 S407D, fixed cells were stained with DAPI and analyzed by immunofluorescence. Confocal microscopy of the DAPI staining revealed that chromatin is excluded from areas where YFP-lamin B2 S407D aggregates are formed (Figure 22 A). The aggregates are spatially confined from chromatin, thus occupying a chromatin-free nuclear space. Chromatin distribution was also analyzed

in U2OS cells stably expressing a CFP fusion protein of histone H2A (Figure 22 B). For this purpose a U2OS cell line stably expressing a CFP fusion protein of histone H2A was generated and was transiently transfected with the YFP-lamin B2 S407D expression plasmid. Confocal microscopy showed that CFP-H2A was eliminated from areas of aggregate formation. Thus it is concluded that YFP-lamin B2 S407D accumulation takes place in the interchromosomal domain (ICD) compartment, eventually occupying a chromatin-free nuclear space.

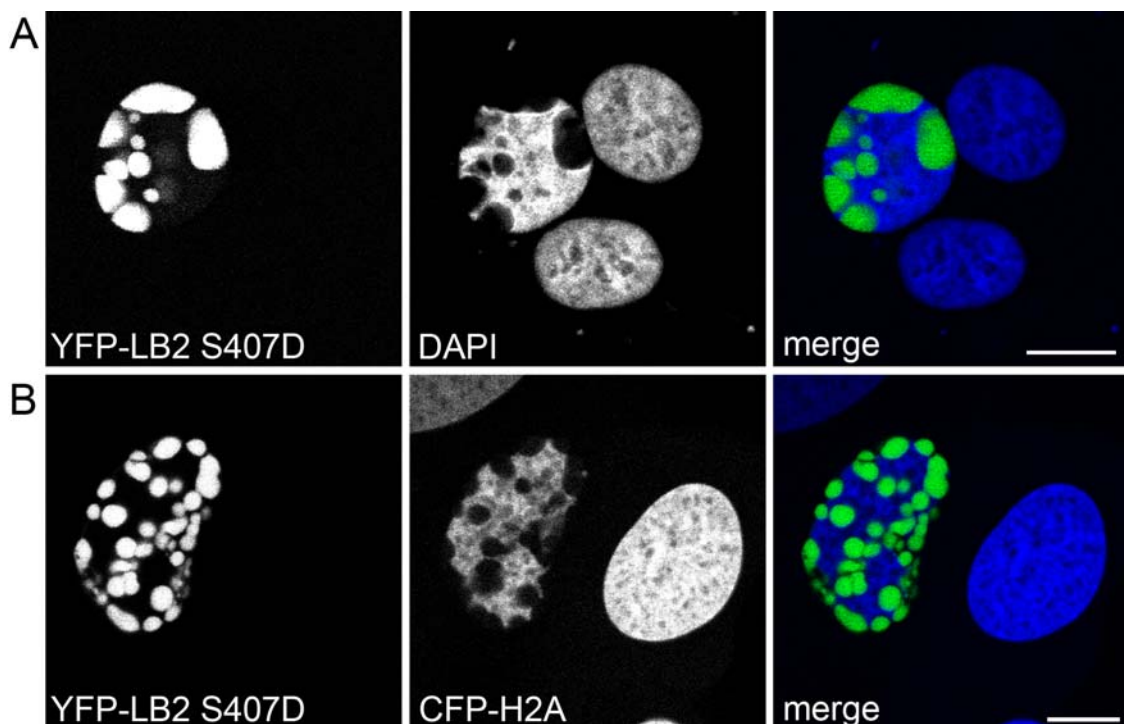


Figure 22: Chromatin organization in U2OS cells expressing YFP-lamin B2 S407D. (A) chromatin distribution revealed by DAPI staining (blue), (B) chromatin distribution in U2OS cells stably expressing CFP-H2A (blue). All images are confocal sections. Bars 10 µm.

4.2.8 Co-transfection of lamin B1 and lamin B2

Both, lamin B1 S→D mutants as well as lamin B2 S→D mutants formed intranuclear aggregates upon expression in U2OS cells. In order to study the spatial relationship of lamin B1 S→D mutants with lamin B2 S→D mutants and to find out whether the aggregates co-localize, co-transfection with both constructs was performed. U2OS cells were co-transfected with GFP-lamin B2 S407D and mCherry-lamin B1 S393D, fixed 24 hours thereafter and analyzed by confocal microscopy (Figure 23). The aggregates formed by the mutants were similarly distributed throughout the nucleus

and appeared to occupy the same nuclear space. However, analysis of confocal stacks in z showed that the GFP-lamin B2 S407D and mCherry-lamin B1 S393D signals did not co-localize completely (see insets Figure 23). Hence, both proteins were rather in very close proximity to each other, overlapping on the borders of the aggregates. These observations suggest that both proteins occupy the same nuclear space but they do not intermingle.

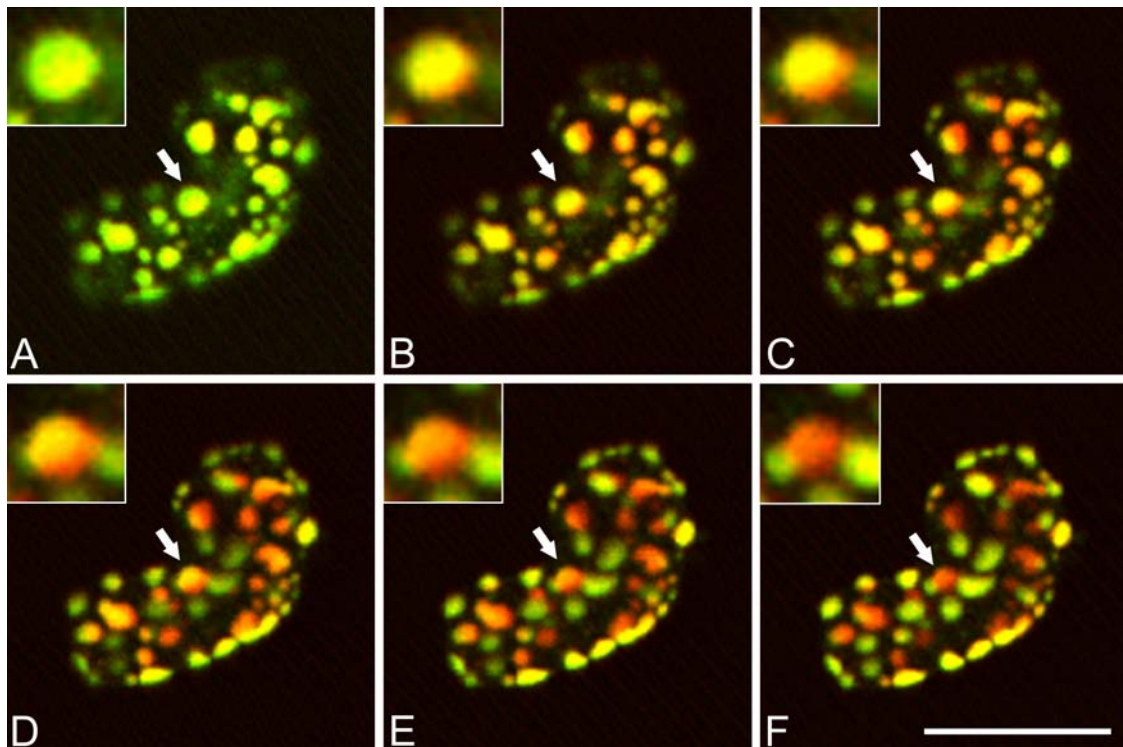


Figure 23: Single confocal sections of a U2OS cell co-expressing GFP-lamin B2 S407D (green) and mCherry-lamin B1 S393D (red). Bar 10 μ m.

4.2.9 Co-transfection of “mitotic” lamins with NLS-vimentin

Several of the “mitotic” lamin B mutants fused to mCherry were also investigated concerning their co-localization to other ectopically expressed proteins. To this aim mCherry-lamin B1 S393D and GFP-*Xenopus laevis* NLS-vimentin were co-transfected in U2OS cells and fixed 24 hours thereafter (Figure 24 A). mCherry-lamin B1 S393D assembled into larger intranuclear aggregates, whereas GFP-*Xenopus laevis* NLS-vimentin was visible as small intranuclear dots. The GFP-*Xenopus laevis* NLS-vimentin dots surrounded the mCherry-lamin B1 S393D aggregates but could also be

observed apart from the aggregates. Hence, they co-localized but were not deposited into the same aggregate.

Co-transfection of mCherry-lamin B2 S407D and GFP-*Xenopus laevis* NLS-vimentin showed similar results (Figure 24 B). mCherry-lamin B2 S407D appeared as irregular aggregates throughout the nucleus. These aggregates co-localized with GFP-*Xenopus laevis* NLS-vimentin, but did not intermingle. These results indicate that ectopically co-expressed mCherry-lamin B2 S407D or mCherry-lamin B1 S393D respectively, and GFP-*Xenopus laevis* NLS-vimentin occupy the same nuclear space, i.e. the ICD but are processed and sorted differently.

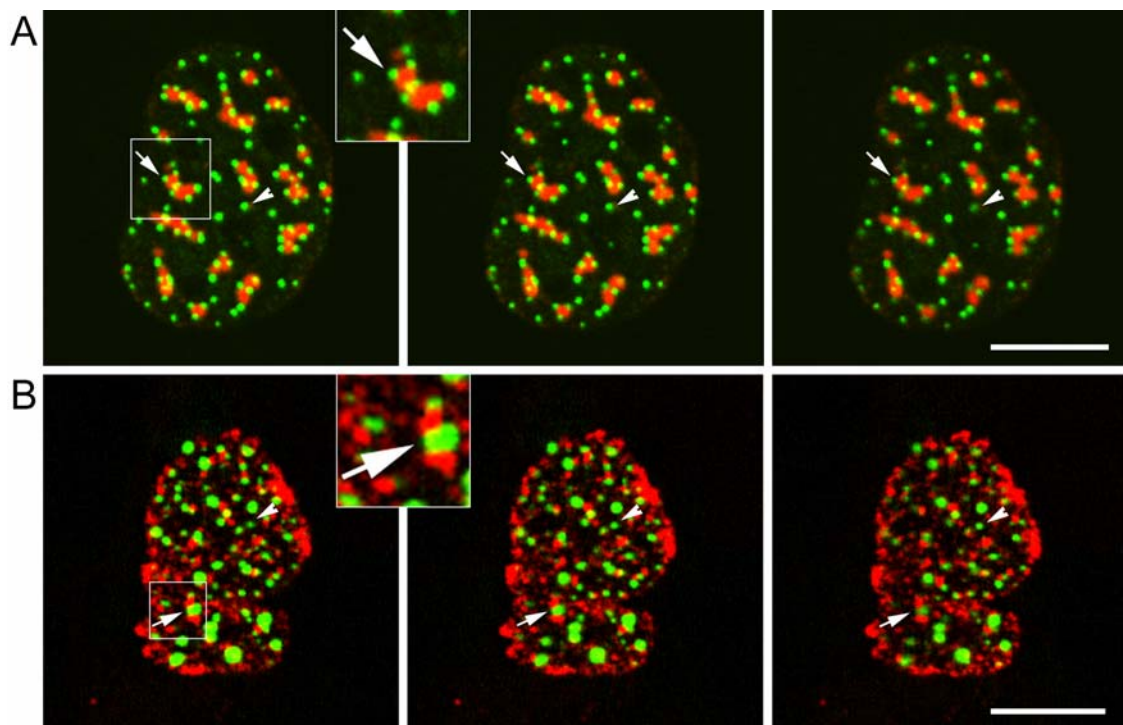


Figure 24: Confocal sections of U2OS cells co-expressing (A) mCherry-lamin B1 S393D (red) and GFP-*Xenopus laevis* NLS-vimentin (green), (B) mCherry-lamin B2 S407D (red) and GFP-*Xenopus laevis* NLS-vimentin (green). Arrows point to GFP-*Xenopus laevis* NLS-vimentin dots lying next to lamin aggregates. Arrowheads indicate single GFP-*Xenopus laevis* NLS-vimentin dots. Bars 10 μ m.

4.2.10 Effects of mitotic lamin expression on PCNA localization

Nuclear lamins are thought to play a role in DNA replication. Several laboratories have demonstrated that nuclear lamin proteins are essential for DNA replication in *Xenopus* egg extracts. Without lamin proteins, nuclear membranes assemble around *Xenopus* sperm chromatin but do not initiate replication. In one case it was shown

that the replication fork protein PCNA (proliferating cell nuclear antigen) is relocated from replication centers to intranuclear lamin aggregates (Spann et al, 1997). Izumi et al. (2000) showed in mammalian cells that dominant negative lamin B1 mutants trapped PCNA into intranuclear aggregates. In order to investigate whether “mitotic” lamin B2 sequesters PCNA from replication centers, fixed cells were analyzed by confocal microscopy. U2OS cells transiently transfected with YFP-lamin B2 S407D were fixed 24 hours thereafter and stained with an antibody specific for PCNA (Figure 25 A). YFP-Lamin B2 S407D trapped PCNA into intranuclear aggregates. In cells co-expressing YFP-lamin B2 S407D and CFP-PCNA, PCNA protein was also recruited into the aggregates formed by YFP-lamin B2 S407D (Figure 25 B).

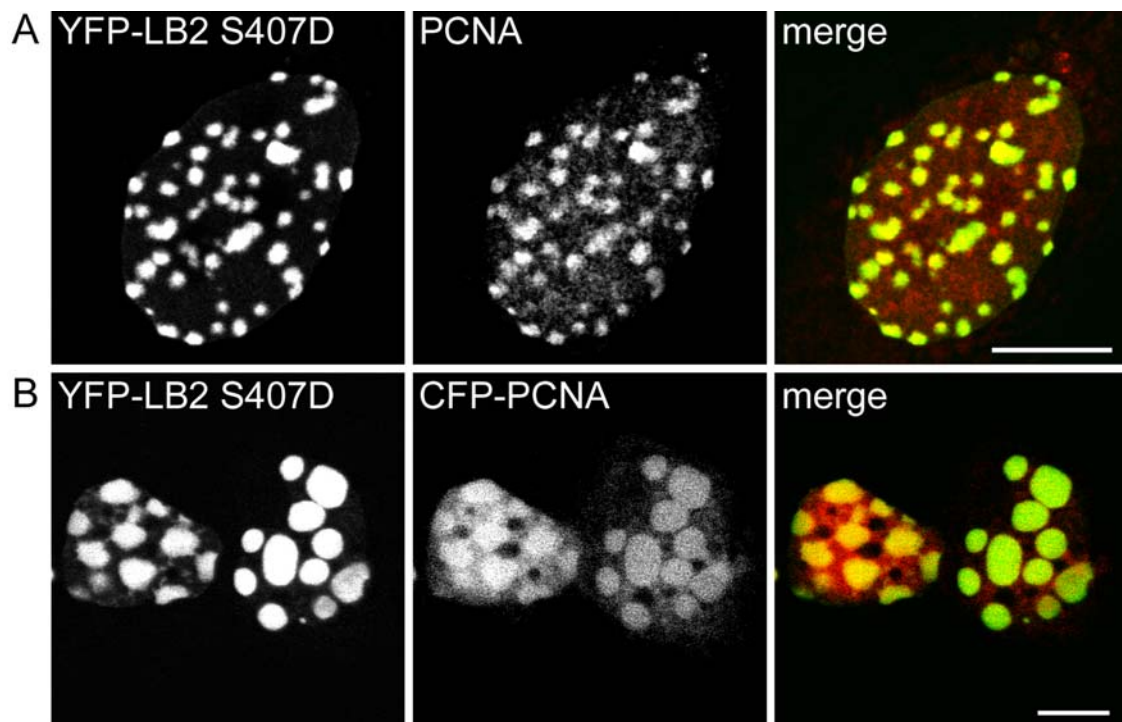


Figure 25: Double labeling of YFP-lamin B2 S407D and PCNA. (A) U2OS cell expressing YFP-lamin B2 S407D (green in merge) stained with an antibody specific for PCNA (red in merge), (B) U2OS cells co-transfected with YFP-lamin B2 S407D (green in merge) and CFP-PCNA (red in merge). All images are confocal sections. Bars 10 μ m.

4.2.11 Biochemical analysis of cells expressing mitotic lamin mutants

In order to characterize the solubility of “mitotic” lamin B2 mutants, transiently transfected U2OS cells were subjected to differential protein extraction (see 3.7.2). Cells have been transfected with the respective expression plasmid about 18-22

hours before the extraction procedure, with an estimated transfection efficiency of about 80-90%. Fractions 1-4 were analyzed in a Western blot by detection with an antibody specific for lamin B2 (Figure 26).

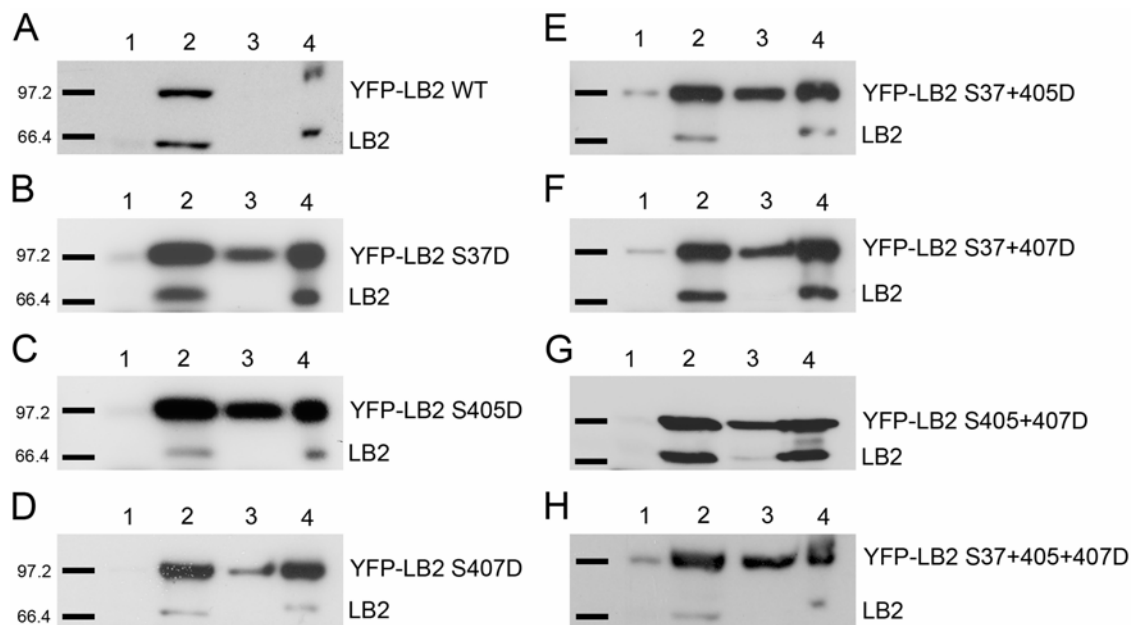


Figure 26: Western blot analysis of differentially extracted fractions from U2OS cells expressing YFP-lamin B2 mutants mimicking the mitotic phosphorylated state using an antibody specific for lamin B2. Extracts of U2OS cells expressing YFP fusion proteins of (A) lamin B2 WT, (B) lamin B2 S37D, (C) lamin B2 S405D, (D) lamin B2 S407D, (E) lamin B2 S37+405D, (F) lamin B2 S37+407D, (G) lamin B2 S405+407D, (H) lamin B2 S37+405+407D. Lane 1, soluble and extractable cytoplasmic proteins, lane 2, total cytoskeletal fraction, lane 3, high-salt and high-detergent soluble cytoskeletal fraction, lane 4, insoluble cytoskeleton proper. It should be considered that the signal intensities of the different immunoblots can not be compared directly, since the exposure times of the X-ray film varied between cell preparations.

In contrast to YFP-lamin B2 WT which was detectable in fractions 2 and 4 (Figure 26 A), YFP-lamin B2 proteins mutated from serine to aspartic acid in mitotic phosphoacceptor sites was detectable in fractions 2-4 (Figure 26 B-H). This higher solubility could be observed in extracts of all mutants analyzed, independent of both the position of the mutated site and the number of mutated sites. Endogenous lamin B2 protein was detectable in fractions 2 and 4 and its solubility was thus not affected by the expression of YFP-lamin B2 proteins mutated in mitotic phosphoacceptor sites. The relative amount of the YFP-fusion proteins was several folds higher than endogenous lamin B2. These results clearly demonstrate that "mitotic" lamin B2 mutants do not form co-polymers with endogenous lamin B2.

4.2.12 Identification of interaction partners of soluble lamins

Lamin B2 YFP-fusion proteins mimicking the mitotic phosphorylated state have been shown to be more soluble than wild type lamin B2 or endogenous lamin B2 protein. Furthermore, they are localized in a chromatin-free nuclear space. In order to identify possible interaction partners of these so-called soluble lamins, which might be responsible for the formation and sorting of the protein into intranuclear lamin aggregates, a co-immunoprecipitation assay was performed followed by MALDI analysis. To optimize the cell extraction conditions for the subsequent co-immunoprecipitation, U2OS cells transfected with the YFP-lamin B2 S407D expression plasmid were sequentially extracted with an extraction buffer containing 10 mM MgCl₂ and 0.2, 0.4, 0.6, 0.8, and 1% Triton X-100, respectively. The gained fractions were analyzed in a Western blot by detection with an antibody specific for lamin B2 (Figure 27 A). A certain amount of YFP-lamin B2 S407D protein with a size of about 97 kD could already be solubilized with 0.2% and 0.4% Triton X-100. In contrast, endogenous lamin B2 could not be extracted with any of the applied Triton X-100 concentrations and resided completely in the insoluble pellet fraction. Western blot analysis with an antibody specific for lamin B2 of extracts of untreated cells, cells expressing wild type YFP-lamin B2, and cells expressing YFP-lamin B2 S407D showed that 0.4% Triton was sufficient to extract a high portion of YFP-lamin B2 S407D protein being thus present in the supernatant (Figure 27 B). On the contrary, wild type YFP-lamin B2 and endogenous lamin B2 (control) remained unaffected and resided completely in the insoluble pellet fraction. These results suggest that wild type and endogenous lamin B2 are in a membranous state.

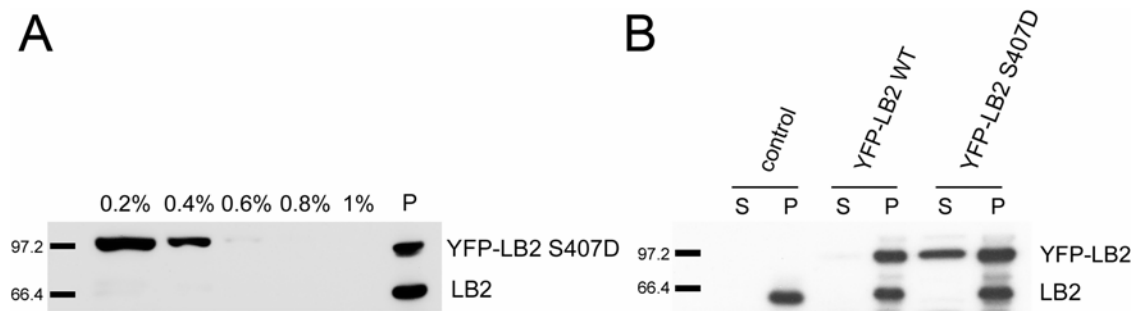


Figure 27: Western blot analysis of Triton X-100 extracted U2OS cells expressing YFP-lamin B2 S407D. (A) Sequential Triton X-100 extraction (0.2%, 0.4%, 0.6%, 0.8%, 1%, insoluble Pellet (P)) of cells expressing YFP-lamin B2 S407D. (B) Extracts of wild type cells, cells expressing wild type YFP-lamin B2, and cells expressing YFP-lamin B2 S407D were treated with 0.4% Triton X-100 and processed for soluble and cytoskeletal fractions, P pellet, S supernatant.

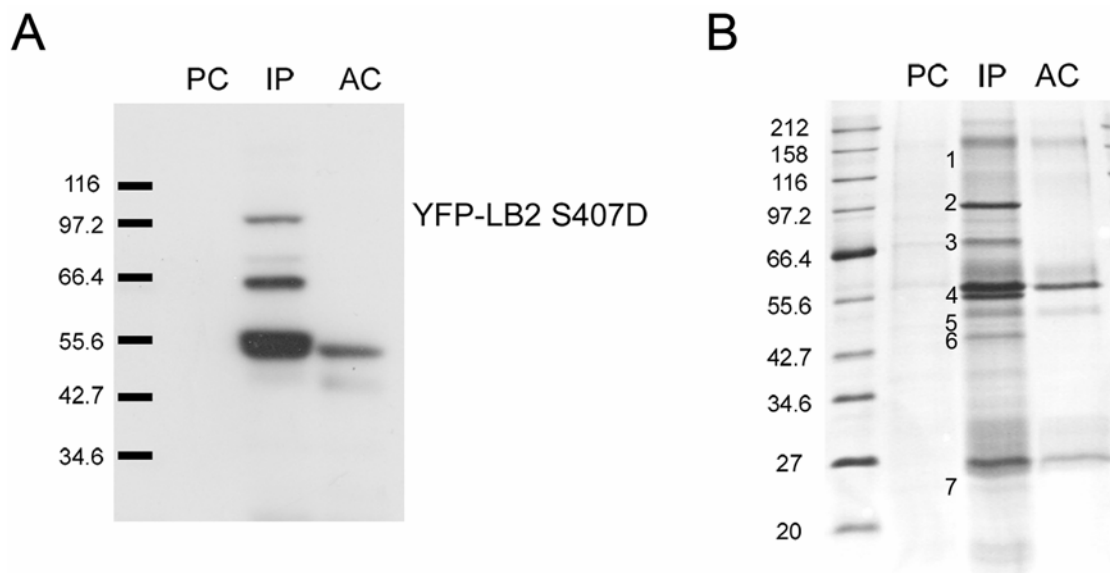


Figure 28: Co-immunoprecipitation of Triton X-100 extracted U2OS cells expressing YFP-lamin B2 S407D using an antibody specific for lamin B2. (A) Immunoprecipitation with an antibody specific for lamin B2, (B) Coomassie staining of immunoprecipitation. Numbers 1-7 indicate the bands cut out for MALDI analysis. PC preclearing sample, IP immunoprecipitation sample, AC antibody control sample.

For the co-immunoprecipitation assay cells expressing YFP-lamin B2 S407D were extracted as described above and the supernatant containing the soluble lamin complexes was subsequently subjected to immunoprecipitation with an antibody specific for lamin B2 as described in 3.7.4. The immunoprecipitation sample (IP), the preclearing sample (PC) and the antibody control sample (AC) were analyzed in a Western blot by detection with an antibody specific for lamin B2 (Figure 28 A). YFP-lamin B2 S407D protein could not be detected in the preclearing sample, thus excluding unspecific binding of the protein to the protein G sepharose beads.

Immunoprecipitation targeted against lamin B2 precipitated YFP-lamin B2 S407D. Western blot analysis with an antibody specific for lamin B2 revealed two additional bands with a size of ~66 kD and ~55kD, respectively. These bands most likely represent degradation products as they are also detected with an antibody specific for GFP (data not shown). An additional band detected was also detected in the antibody control sample, and thus probably corresponded to the heavy chains of the antibody.

For MALDI analysis, preclearing sample, immunoprecipitation sample, and antibody control sample were subjected to SDS-PAGE and the gel was subsequently stained with Coomassie staining solution (Figure 28 B). Seven bands (1-7) were cut out of the gel and MALDI-TOF analysis was performed. The results are listed in Table 10 in the appendix. The IMALDI-TOF analysis was performed in cooperation with Dr. M. Schnölzer, DKFZ Heidelberg.

4.3 Characterization of a laminopathy causing lamin A mutant

Zeller et al. (2006) recently published a novel mutation in the lamin A gene, a p.R321X nonsense mutation, found in a family with dilated cardiomyopathy. Three family members were heterozygous for the mutation and revealed variable degrees of cardiac contractile dysfunction in addition to severe rhythm disturbances. In order to characterize the mutation on a cellular level, explanted cardiac tissue and cultivated skin fibroblasts from two patients carrying this mutation were analyzed. Patient IV-1 required heart transplantation at the age of 34, and his sister (IV-3) suffers from mildly reduced left ventricular systolic function and first degree atrioventricular conduction block. The pedigree of the affected family is shown in the appendix (Figure 34).

4.3.1 Downregulation of the mutant *LMNA* allele by nonsense-mediated decay (NMD)

An allele specific Taqman assay was employed to determine the ratio of wild type to mutant transcripts in patient samples (Table 9). In cultured skin fibroblasts of both patients IV-1 and IV-3, the wild type transcripts exceeded the mutant transcripts

about 30-fold. Similarly, the wild type transcripts were ~7- and ~9-fold higher in the left and right ventricular myocardium, respectively, of patient IV-1, than the mutant transcripts. In control fibroblasts, a wild type to mutant mRNA ratio of 304:1 was obtained, demonstrating negligible unspecific recognition of the wild type allele by the Taqman probe for the mutant allele.

Table 9: Allele specific quantitation of *LMNA* transcripts.

Sample	Allele	C _T	Δ C _T (C _{Twt} -C _{Tmut})	2 ^{-Δ C_T}	Corrected ratio ¹ wild type/mutant
Patient IV-3 fibroblasts	wild type	28.03	-3.91	15.0	30.0
	mutant	31.94			
Patient IV-1 fibroblasts	wild type	27.73	-3.87	14.6	29.2
	mutant	31.60			
Patient IV-1 left ventricle	wild type	32.86	-1.71	3.3	6.6
	mutant	34.57			
Patient IV-1 right ventricle	wild type	29.13	-2.22	4.7	9.4
	mutant	31.35			
Wild type control fibroblasts	wild type	27.80	-7.25	152.2	304.4
	mutant	35.05			

¹The Δ C_T value (C_{Twt}-C_{Tmut}) at equal quantities of both alleles, as is the case in the genomic DNA of patient IV-1 and IV-3, was ~1. Accordingly, the 2^{-Δ C_T} values have to be corrected by a factor of 2.

4.3.2 Biochemical characterization of cardiac tissue and skin fibroblasts

In order to investigate the expression levels of wild type and mutant p.R321X protein a specimen of left ventricular myocardium obtained from patient IV-1 at the time of cardiac transplantation and cultured skin fibroblast cells from patients IV-1 and IV-3 were analyzed by Western blotting. For control, primary skin fibroblasts obtained from a healthy person and cardiac muscle tissue from a patient, who underwent cardiac transplantation due to ischemic cardiomyopathy and harbored no *LMNA* mutation, were used. Cardiac tissue was disrupted and homogenized as described in

section 3.7.1 and cell lysates were subjected to SDS-PAGE. Equal protein amounts of control and patient cardiac tissue were loaded onto the gel as validated by Coomassie staining (Figure 29). Cultured skin fibroblast cells from patients IV-1 and IV-3 were analyzed by differential protein extraction (see 3.7.2). Western blots of cardiac tissue and skin fibroblasts were detected with an antibody raised against the amino-terminal domain of lamin A/C. No differences between the relative amounts of wild type lamin A/C protein could be observed, neither in the controls and in cardiac muscle from patient IV-1 (Figure 29 A), nor in the cytoskeletal fractions 2 and 4 of cultured fibroblast cells from both patients examined (IV-1 and IV-3; exemplified for patient IV-1, Figure 29 B). These data suggest that the single wild type *LMNA* allele in the heterozygous patient is sufficient to produce 'normal' quantities of lamin A/C protein. In agreement with the finding of down regulation of the mutant *LMNA* allele at the mRNA level, the truncated p.R321X lamin A protein with an expected molecular weight of ~37 kDa could not be detected in all patient tissues analyzed at our level of sensitivity (Figure 29 A + B).

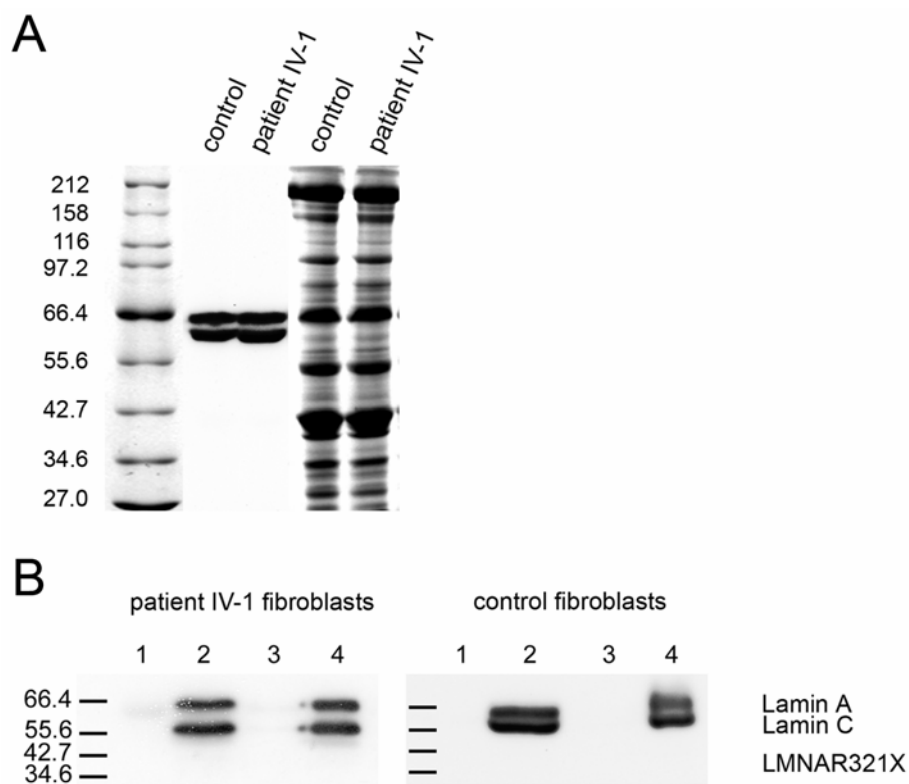


Figure 29: Western blot analysis of patient and control samples using an antibody specific for lamin A. (A) Whole cell lysate of left ventricular myocardial tissue. Coomassie staining (two lanes on the right), (B) Differential protein extraction of fibroblasts. Lane 1, soluble and extractable cytoplasmic proteins, lane 2, total cytoskeletal fraction, lane 3, high-salt and high-detergent soluble cytoskeletal fraction, lane 4, insoluble cytoskeleton proper.

4.3.3 Inhibition of the proteasome uncovers the truncated *LMNAR321X* protein

We have demonstrated that the mutant *LMNA* allele was significantly down regulated but not completely shut off. This leaves the possibility that the truncated message could be translated into a short-lived protein. Since such misfolded proteins are particularly prone to proteasomal degradation, the proteasomal function in cultured fibroblasts was suppressed with the proteasome inhibitor epoxomicin. The cells were treated for 24 hours with 100 nM epoxomicin and subjected to differential protein extraction. The isolated fractions 1-4 were analyzed in a Western blot by detection with an antibody specific for the N-terminal segment of lamin A/C. The truncated p.R321X protein was readily detectable in the cytoskeletal fractions 2 and 4 of patient IV-1 but not in control fibroblasts (Figure 30). In fibroblasts derived from patient IV-3, however, no truncated p.R321X protein was detected. This indicates that NMD may not fully prevent the synthesis of the truncated protein in patient IV-1. Moreover, the relative amount of lamin A to lamin C in epoxomicin treated fibroblasts of patient IV-1 was reduced compared to control fibroblasts. The reason for this reduction in lamin A is at present completely elusive.

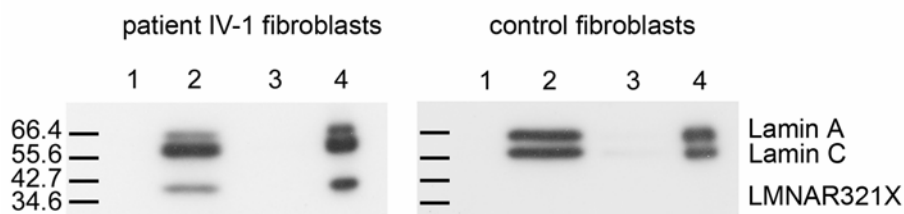


Figure 30: Western blot analysis of detergent-extracted fractions from patient and control fibroblasts treated with epoxomicin using an antibody specific for lamin A. Left panel: patient IV-1, right panel: control patient. Lane 1, soluble and extractable cytoplasmic proteins, lane 2, total cytoskeletal fraction, lane 3, high-salt and high-detergent soluble cytoskeletal fraction, lane 4, insoluble cytoskeleton proper.

4.3.4 Nuclear morphology, chromatin distribution and localization of nuclear proteins in patient tissues

The nuclear morphology and the distribution of nuclear proteins were examined in cardiac tissue of patient IV-1 and in cultured fibroblasts of patient IV-1 and IV-3 (Figure 31). The fixed cells or tissues were labeled with a lamin A/C specific antibody and chromatin organization was investigated by DAPI staining. Lamin A/C staining patterns and nuclear morphology of patient IV-1 fibroblasts and cardiac tissue was indistinguishable from those obtained for the healthy controls. DNA staining revealed a normal heterochromatin distribution (Figure 31).

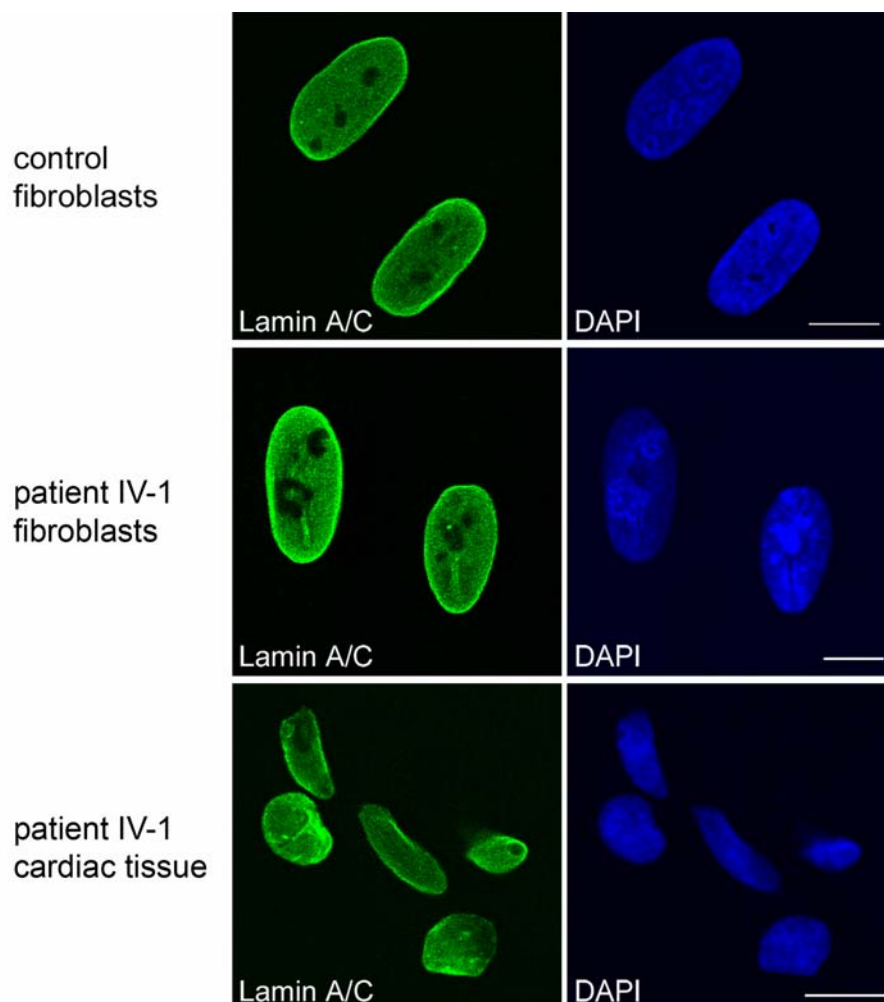


Figure 31: Confocal sections of control fibroblasts (upper row), patient fibroblasts (middle row) and patient left ventricular myocardium (lower row) stained with an antibody specific for lamin A (shown in green). Note the typical rim staining for lamin A in all cells and the normal heterochromatin distribution as indicated by DAPI staining (shown in blue). Bars 10 μ m.

Immunofluorescence staining of fibroblasts obtained from patient IV-1 and IV-3 for lamin B2, emerin, and LBR (exemplified for patient IV-1 fibroblasts; Figure 32) showed staining patterns indistinguishable from those obtained for healthy controls. The same was true for immunofluorescence studies done after treatment with epoxomicin for 24 hours (data not shown).

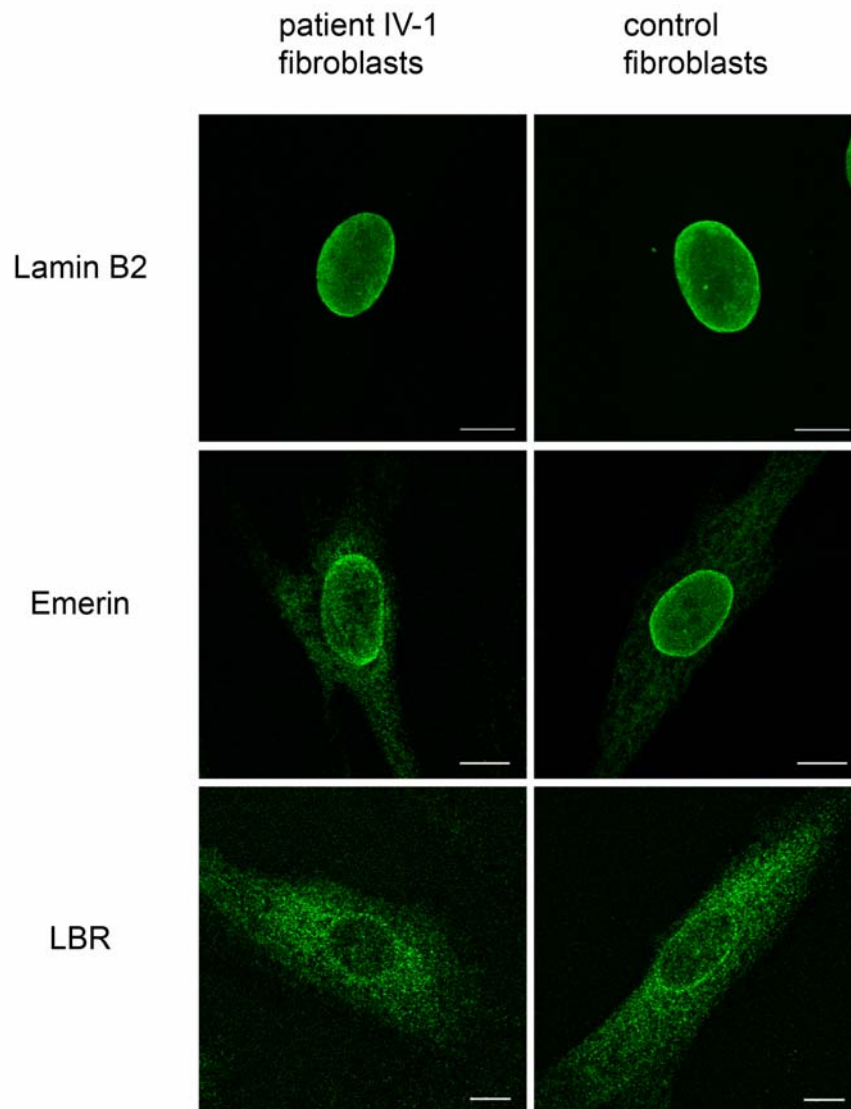


Figure 32: Representative immunofluorescence staining of lamin B2 (upper row), emerin (middle row), and lamin B receptor (LBR, lower row) in control (left column) as well as in patient (right column) cultured fibroblasts. All images are confocal sections. Bars 10 μ m.

4.3.5 Transfection of the lamin A p.R321X mutant

In order to reveal potential toxic effects of the truncated protein on the nuclear morphology and chromatin distribution, an EGFP-tagged expression construct for both wild type LMNA and mutant p.R321X was generated. Transient transfection of HeLa cells with the wild type *LMNA* cDNA revealed a typical “rim-staining” at the nuclear periphery. The mutant lamin A was found to be partially targeted to the nucleus, where it accumulated in the nucleoplasm and, to some extent, in the nuclear lamina (Figure 33). Additionally, the mutant protein was distributed throughout the cytoplasm. The heterochromatin distribution, the nuclear shape and the distribution of lamin B2 and emerin appeared not to be affected by transient overexpression of the truncated lamin A variant.

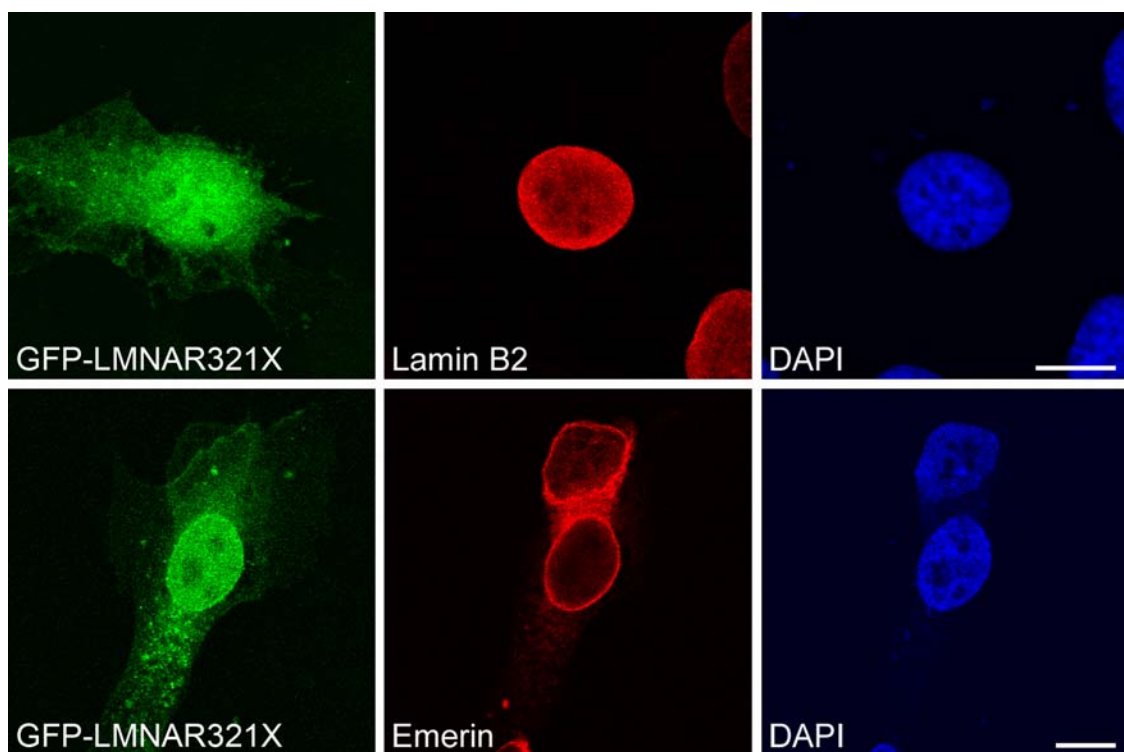


Figure 33: Transient transfection study of EGFP-tagged p.R321X in HeLa cells. Note the diffuse cytoplasmic and nucleoplasmic distribution of the truncated protein (green, left column) in transfected cells. Some mutant protein is also recruited to the nuclear lamina as indicated by the rim staining. Immunofluorescence stainings with antibodies specific for lamin B2 or emerin respectively are shown in red (middle column). DNA is detected with DAPI (blue, right column). All images are confocal sections. Bars 10 μm .

5 Discussion

5.1 Topogenesis of lamins/lamina

5.1.1 Role of the lamin head and tail domains in cellular localization

To determine the influence of the distinct head and tail domains on lamin filament organization and cellular localization, human cultured cells were transfected with cDNAs coding for the $\Delta 32$ head, headless, tailless, $\Delta 32$ head/tailless, and the rod of human lamin B2 fused to YFP. Deletion of the head domain or the tail domain was essential for the formation of a dominant negative lamin mutant. Mutants with partial (LB2 $\Delta 32$ head) or complete deletion of the head domain (LB2 headless) localized to the nuclear rim but nuclear shape was highly impaired. Double mutants exhibiting both head domain deletions and tail domain deletions (LB2 $\Delta 32$ head/tailless and LB2 rod) were effective as dominant negative mutants and their effects were almost identical to those of the mutants carrying only the tail deletion (LB2 tailless).

Tailless lamin B2 mutants

We could show that the lamin B2 tail domain is indispensable for targeting the protein to the nuclear rim and its proper integration into the nuclear envelope. However, it seems to be dispensable for nuclear localization. Lamin B2 mutants devoid of the tail domain were not only distributed throughout the cytoplasm but were also found in the nucleoplasm. Furthermore, tailless lamin mutants could not be integrated into the nuclear rim. These observations are in agreement with previous studies. The C-terminal tail domains of lamins contain several motifs that are essential for their correct localization: a nuclear localization signal (NLS) and a CAAX box motif, which are thought to be required for proper targeting of lamins into the nucleus and nuclear envelope, respectively. Although tailless lamin B2 mutants are devoid of the NLS a significant portion of the mutant protein localized to the nucleoplasm. The nuclear localization of tailless lamin B2 can be explained by the presence of an evolutionary conserved motif at the end of coil 2 of the α -helical rod domain. This motif has been shown to direct vimentin, a cytoplasmic IF protein, to

the nucleus when its tail domain is deleted (Rogers et al, 1995). The inability of tailless lamin B2 to incorporate into the nuclear lamina is suggested to be due to the lack of the CAAX motif. Chicken lamin B2 CAAX-less mutant proteins were reported to be distributed diffusely throughout the nucleoplasm (Nigg et al, 1992). B-type lamins are permanently farnesylated and this modification, although necessary, is not sufficient for anchorage at the nuclear envelope, and a prenyl receptor is required for this association. Two nuclear membrane proteins bind to B-type lamins in domains that are not deleted in any of the tail deleted lamin B2 mutants reported here, namely LBR (Mical & Monteiro, 1998) and LAP2 β (Furukawa & Kondo, 1998). Although it has been concluded previously that the LBR binding domain is not sufficient for nuclear envelope localization of lamin B (Mical & Monteiro, 1998), LAP2 β does appear to have an important role in lamin filament assembly (Yang et al, 1997). We conclude from our results that the tail domain of lamin B2 contains those elements that are necessary for effectively guiding these lamins to the nuclear envelope.

Lamin B2 head deletion mutants

A major result of our study was that the lamin B2 head domain is dispensable for localization of the protein to the nuclear rim. Wild type lamin B2 contains in its head domain a highly conserved sequence. This is deleted in lamin B2 headless but not in lamin B2 Δ 32head. Interestingly both, lamin B2 protein deleted in the N-terminal 32 amino acids (LB2 Δ 32head) and lamin B2 protein deleted in the complete head domain (LB2 headless) localized to the nuclear rim. It is thus clear that the conserved sequence in the lamin B2 head domain is dispensable for nuclear envelope targeting. However, nuclear shape was highly impaired by both mutants. This finding suggests that headless lamin B2 protein interferes with proper lamina assembly and thus impairs the structural function of the nuclear lamina. Several important studies have highlighted the role of the lamina in determining the shape of the nucleus. In mouse spermatocytes, nuclei are hook shaped rather than spherical, and a spermatocyte-specific lamin - lamin B3 – is expressed in these cells. Indeed, exogenous expression of lamin B3 in somatic cells resulted in their nuclei adopting a hook-shaped morphology (Furukawa & Hotta, 1993). Schirmer et al. (2001) constructed a dominant-negative mutant of lamin B1 that lacked four-fifths of the

rod domain (B1 Δ rod). This mutant was still able to self-assemble into filaments *in vitro* and, when transfected into cultured cells, was incorporated into the lamina. However, its incorporation into the lamina caused massive deformation of the nuclear envelope. In support of this, deletion of the head domain of both lamin B1 (Ellis et al, 1997) and lamin A (Spann et al, 1997) lead to the formation of very fragile nuclei when used to assemble artificial nuclei using detergent extracted sperm nuclei in the presence of *Xenopus* egg extracts.

5.1.2 "Mitotic" lamins

The amino acid sequence of three phosphorylation sites of human lamin B2 and lamin B1 were altered and the mutated proteins were expressed in U2OS cells. The mutations affected three highly conserved serine residues flanking the α -helical rod domain. These serine residues (i.e. serine 37 and serine 405 or 407 in the human lamin B2 sequence; serine 23 and serine 391 or 393 in the human lamin B1 sequence) have been shown to be phosphorylated in response to a cdc2 kinase in mitosis (Heald & McKeon, 1990; Nigg, 1992; Peter et al, 1990).

If the phosphorylation of Ser-37/23, Ser-405/391, and Ser-407/393 participated in the active disassembly of higher order lamin associations, it would be expected that an amino acid exchange of these serine residues to negatively charged aspartic acid residues would either prohibit the integration of these mutants into the nuclear lamina or lead to the disassembly of the nuclear lamina. Indeed, the mutant proteins were not incorporated into the lamina but formed intranuclear aggregates when expressed in U2OS cells. Both, lamin B1 mutants and lamin B2 mutants localized to nuclear aggregates. The aggregates varied in size, and those observed for lamin B1 mutants were in general smaller than mutant lamin B2 aggregates. Some of these aggregates appeared to be associated with the nuclear membrane whereas others were not as judged by confocal microscopy. Interestingly, the effect of nuclear aggregate formation was independent of both the position of the mutated site and the number of mutated sites. Early on, using polymers reconstituted *in vitro* from bacterially expressed chicken lamin B2 proteins, it could be shown that phosphorylation of mitotic phosphoacceptor sites caused disassembly of longitudinal head-to-tail polymers into dimers but not dissociation of dimers (Nigg, 1992; Peter et

al, 1991). A molecular description of the effects of phosphorylation on lamin assembly remains to be established: what is the structure of the non-helical regions surrounding the mitotic phosphoacceptor sites before phosphorylation and how do these sites change in response to phosphorylation? It is conceivable that the major effects on lamin disassembly are not directly mediated by the placement of negative charge but rather through conformational changes of the surrounding regions.

The observed nuclear aggregates might represent a deposit for excess/surplus produced proteins, or proteins which might interfere/are harmful with cellular integrity. About the ultrastructure of the aggregates it can only be speculated. It is not clear whether the aggregates represent accumulations of the mutant protein or if they represent intranuclear membrane assemblies. Previous electron microscopic analysis demonstrated that the exogenous expression of CAAX-containing lamin proteins in *Xenopus* A6 cells, *Xenopus* oocytes, and COS-7 cells lead to the formation of intranuclear membrane assemblies (Prufert et al, 2004 2004). It has been shown that in *Xenopus* oocytes these intranuclear membranes are covered by single lamin filament layers (R. Stick, personal communication). It has been proved to be difficult to solubilize intranuclear NLS-vimentin aggregates (H. Herrmann, personal communication) which have been shown to consist of loose protein accumulations. The higher solubility of "mitotic" lamin B2 mutants compared to wild type lamin B2 would argue for intranuclear membrane assemblies. However, as observed in immunofluorescence stainings with antibodies specific for inner nuclear membrane proteins, LBR and emerin were not localized to the nuclear aggregates. They were furthermore excluded from the nuclear rim at the sites of "mitotic" lamin B2 aggregates. In contrast, Nup153 was enriched at the sites of nuclear aggregates but did not relocalize from the nuclear rim. These results argue against the formation of intranuclear membrane assemblies. It will be necessary to analyze cells expressing "mitotic" lamin B mutants by means of electron microscopy to clarify the ultrastructure of the aggregates observed.

The structure and the mobility of lamin proteins in these aggregates is not characterized so far. Fluorescence recovery after photobleaching (FRAP) analysis of the nuclear lamina in interphase cells revealed that both lamin A and lamin B1 are almost immobile in the lamina (Broers et al, 1999; Daigle et al, 2001). However, in our study extracts from differentially extracted cells expressing mutant lamin B2

showed an increased solubility of mutant proteins compared to endogenous lamin B2 suggesting a higher mobility of the proteins in the aggregates. In live cell imaging experiments we could show that the nuclear aggregates are rather dynamic structures. The aggregates fused, forming single large lamin territories. Preliminary data from FRAP analysis suggest a higher mobility of lamin mutants in the aggregates as in the nuclear lamina (data not shown). Further FRAP analysis will be performed to verify this observation.

The mechanism underlying aggregate formation is yet unknown. Upon co-transfection, aggregates of "mitotic" lamin B1 did not co-localize completely with "mitotic" lamin B2 aggregates but rather showed an overlap of aggregates on the borders. Similar results were obtained when co-expressing *Xenopus* NLS-vimentin and "mitotic" lamin B1 or "mitotic" lamin B2 protein. *Xenopus* NLS-vimentin formed nuclear dots localizing next to mutant lamin aggregates but were also found in separate locations. Nuclear *Xenopus* NLS-vimentin accumulations have been suggested to represent deposit structures for proteins produced in excess or proteins incapable of filament formation (Reichenzeller, 2002). However, in stable cell lines NLS-vimentin formed few and very small aggregates indicating that this ectopically expressed protein is recruited to specific loci within the nucleus (Bridger, 2005). The nuclear space occupied by NLS-vimentin has been shown to be the interchromosomal domain (ICD) compartment (Bridger et al, 1998). Mutant lamin aggregates were also clearly separated from chromatin and in close spatial proximity to vimentin-NLS accumulations. This suggests that both aggregates formed from mutant lamin proteins and NLS-vimentin accumulations are deposited in the ICD. Although all of the above mentioned ectopic or mutant proteins are localized to nuclear aggregates occupying the same nuclear space, intermingling could not be observed. Although the mechanism underlying aggregate formation of "mitotic" lamin B1, "mitotic" lamin B2, and NLS-vimentin remains elusive, our results strongly suggest the existence of nuclear "protein processing centers". Their functions may relate to the prevention of macromolecular crowding as well as to the organization and distribution of nuclear proteins in general.

In a recent study it was demonstrated that EGFP and EGFP fusion proteins inhibit polyubiquitination, a posttranslational modification that controls a wide variety of cellular processes, like activation of kinase signaling or protein degradation (Baens et

al, 2006). Thus proteasomal degradation of the aggregate forming mutants might be inhibited by the presence of their tag.

5.2 Influence of lamin B mutants on the endogenous lamina and lamina assembly

Several studies indicate that there might be a hierarchy of lamin-lamin associations at the INM. In this hierarchy, the B-type lamins are assembled into lamina filaments first, followed by lamin A and then by lamin C (Hutchison et al, 2001). In *Xenopus* egg extracts, recombinant lamin A is assembled at the NE of in-vitro-assembled sperm pronuclei only in the presence of the endogenous lamin B3, indicating that lamin A might be incorporated into existing B-type lamina filaments (Dyer et al, 1999). In tissue culture cells, lamin A remains in the nucleoplasm until B-type lamin filaments are assembled in the telophase nuclei (Dechat et al, 2000; Moir et al, 2000). Finally, dominant negative lamin mutants that have altered lamin-assembly properties have distinctively different effects on A-type and B-type lamins (Izumi et al, 2000; Schirmer et al, 2001; Vaughan et al, 2001) indicating that the two types of lamin might be incorporated into the lamina in different ways.

Lamin B2 head deletion mutants

Both lamin B2 head deletion mutants localized to the nuclear rim and did not influence endogenous lamin A and lamin B2 distribution. However, in cells expressing lamin B2 head deletion mutants nuclear shape was highly impaired. Biochemical fractionation showed that lamin B2 headless and lamin B2 $\Delta 32$ head were more soluble than transfected YFP-tagged wild type and endogenous lamin B2. These results are in support of previous studies which suggested that the head domain is required for efficient lamin assembly. *In vitro* analysis of headless lamin mutants demonstrated that the mutant proteins lose their ability to associate head to tail (Heitlinger et al, 1992; Stuurman et al, 1996). Other support for the role of the head domain in lamin assembly comes from experiments of nuclei assembled in *Xenopus* extracts, in which the nuclei failed to establish a normal organization of lamin B3 in the presence of headless lamin mutants (Moir et al, 2000; Spann et al, 1997). In mammalian cells, deletion of the head domain in lamin A lead to the formation of

nuclear aggregates, which resulted in the disruption of endogenous lamins A/C. In contrast, headless lamin B1 was shown to localize to the nuclear rim without any detectable effect on the nuclear lamina (Izumi et al, 2000). Therefore, the large majority of the results obtained from experiments with headless lamins demonstrated that their non-helical amino-terminal head domains are required for the formation of the head to tail interactions necessary for normal lamin assembly. They also showed that the function of the head domain in filament assembly is evolutionary conserved. The discrepancies in the behavior of headless lamin B2 protein and headless lamin B1 could reflect genuine differences between lamin B2 and lamin B1. We conclude from our results that the head domain of human lamin B2 is necessary for efficient lamin assembly. It is however not possible to decide from light microscopy data whether the shortened lamin B2 is only targeted correctly but not assembled properly, or if the head domain of lamin B2 is not engaged in lamina formation but the organization of other factors within the nuclear envelope.

Tailless lamin B2 mutants

The tailless lamin mutants LB2 tailless, LB2 Δ 32head/tailless, and LB2 rod did not localize to the nuclear rim and were distributed throughout the cytoplasm and the nucleoplasm. Immunofluorescence stainings with antibodies specific for lamin A and lamin B2 showed that the tailless lamin B2 proteins were not incorporated into the nuclear rim. However, endogenous lamin A and at least a portion of endogenous lamin B2 protein resided in the nuclear lamina. These findings indicate that a functional lamina can be assembled in the presence of tail deleted lamin B2 mutants. In cells expressing lamin B2 tailless, a fraction of lamin A co-localized with the mutant lamin B2 in the cytoplasm. It is conceivable that lamin B2 tailless forms heteropolymers with lamin A already in the cytoplasm and thus restrains it from being transported into the nucleus. However, it is also conceivable that LB2 tailless protein in the nucleus recruits lamin A from the nuclear lamina (see below) and is transported as heteromeric complex into the cytoplasm. Both possibilities suggest an important role of the lamin B2 head domain in heteropolymer formation and in the latter case also in the recruitment of lamin A from the nuclear envelope.

“Mitotic” lamins

The effect of lamin proteins mutated in the mitotic phosphoacceptor sites on the endogenous lamina has been analyzed by confocal laser scanning microscopy with antibodies specific for lamin A and lamin B2. Endogenous lamin A was localized at the nuclear rim but was also co-localizing with “mitotic” lamin B1 and “mitotic” lamin B2 at nuclear aggregates. Endogenous lamin B2 remained unaffected by the expression of mutant lamin B1 and localized at the nuclear rim. These findings are consistent with the fact that several dominant negative A-type and B-type lamin mutants that form nucleoplasmic aggregates cause the relocation of A-type lamins from the NE to the aggregates but do not affect the distribution of B-type lamins (Izumi et al, 2000; Vaughan et al, 2001). These findings suggest distinct differences in the organization of A-type and B-type lamins within lamina filaments. One explanation for this difference is related to the way in which the different lamin types are anchored to the nuclear envelope. B-type lamins remain farnesylated throughout their lifespan (Moir et al, 1995). The farnesylated modification is important but not sufficient for targeting and anchoring the protein to the INM, and a prenyl receptor is required for this association. In addition, the integral membrane protein LAP2 β also binds specifically to B-type lamins (Foisner & Gerace, 1993). Therefore it seems likely that B-type lamins are anchored to the nuclear envelope by interactions with integral membrane proteins at two separate points along the axis of the lamin dimer. In contrast, A-type lamins are not anchored through their tail domains and although there are integral membrane proteins that bind to A-type lamins (LAPs 1A, 1B, and emerin) these proteins also bind to B-type lamins (Gruenbaum et al, 2003). Therefore, specific associations between A-type lamins and integral membrane proteins may either not occur or may be less stable than associations between integral membrane proteins and B-type lamins. In light of the large number of integral membrane proteins, many more proteins may bind at the same time. Hence these are all preliminary speculations and it will be important in the future to define the network of interactions that tether lamins to the nuclear envelope. It has been suggested previously that dominant negative lamin mutants exert their effects by trapping lamins that are in a dynamic equilibrium between filamentous and soluble nucleoplasmic state (Ellis et al, 1997; Schmidt et al, 1994). Presumably in somatic cells A-type lamins are more mobile than B-type lamins for the reasons stated above.

Indeed, a significant proportion of A-type lamins is readily extracted from the lamina of a range of cell lines, whereas B-type lamins are completely insoluble (Hutchison et al, 2001). Thus, a combination of the greater affinity of A-type lamins for the mutant proteins and the greater solubility of A-type lamins means that these proteins are readily sequestered from the lamina to nucleoplasmic lamin aggregates, whereas B-type lamins are not.

In cells expressing "mitotic" lamin B2, the lamin B2 antibody staining was visible as rim-like structures surrounding the intranuclear aggregates. This effect might be due to sterical hindering of the lamin B2 antibody. It is conceivable that the lamin B2 antibody used first binds massively on the surface of the nuclear aggregates and thus hinders antibody penetration into the aggregates.

Biochemical fractionation showed that a portion of "mitotic" lamin B2 protein is more soluble as wild type lamin B2 protein. The solubility properties of endogenous lamin B2 were not influenced by the expression of "mitotic" lamin B2 mutants. This indicates that "mitotic" lamin B2 mutant proteins probably do not form heteropolymers with wild type lamin B2 due to their "mitotic" signal. We conclude from our results that a lamina structure can be assembled in the presence of both "mitotic" lamin B1 and "mitotic" lamin B2, however, "mitotic" lamin B2 segregates from endogenous lamin B2 protein.

5.3 Organization of the nuclear envelope

The lamina has important functions in anchoring the elements of the NE to their correct position, and the lamins as major elements of the lamina are crucial in this process. Anchorage functions of the lamins include the spacing of NPCs and the recruitment of proteins to the INM (Lenz-Bohme et al, 1997). In *Xenopus* sperm pronuclei B-type lamins interact with the nuclear pore protein nucleoporin 153 (Nup153). Moreover, disruption of lamina filaments with dominant negative lamin mutants causes a selective loss of Nup153 from NPCs (Smythe et al, 2000). Nup153 is located within the nucleoplasmic ring of NPCs (Walther et al, 2001). Hence it is in good proximity to lamin filaments and therefore it was proposed that lamina filaments interact with the nucleoplasmic ring of NPCs via Nup153, thereby anchoring NPCs within the NE. We could show that in cells expressing "mitotic" lamin B2

mutants Nup153 was accumulated at sites of membrane associated aggregates formed by the mutant protein. This suggests that the lamina filament structure necessary for correct positioning of the NPCs is interrupted by the presence of "mitotic" lamin B2 causing the observed rearrangement of Nup153.

Emerin and LAP1 are thought to be anchored at the INM through interactions with lamin A/C (Manilal et al, 1996; Nagano et al, 1996; Senior & Gerace, 1988; Sullivan et al, 1999). In contrast, members of the LAP2 family of INM proteins and LBR are believed to be anchored at the INM through interactions with lamin B (Harris et al, 1995; Ye & Worman, 1994). However, it was shown recently, that CAAX motif deleted lamin B protein fractionated independently of LBR, indicating that these two proteins do not bind directly to each other (Mical & Monteiro, 1998). We could show that deletion of the head or tail domain of lamin B2 does not interfere with proper emerin localization. In contrast, LBR was partially localized to the ER by the expression of head deleted lamin B2 mutants. Deletion of the lamin B2 head domain may lead to a weakening of a structural support network and thus LBR may either be partially retained in the ER after synthesis or be partially redistributed from the nuclear envelope to the ER. Further experiments will be needed to clarify whether the lamin B2 head domain is involved in a direct interaction with LBR. In cells expressing "mitotic" lamin B2 mutants, both emerin and LBR localized to the nuclear rim. However, LBR and emerin distribution was interrupted at sites where membrane associated "mitotic" lamin B2 aggregates occurred. These results clearly demonstrate that proper lamin filament assembly is a prerequisite for proper nuclear envelope organization.

5.4 The role of lamins in DNA replication

It is widely accepted that lamins play a role in DNA replication, but the mechanism how lamins take part in this process is elusive. Several laboratories have demonstrated that nuclear lamin proteins are essential for DNA replication in *Xenopus* egg extracts. Without lamin proteins, nuclear membranes assemble around *Xenopus* sperm chromatin but do not initiate replication. This has been observed when lamin-free nuclei are assembled either from extracts that were immunodepleted for lamins (Jenkins et al, 1993; Meier et al, 1991; Newport et al,

1990) or by supplementing extracts with dominant negative, i.e. headless lamin mutants (Ellis et al, 1997; Spann et al, 1997). When purified lamin B (but not lamin A) is re-added to depleted extracts, DNA replication is initiated, indicating that lamins might have a direct role in DNA replication (Goldberg et al, 1995). Further experiments employing dominant negative lamin mutants showed that intranuclear lamin aggregates formed by the mutant proteins had recruited endogenous B-type lamins to the aggregates as well as proliferating cell nuclear antigen (PCNA) and replication factor complex (RFC) (Ellis et al, 1997; Moir et al, 2000; Spann et al, 1997). This strongly suggests that lamins are involved in the elongation phase of DNA replication. In somatic cells, similar mutants still formed intranuclear aggregates. However, whereas A-type lamins were recruited to the aggregates, B-type lamins were not. In this case PCNA and prereplication complex Mcm proteins localized to mutant lamin aggregates demonstrating that, in mammalian cells, the association of nuclear proteins with dominant negative lamin mutants is not restricted to proteins exclusively present at the replication fork. Furthermore, DNA replication was not inhibited by the presence of the mutant proteins (Izumi et al, 2000). The interaction of "mitotic" lamin B2 mutant with PCNA is consistent with the observation of Moir et al. (Moir et al) and Izumi et al. (2000) that B-type lamins associate with late replication centers. Further studies are needed to clarify whether DNA replication is influenced by the presence of "mitotic" lamin proteins and whether other replication proteins are recruited to the intranuclear aggregates.

Although it appears clear that B-type lamins associate with sites of DNA replication and replication proteins, the role of lamins in DNA replication is still far from being resolved. The prospect of using RNAi to knock down the expression of specific lamins in mammalian cells probably provides the best opportunity to address this important issue (Harborth et al, 2001).

5.5 Role of lamins in chromatin organization

Due to the intimate spatial relationship between lamins and chromatin, it has been suggested that chromosomes are anchored, at least to some extent by the nuclear lamina. Indeed, all lamin subtypes have affinity for chromosomes, chromatin and/or DNA (Mattout-Drubezki & Gruenbaum, 2003). Several studies indicate that lamins

influence chromosome position in interphase (Bridger et al, 2007; Malhas et al, 2007). Further support for a role of lamins in chromatin organization comes from studies in laminopathy cell lines whereby chromatin is disorganized and observed coming away from the nuclear periphery (Columbaro et al, 2005; Filesi et al, 2005; Sewry et al, 2001). It is, however, not clear how changes in chromosome positioning take place and what the consequences for genome function are, i.e. gene expression. It is plausible that lamins are not purely anchorage sites for the genome but that they are involved in signaling pathways. In diseased cells these pathways may be perturbed, eliciting a reorganization of the genome and thereby changing the normal status of the cells. Heterochromatin, including centromeres, telomeres and repetitive DNA, is preferentially positioned near the nuclear envelope. Several studies suggest that the nuclear periphery may be a repressive environment for transcription of many genes (Mattout-Drubezki & Gruenbaum, 2003). Indeed, a growing number of transcription factors, including the transcriptional repressor germ-cell-less (GCL), Oct-1 and pRb either co-localize with the nuclear lamina or interact with proteins anchored to the lamina (Shaklai et al, 2007). Despite of this circumstantial evidence, still little is known about the molecular mechanisms responsible for nuclear-lamina dependent gene regulation. Although expression of lamin B2 deletion mutants in U2OS cells did not influence overall chromatin distribution as revealed by DAPI staining, it is possible that gene expression is altered by their presence. This issue should also be addressed in cells expressing "mitotic" lamin mutants, as chromatin distribution is massively affected by the formation of "mitotic" lamin nuclear aggregates. Lamin mutants together with the remarkable sensitivity of gene chip technology may provide the means to directly test if normal lamin organization is a requirement for transcription.

5.6 Lamins in ES cells

Only a few aspects of nuclear architecture have been characterized in detail in ES cells, but cursory observations indicate that many nuclear features, including the nuclear lamina, the nucleolus, heterochromatin structure and nuclear speckles, undergo morphological changes during the differentiation process (Meshorer & Misteli, 2006). In both mouse and human ES cells, lamin B1 and lamin B2 are

expressed in high levels (Constantinescu et al, 2006). In contrast, ES cells do not express A-type lamins. The absence of lamin A even serves as a specific stem cell marker in both mouse and human ES cells (Constantinescu et al, 2006). So far, there is no report about exogenous expression of lamins in ES cells and the influence of lamin mutants on cellular integrity. We have expressed YFP-lamin B1 and YFP-lamin B2 in mouse ES cells. As expected, both proteins localized to the nuclear periphery. In some cells transiently transfected with the respective expression plasmids, the nuclear envelope appeared as a rather thick structure. The variation of the thickness of the nuclear envelope might be explained by different expression levels of the proteins. It could further be shown that cells stably expressing YFP-lamin B1 and lamin B2 respectively, did not have a higher tendency to differentiate than untransfected cells. This indicates that exogenous expression of YFP-lamin B1 and YFP-lamin B2 fusion proteins does not influence the stem cell status of the cells. ES cells stably expressing YFP-lamin B1/B2 may provide the means to follow possible changes in lamina morphology during ES cell differentiation by time-lapse microscopy.

Expression of lamin B2 deletion mutants in mouse ES cells showed similar effects as those observed in U2OS cells. Both the YFP-lamin B2 Δ 32head and YFP-lamin B2 headless protein integrated into the nuclear rim. In some cells small aggregates along the nuclear envelope or invaginations of the nuclear lamina were observed. In contrast, YFP-lamin B2 tailless and YFP-lamin B2 rod were diffusely distributed throughout the cytoplasm and the nucleoplasm. These results suggest that lamin proteins are similarly processed and assembled into the nuclear lamina in both differentiated and ES cells. To date we can not make any statement about the influence of lamin B2 deletion mutants on differentiation.

ES cells are a valuable tool for further cell biological studies. They can be differentiated into all specialized cell types found in the adult mouse and exhibit and maintain a normal diploid complement of chromosomes. A complete characterization of the nuclear landscape in pluripotent ES cells will be a useful basis for a cell-biological understanding of these cells.

5.7 Identification of novel putative lamin interaction partners

With co-immunoprecipitation and mass spectrometry-based methodology we have identified new proteins potentially interacting with the soluble lamin B2 protein mutated from serine to aspartic acid in mitotic phosphorylation sites. Among the putative "mitotic" lamin B2 partners were found several ribosomal proteins (L4, L17, L18, S5, and S9). Ribosomal proteins are synthesized in the cytoplasm and are imported into the nucleolus where they, together with rRNA, are assembled to the ribosomal subunits. On their way to the nucleolus they might be trapped by the "mitotic" lamin B2 aggregates. Immunofluorescence stainings with antibodies specific for the ribosomal subunits could give further proof of this interaction.

Another putative "mitotic" lamin B2 interaction partner was identified as the heat shock protein 70 (Hsp70) family member mortalin which is heat-uninducible. Members of the Hsp70 family have been reported to be localized in almost all subcellular compartments including the nuclear matrix (Jethmalani & Henle, 1997; Pouchelet et al, 1983). Moreover, a recent study suggested that Hsp70 may play a role in the protection of nuclear lamins within the nuclear matrix (Willsie & Clegg, 2002). All Hsps70, regardless of location, bind proteins, particularly unfolded ones. The molecular chaperones of the Hsp70 family recognize and bind to nascent polypeptide chains as well as partially folded intermediates of proteins preventing their aggregation and misfolding. The binding of ATP triggers a critical conformational change leading to the release of the bound substrate protein (Fink, 1999). The universal ability of Hsp70 to undergo cycles of binding to and release from hydrophobic stretches of partially unfolded proteins determines their role in a great variety of vital intracellular functions such as protein synthesis, protein folding and oligomerization and protein transport. Mortalin is the major mitochondrial protein and it plays a central role in the elaborate translocation system for efficient import and export of proteins (Kaul et al., 2007). The biological function of mortalin is not restricted to its mitochondrial locale. Subcellular fractionation and immunofluorescence microscopy have revealed that mortalin is not only present in mitochondria but also in other extra-mitochondrial sites (Ran et al, 2000). Mortalin might keep "mitotic" lamin B2 in aggregates, thus preventing its refolding and assembly to its native oligomeric state.

It was recently suggested that mortalin is a regulator of oxidative stress and apoptosis, and contributes to aging and old-age pathologies (Kaul et al, 2007). Interestingly, overexpression of mortalin resulted in lifespan extension of normal human fibroblasts (Wadhwa et al, 2005). Hsp70F siRNA caused reduction in *C. elegans* lifespan and early appearance of progeria-like phenotype and age pigments (Yokoyama et al, 2002). So far nothing is known about a role of Hsp70/mortalin in HGPS, a disease caused by a mutation in the lamin A gene, which is characterized by accelerated aging. Whether this interaction is functional has to be tested by the use of different antibodies specific for mortalin.

Beside the above mentioned putative "mitotic" lamin B2 partners, other proteins were identified with which interaction seems very unlikely. Further experiments will be necessary to verify these interactions and to reduce unspecific interactions. One attempt would be to increase the buffer stringency and/or to perform the extraction of the cells in two steps, with the first one removing all cytoplasmic proteins and thus reducing cytoplasmic impurities. Furthermore, antibodies specific for the respective proteins will be needed to verify putative interactions by microscopical and biochemical methods.

5.8 Laminopathy

Transcripts with premature termination codons are rapidly degraded by NMD, if the premature stop locates 50-55 nucleotides 5' of a splicing-generated exon-exon junction (Nagy & Maquat, 1998). NMD is considered to be a surveillance pathway to prevent accumulation of potentially harmful truncated proteins and to properly regulate the expression of alternative splice products (Maquat, 2005). In a growing number of studies, modulating and protecting effects of NMD on the phenotype of hereditary disorders have already been demonstrated (Holbrook et al, 2004).

Here, a p.R321X nonsense mutation in the *LMNA* gene discovered in a family with cardiac conduction system disease and dilated cardiomyopathy was examined by immunohistochemistry, immunoblotting and quantitative PCR analysis. The mutation was most likely responsible for the disease for four reasons: i) the mutation clearly segregated with the disease: among eight family members examined, three members were affected and mutation carriers, while five members were healthy and

exhibited the wild type genotype; ii) screening of 434 control individuals only revealed the wild type genotype; iii) the mutation is not listed as a polymorphism in public databases, despite extensive screening of *LMNA* in many laboratories; iv) mutation screening of 24 additional known or novel candidate genes for DCM in patient III-5, including those for β -myosin heavy chain (*MYH7*), cardiac myosin binding-protein C (*MYBPC-3*) and cardiac troponin T (*TNNT2*), did not reveal extra mutations (Zeller et al, 2006).

Since the p.R321X nonsense mutation resides within the sixth of twelve *LMNA* exons, it was a likely target for NMD. In fact, quantitative analysis of *LMNA* transcripts in myocardial tissue and cultured fibroblasts clearly indicated significant downregulation of the mutant allele by NMD. Correspondingly, a truncated *LMNA* protein could not be detected at standard sensitivity of Western blotting, neither in myocardial tissue, nor in cultivated patient fibroblasts. Moreover, no indication of gross nuclear abnormalities or an aberrant cellular distribution of lamin A/C or its interaction partners LBR, emerin and lamin B2 could be observed: nuclei exhibited a normal ovoid shape, the heterochromatin appeared to be distributed normally, and all proteins investigated were properly targeted to the nuclear envelope. Similar observations of normal nuclear morphology and protein distribution have been made in a large number of patients heterozygous for missense mutations in the *LMNA* gene. In contrast, cells obtained from patients harbouring other *LMNA* mutations displayed a spectrum of nuclear abnormalities such as excess lobulation, extra nuclear speckles or even disruption of the nuclear membrane as well as dislocation of lamin A/C and associated proteins (Sylvius & Tesson, 2006). In a recent study, a comparable *LMNA* nonsense mutation, p.Y259X, was discovered in a heterozygous patient who suffered from autosomal dominant limb-girdle muscular dystrophy associated with conduction disturbances (LGMD1B) (Muchir et al, 2003). This mutation resided in the same region of lamin A/C's central α -helical coiled-coil rod domain, i.e. coil 2B, as the nonsense mutation described here. Like in our study, the heterozygous patient displayed normal nuclear morphology and protein distribution. In contrast, a newborn homozygous for the respective mutation died at birth. Cells of this patient displayed aberrant lobulation of nuclei and absence of lamin A/C and several of its interaction partners. Apparently, the wild type allele was sufficient in the heterozygous situation to prevent the dramatic phenotype and the cellular

abnormalities documented in the homozygote. The authors proposed haploinsufficiency as a likely explanation for the LGMD1B phenotype of the heterozygote, as they detected reduced levels of wild type lamin A/C in the affected patient. Haploinsufficiency, however, is not a likely explanation for the cardiac phenotype in patients analyzed in this study, as no obvious reduction in the absolute amount of wild type lamin A/C protein both in cardiac tissue and in cultured patient fibroblasts was observed.

Instead, insufficient NMD as the most likely reason for the observed disease phenotype is proposed. It was demonstrated a significantly reduced amount of mutant *LMNA* mRNA in both cardiac tissue and cultivated fibroblasts of affected patients. Although the mutant protein could not be detected in these specimens, the truncated protein was readily detectable after inhibition of the proteasomal protein degradation pathway in cultured fibroblasts of the more severely affected patient. Even though any obvious changes in nuclear shape or distribution of major inner nuclear membrane proteins such as emerin and LBR were not observed, a potential dominant negative effect of this mutant protein is likely to be responsible for the development of cardiomyopathy in the patients analyzed. Interestingly, the truncated protein was not detectable in another patient harbouring the mutation after treatment with epoxomicin at the level of sensitivity employed here, suggesting a more effective NMD and/or proteasomal degradation of the truncated mutant protein in this patient. Correspondingly, the disease phenotype in this patient is markedly less pronounced.

The question why patients with mutations in the *LMNA* gene develop distinct disease phenotypes, despite the lack of readily detectable nuclear abnormalities, still awaits a conclusive answer (Sylvius & Tesson, 2006). Presumably, gross structural abnormalities are not the primary pathogenic event in various types of laminopathies, but rather a reflection of disturbances in the more subtle regulatory functions of lamin A/C. A possible clue to explain the cardiac phenotype in the patients analyzed in this study may be derived from apparent tissue-dependent differences in the efficiency of NMD. A relatively weak reduction of mutant transcripts was observed in the left and right myocardium as compared to skin fibroblasts which displayed an up to 5-fold stronger reduction of mutant transcripts. It may therefore be suspected that NMD is not efficient enough in affected tissues to prevent the

deleterious effects of the expressed mutant p.R321X allele. Because of the lifelong high stress and intricate mechanical coupling of myocytes, the myocardium is apparently an especially critical tissue and, hence, particularly prone to disturbances by even weak cellular imbalances.

In summary, a family with DCM and conduction system disturbances most likely due to a nonsense mutation in the lamin A/C gene was described. It is proposed that NMD, though clearly measurable, cannot completely prevent the expression of truncated lamin A which may negatively interfere with structural and/or regulatory functions of lamin A/C, thus leading to the disease phenotype.

6 References

Aaronson RP, Blobel G (1975) Isolation of nuclear pore complexes in association with a lamina. *Proceedings of the National Academy of Sciences of the United States of America* **72**: 1007-1011

Aebi U, Cohn J, Buhle L, Gerace L (1986) The nuclear lamina is a meshwork of intermediate-type filaments. *Nature* **323**: 560-564

Akey CW (1989) Interactions and structure of the nuclear pore complex revealed by cryo-electron microscopy. *The Journal of cell biology* **109**: 955-970

Baens M, Noels H, Broeckx V, Hagens S, Fevery S, Billiau AD, Vankelecom H, Marynen P (2006) The dark side of EGFP: defective polyubiquitination. *PLoS ONE* **1**: e54

Barbie DA, Kudlow BA, Frock R, Zhao J, Johnson BR, Dyson N, Harlow E, Kennedy BK (2004) Nuclear reorganization of mammalian DNA synthesis prior to cell cycle exit. *Molecular and cellular biology* **24**: 595-607

Biamonti G, Giacca M, Perini G, Contreas G, Zentilin L, Weighardt F, Guerra M, Della Valle G, Saccone S, Riva S, et al. (1992) The gene for a novel human lamin maps at a highly transcribed locus of chromosome 19 which replicates at the onset of S-phase. *Molecular and cellular biology* **12**: 3499-3506

Bridger JM (2005) In *Visions of the cell nucleus*, Hemmerich P, Diekmann S (eds). American Scientific Publishers

Bridger JM, Foeger N, Kill IR, Herrmann H (2007) The nuclear lamina. Both a structural framework and a platform for genome organization. *The FEBS journal* **274**: 1354-1361

Bridger JM, Herrmann H, Munkel C, Lichter P (1998) Identification of an interchromosomal compartment by polymerization of nuclear-targeted vimentin. *Journal of cell science* **111 (Pt 9)**: 1241-1253

Bridger JM, Kill IR, O'Farrell M, Hutchison CJ (1993) Internal lamin structures within G1 nuclei of human dermal fibroblasts. *Journal of cell science* **104 (Pt 2)**: 297-306

Broers JL, Machiels BM, van Eys GJ, Kuijpers HJ, Manders EM, van Driel R, Ramaekers FC (1999) Dynamics of the nuclear lamina as monitored by GFP-tagged A-type lamins. *Journal of cell science* **112 (Pt 20)**: 3463-3475

Broers JL, Peeters EA, Kuijpers HJ, Endert J, Bouten CV, Oomens CW, Baaijens FP, Ramaekers FC (2004) Decreased mechanical stiffness in LMNA-/- cells is caused by defective nucleo-cytoskeletal integrity: implications for the development of laminopathies. *Human molecular genetics* **13**: 2567-2580

- Broers JL, Ramaekers FC, Bonne G, Yaou RB, Hutchison CJ (2006) Nuclear lamins: laminopathies and their role in premature ageing. *Physiological reviews* **86**: 967-1008
- Capell BC, Collins FS (2006) Human laminopathies: nuclei gone genetically awry. *Nat Rev Genet* **7**: 940-952
- Cohen M, Lee KK, Wilson KL, Gruenbaum Y (2001) Transcriptional repression, apoptosis, human disease and the functional evolution of the nuclear lamina. *Trends in biochemical sciences* **26**: 41-47
- Columbaro M, Capanni C, Mattioli E, Novelli G, Parnaik VK, Squarzoni S, Maraldi NM, Lattanzi G (2005) Rescue of heterochromatin organization in Hutchinson-Gilford progeria by drug treatment. *Cell Mol Life Sci* **62**: 2669-2678
- Constantinescu D, Gray HL, Sammak PJ, Schatten GP, Csoka AB (2006) Lamin A/C expression is a marker of mouse and human embryonic stem cell differentiation. *Stem cells (Dayton, Ohio)* **24**: 177-185
- Corrigan DP, Kuszczak D, Rusinol AE, Thewke DP, Hrycyna CA, Michaelis S, Sinensky MS (2005) Prelamin A endoproteolytic processing in vitro by recombinant Zmpste24. *The Biochemical journal* **387**: 129-138
- Daigle N, Beaudouin J, Hartnell L, Imreh G, Hallberg E, Lippincott-Schwartz J, Ellenberg J (2001) Nuclear pore complexes form immobile networks and have a very low turnover in live mammalian cells. *The Journal of cell biology* **154**: 71-84
- Dechat T, Korbei B, Vaughan OA, Vlcek S, Hutchison CJ, Foisner R (2000) Lamina-associated polypeptide 2alpha binds intranuclear A-type lamins. *Journal of cell science* **113 Pt 19**: 3473-3484
- Dimitrova DS, Berezney R (2002) The spatio-temporal organization of DNA replication sites is identical in primary, immortalized and transformed mammalian cells. *Journal of cell science* **115**: 4037-4051
- Dreger CK, Konig AR, Spring H, Lichter P, Herrmann H (2002) Investigation of nuclear architecture with a domain-presenting expression system. *Journal of structural biology* **140**: 100-115
- Dwyer N, Blobel G (1976) A modified procedure for the isolation of a pore complex-lamina fraction from rat liver nuclei. *The Journal of cell biology* **70**: 581-591
- Dyer JA, Lane BE, Hutchison CJ (1999) Investigations of the pathway of incorporation and function of lamin A in the nuclear lamina. *Microscopy research and technique* **45**: 1-12
- Ellis DJ, Jenkins H, Whitfield WG, Hutchison CJ (1997) GST-lamin fusion proteins act as dominant negative mutants in Xenopus egg extract and reveal the function of the lamina in DNA replication. *Journal of cell science* **110 (Pt 20)**: 2507-2518

- Erber A, Riemer D, Hofemeister H, Bovenschulte M, Stick R, Panopoulou G, Lehrach H, Weber K (1999) Characterization of the Hydra lamin and its gene: A molecular phylogeny of metazoan lamins. *Journal of molecular evolution* **49**: 260-271
- Fawcett DW (1966) On the occurrence of a fibrous lamina on the inner aspect of the nuclear envelope in certain cells of vertebrates. *The American journal of anatomy* **119**: 129-145
- Filesi I, Gullotta F, Lattanzi G, D'Apice MR, Capanni C, Nardone AM, Columbaro M, Scarano G, Mattioli E, Sabatelli P, Maraldi NM, Biocca S, Novelli G (2005) Alterations of nuclear envelope and chromatin organization in mandibuloacral dysplasia, a rare form of laminopathy. *Physiological genomics* **23**: 150-158
- Fink AL (1999) Chaperone-mediated protein folding. *Physiological reviews* **79**: 425-449
- Fisher DZ, Chaudhary N, Blobel G (1986) cDNA sequencing of nuclear lamins A and C reveals primary and secondary structural homology to intermediate filament proteins. *Proceedings of the National Academy of Sciences of the United States of America* **83**: 6450-6454
- Foisner R, Gerace L (1993) Integral membrane proteins of the nuclear envelope interact with lamins and chromosomes, and binding is modulated by mitotic phosphorylation. *Cell* **73**: 1267-1279
- Franke WW (1988) Matthias Jacob Schleiden and the definition of the cell nucleus. *Eur J Cell Biol* **47**: 145-156
- Fricker M, Hollinshead M, White N, Vaux D (1997) Interphase nuclei of many mammalian cell types contain deep, dynamic, tubular membrane-bound invaginations of the nuclear envelope. *The Journal of cell biology* **136**: 531-544
- Furukawa K, Hotta Y (1993) cDNA cloning of a germ cell specific lamin B3 from mouse spermatocytes and analysis of its function by ectopic expression in somatic cells. *The EMBO journal* **12**: 97-106
- Furukawa K, Inagaki H, Hotta Y (1994) Identification and cloning of an mRNA coding for a germ cell-specific A-type lamin in mice. *Experimental cell research* **212**: 426-430
- Furukawa K, Kondo T (1998) Identification of the lamina-associated-polypeptide-2-binding domain of B-type lamin. *European journal of biochemistry / FEBS* **251**: 729-733
- Geiger SK, Bär H, Ehlermann P, Wälde S, Rutschow D, Zeller R, Ivandic BT, Zentgraf H, Katus HA, Herrmann H, Weichenhan D (2008) Incomplete nonsense-mediated decay of mutant lamin A/C mRNA provokes dilated cardiomyopathy and ventricular tachycardia. *Journal of molecular medicine* **86**: 281-289

- Gerace L, Blum A, Blobel G (1978) Immunocytochemical localization of the major polypeptides of the nuclear pore complex-lamina fraction. Interphase and mitotic distribution. *The Journal of cell biology* **79**: 546-566
- Gerace L, Burke B (1988) Functional organization of the nuclear envelope. *Annual review of cell biology* **4**: 335-374
- Glass CA, Glass JR, Taniura H, Hasel KW, Blevitt JM, Gerace L (1993) The alpha-helical rod domain of human lamins A and C contains a chromatin binding site. *The EMBO journal* **12**: 4413-4424
- Goldberg M, Harel A, Gruenbaum Y (1999) The nuclear lamina: molecular organization and interaction with chromatin. *Critical reviews in eukaryotic gene expression* **9**: 285-293
- Goldberg M, Jenkins H, Allen T, Whitfield WG, Hutchison CJ (1995) Xenopus lamin B3 has a direct role in the assembly of a replication competent nucleus: evidence from cell-free egg extracts. *Journal of cell science* **108 (Pt 11)**: 3451-3461
- Goldberg MW, Allen TD (1996) The nuclear pore complex and lamina: three-dimensional structures and interactions determined by field emission in-lens scanning electron microscopy. *Journal of molecular biology* **257**: 848-865
- Goldman AE, Maul G, Steinert PM, Yang HY, Goldman RD (1986) Keratin-like proteins that coisolate with intermediate filaments of BHK-21 cells are nuclear lamins. *Proceedings of the National Academy of Sciences of the United States of America* **83**: 3839-3843
- Goldman AE, Moir RD, Montag-Lowy M, Stewart M, Goldman RD (1992) Pathway of incorporation of microinjected lamin A into the nuclear envelope. *The Journal of cell biology* **119**: 725-735
- Gruenbaum Y, Goldman RD, Meyuhas R, Mills E, Margalit A, Fridkin A, Dayani Y, Prokocimer M, Enosh A (2003) The nuclear lamina and its functions in the nucleus. *International review of cytology* **226**: 1-62
- Gruenbaum Y, Margalit A, Goldman RD, Shumaker DK, Wilson KL (2005) The nuclear lamina comes of age. *Nature reviews* **6**: 21-31
- Harborth J, Elbashir SM, Bechert K, Tuschl T, Weber K (2001) Identification of essential genes in cultured mammalian cells using small interfering RNAs. *Journal of cell science* **114**: 4557-4565
- Harris CA, Andryuk PJ, Cline SW, Mathew S, Siekierka JJ, Goldstein G (1995) Structure and mapping of the human thymopoietin (TMPO) gene and relationship of human TMPO beta to rat lamin-associated polypeptide 2. *Genomics* **28**: 198-205
- Heald R, McKeon F (1990) Mutations of phosphorylation sites in lamin A that prevent nuclear lamina disassembly in mitosis. *Cell* **61**: 579-589

- Heitlinger E, Peter M, Lustig A, Villiger W, Nigg EA, Aebi U (1992) The role of the head and tail domain in lamin structure and assembly: analysis of bacterially expressed chicken lamin A and truncated B2 lamins. *Journal of structural biology* **108**: 74-89
- Herrmann H, Bar H, Kreplak L, Strelkov SV, Aebi U (2007) Intermediate filaments: from cell architecture to nanomechanics. *Nature reviews* **8**: 562-573
- Herrmann H, Eckelt A, Brettel M, Grund C, Franke WW (1993) Temperature-sensitive intermediate filament assembly. Alternative structures of *Xenopus laevis* vimentin in vitro and in vivo. *Journal of molecular biology* **234**: 99-113
- Herrmann H, Foisner R (2003) Intermediate filaments: novel assembly models and exciting new functions for nuclear lamins. *Cell Mol Life Sci* **60**: 1607-1612
- Hoger TH, Grund C, Franke WW, Krohne G (1991) Immunolocalization of lamins in the thick nuclear lamina of human synovial cells. *European journal of cell biology* **54**: 150-156
- Holbrook JA, Neu-Yilik G, Hentze MW, Kulozik AE (2004) Nonsense-mediated decay approaches the clinic. *Nature genetics* **36**: 801-808
- Hozak P, Sasseville AM, Raymond Y, Cook PR (1995) Lamin proteins form an internal nucleoskeleton as well as a peripheral lamina in human cells. *Journal of cell science* **108 (Pt 2)**: 635-644
- Hutchison CJ, Alvarez-Reyes M, Vaughan OA (2001) Lamins in disease: why do ubiquitously expressed nuclear envelope proteins give rise to tissue-specific disease phenotypes? *Journal of cell science* **114**: 9-19
- Izumi M, Vaughan OA, Hutchison CJ, Gilbert DM (2000) Head and/or CaaX domain deletions of lamin proteins disrupt preformed lamin A and C but not lamin B structure in mammalian cells. *Molecular biology of the cell* **11**: 4323-4337
- Jagatheesan G, Thanumalayan S, Muralikrishna B, Rangaraj N, Karande AA, Parnaik VK (1999) Colocalization of intranuclear lamin foci with RNA splicing factors. *Journal of cell science* **112 (Pt 24)**: 4651-4661
- Jenkins H, Holman T, Lyon C, Lane B, Stick R, Hutchison C (1993) Nuclei that lack a lamina accumulate karyophilic proteins and assemble a nuclear matrix. *Journal of cell science* **106 (Pt 1)**: 275-285
- Jethmalani SM, Henle KJ (1997) Intracellular distribution of stress glycoproteins in a heat-resistant cell model expressing human HSP70. *Biochemical and biophysical research communications* **237**: 382-387
- Kaul SC, Deocaris CC, Wadhwa R (2007) Three faces of mortalin: a housekeeper, guardian and killer. *Experimental gerontology* **42**: 263-274

- Kennedy BK, Barbie DA, Classon M, Dyson N, Harlow E (2000) Nuclear organization of DNA replication in primary mammalian cells. *Genes & development* **14**: 2855-2868
- Kumaran RI, Muralikrishna B, Parnaik VK (2002) Lamin A/C speckles mediate spatial organization of splicing factor compartments and RNA polymerase II transcription. *The Journal of cell biology* **159**: 783-793
- Lammerding J, Schulze PC, Takahashi T, Kozlov S, Sullivan T, Kamm RD, Stewart CL, Lee RT (2004) Lamin A/C deficiency causes defective nuclear mechanics and mechanotransduction. *The Journal of clinical investigation* **113**: 370-378
- Lamond AI, Sleeman JE (2003) Nuclear substructure and dynamics. *Curr Biol* **13**: R825-828
- Lenz-Bohme B, Wismar J, Fuchs S, Reifegerste R, Buchner E, Betz H, Schmitt B (1997) Insertional mutation of the *Drosophila* nuclear lamin Dm0 gene results in defective nuclear envelopes, clustering of nuclear pore complexes, and accumulation of annulate lamellae. *The Journal of cell biology* **137**: 1001-1016
- Leonhardt H, Rahn HP, Weinzierl P, Sporbert A, Cremer T, Zink D, Cardoso MC (2000) Dynamics of DNA replication factories in living cells. *The Journal of cell biology* **149**: 271-280
- Lin F, Worman HJ (1995) Structural organization of the human gene (LMNB1) encoding nuclear lamin B1. *Genomics* **27**: 230-236
- Loewinger L, McKeon F (1988) Mutations in the nuclear lamin proteins resulting in their aberrant assembly in the cytoplasm. *The EMBO journal* **7**: 2301-2309
- Luderus ME, de Graaf A, Mattia E, den Blaauwen JL, Grande MA, de Jong L, van Driel R (1992) Binding of matrix attachment regions to lamin B1. *Cell* **70**: 949-959
- Machiels BM, Zorenc AH, Endert JM, Kuijpers HJ, van Eys GJ, Ramaekers FC, Broers JL (1996) An alternative splicing product of the lamin A/C gene lacks exon 10. *The Journal of biological chemistry* **271**: 9249-9253
- Malhas A, Lee CF, Sanders R, Saunders NJ, Vaux DJ (2007) Defects in lamin B1 expression or processing affect interphase chromosome position and gene expression. *The Journal of cell biology* **176**: 593-603
- Manilal S, Nguyen TM, Sewry CA, Morris GE (1996) The Emery-Dreifuss muscular dystrophy protein, emerin, is a nuclear membrane protein. *Human molecular genetics* **5**: 801-808
- Maquat LE (2005) Nonsense-mediated mRNA decay in mammals. *Journal of cell science* **118**: 1773-1776

- Markiewicz E, Dechat T, Foisner R, Quinlan RA, Hutchison CJ (2002) Lamin A/C binding protein LAP2alpha is required for nuclear anchorage of retinoblastoma protein. *Molecular biology of the cell* **13**: 4401-4413
- Mattout-Drubezki A, Gruenbaum Y (2003) Dynamic interactions of nuclear lamina proteins with chromatin and transcriptional machinery. *Cell Mol Life Sci* **60**: 2053-2063
- Mattout A, Dechat T, Adam SA, Goldman RD, Gruenbaum Y (2006) Nuclear lamins, diseases and aging. *Current opinion in cell biology* **18**: 335-341
- McKeon FD, Kirschner MW, Caput D (1986) Homologies in both primary and secondary structure between nuclear envelope and intermediate filament proteins. *Nature* **319**: 463-468
- Meier J, Campbell KH, Ford CC, Stick R, Hutchison CJ (1991) The role of lamin LIII in nuclear assembly and DNA replication, in cell-free extracts of *Xenopus* eggs. *Journal of cell science* **98 (Pt 3)**: 271-279
- Meshorer E, Misteli T (2006) Chromatin in pluripotent embryonic stem cells and differentiation. *Nature reviews* **7**: 540-546
- Mical TI, Monteiro MJ (1998) The role of sequences unique to nuclear intermediate filaments in the targeting and assembly of human lamin B: evidence for lack of interaction of lamin B with its putative receptor. *Journal of cell science* **111 (Pt 23)**: 3471-3485
- Moir RD, Donaldson AD, Stewart M (1991) Expression in *Escherichia coli* of human lamins A and C: influence of head and tail domains on assembly properties and paracrystal formation. *Journal of cell science* **99 (Pt 2)**: 363-372
- Moir RD, Montag-Lowy M, Goldman RD (1994) Dynamic properties of nuclear lamins: lamin B is associated with sites of DNA replication. *The Journal of cell biology* **125**: 1201-1212
- Moir RD, Spann TP, Goldman RD (1995) The dynamic properties and possible functions of nuclear lamins. *International review of cytology* **162B**: 141-182
- Moir RD, Spann TP, Lopez-Soler RI, Yoon M, Goldman AE, Khuon S, Goldman RD (2000) Review: the dynamics of the nuclear lamins during the cell cycle-- relationship between structure and function. *Journal of structural biology* **129**: 324-334
- Muchir A, van Engelen BG, Lammens M, Mislow JM, McNally E, Schwartz K, Bonne G (2003) Nuclear envelope alterations in fibroblasts from LGMD1B patients carrying nonsense Y259X heterozygous or homozygous mutation in lamin A/C gene. *Experimental cell research* **291**: 352-362

- Nagano A, Koga R, Ogawa M, Kurano Y, Kawada J, Okada R, Hayashi YK, Tsukahara T, Arahata K (1996) Emerin deficiency at the nuclear membrane in patients with Emery-Dreifuss muscular dystrophy. *Nature genetics* **12**: 254-259
- Nagy E, Maquat LE (1998) A rule for termination-codon position within intron-containing genes: when nonsense affects RNA abundance. *Trends in biochemical sciences* **23**: 198-199
- Newport JW, Wilson KL, Dunphy WG (1990) A lamin-independent pathway for nuclear envelope assembly. *The Journal of cell biology* **111**: 2247-2259
- Nigg EA (1989) The nuclear envelope. *Current opinion in cell biology* **1**: 435-440
- Nigg EA (1992) Assembly and cell cycle dynamics of the nuclear lamina. *Seminars in cell biology* **3**: 245-253
- Nigg EA, Kitten GT, Vorburger K (1992) Targeting lamin proteins to the nuclear envelope: the role of CaaX box modifications. *Biochemical Society transactions* **20**: 500-504
- Nikolova V, Leimena C, McMahon AC, Tan JC, Chandar S, Jogia D, Kesteven SH, Michalick J, Otway R, Verheyen F, Rainer S, Stewart CL, Martin D, Feneley MP, Fatkin D (2004) Defects in nuclear structure and function promote dilated cardiomyopathy in lamin A/C-deficient mice. *The Journal of clinical investigation* **113**: 357-369
- Peter M, Heitlinger E, Haner M, Aebi U, Nigg EA (1991) Disassembly of in vitro formed lamin head-to-tail polymers by CDC2 kinase. *The EMBO journal* **10**: 1535-1544
- Peter M, Kitten GT, Lehner CF, Vorburger K, Bailer SM, Maridor G, Nigg EA (1989) Cloning and sequencing of cDNA clones encoding chicken lamins A and B1 and comparison of the primary structures of vertebrate A- and B-type lamins. *Journal of molecular biology* **208**: 393-404
- Peter M, Nakagawa J, Doree M, Labbe JC, Nigg EA (1990) In vitro disassembly of the nuclear lamina and M phase-specific phosphorylation of lamins by cdc2 kinase. *Cell* **61**: 591-602
- Pouchelet M, St-Pierre E, Bibor-Hardy V, Simard R (1983) Localization of the 70 000 dalton heat-induced protein in the nuclear matrix of BHK cells. *Experimental cell research* **149**: 451-459
- Prufert K, Vogel A, Krohne G (2004) The lamin CxxM motif promotes nuclear membrane growth. *Journal of cell science* **117**: 6105-6116
- Ralle T, Grund C, Franke WW, Stick R (2004) Intranuclear membrane structure formations by CaaX-containing nuclear proteins. *Journal of cell science* **117**: 6095-6104

- Ran Q, Wadhwa R, Kawai R, Kaul SC, Sifers RN, Bick RJ, Smith JR, Pereira-Smith OM (2000) Extramitochondrial localization of mortalin/mthsp70/PBP74/GRP75. *Biochemical and biophysical research communications* **275**: 174-179
- Rao L, Perez D, White E (1996) Lamin proteolysis facilitates nuclear events during apoptosis. *The Journal of cell biology* **135**: 1441-1455
- Reichenzeller M (2002) Strukturelle und dynamische Analyse des Interchromosomal Domänen Kompartiments. Biologische Fakultät, Ruprecht-Karls-Universität, Heidelberg,
- Reichenzeller M, Burzlaff A, Lichter P, Herrmann H (2000) In vivo observation of a nuclear channel-like system: evidence for a distinct interchromosomal domain compartment in interphase cells. *Journal of structural biology* **129**: 175-185
- Riemer D, Wang J, Zimek A, Swalla BJ, Weber K (2000) Tunicates have unusual nuclear lamins with a large deletion in the carboxyterminal tail domain. *Gene* **255**: 317-325
- Rober RA, Weber K, Osborn M (1989) Differential timing of nuclear lamin A/C expression in the various organs of the mouse embryo and the young animal: a developmental study. *Development (Cambridge, England)* **105**: 365-378
- Rogers KR, Eckelt A, Nimmrich V, Janssen KP, Schliwa M, Herrmann H, Franke WW (1995) Truncation mutagenesis of the non-alpha-helical carboxyterminal tail domain of vimentin reveals contributions to cellular localization but not to filament assembly. *European journal of cell biology* **66**: 136-150
- Ruchaud S, Korfali N, Villa P, Kottke TJ, Dingwall C, Kaufmann SH, Earnshaw WC (2002) Caspase-6 gene disruption reveals a requirement for lamin A cleavage in apoptotic chromatin condensation. *The EMBO journal* **21**: 1967-1977
- Sasseville AM, Raymond Y (1995) Lamin A precursor is localized to intranuclear foci. *Journal of cell science* **108 (Pt 1)**: 273-285
- Scheer U, Kartenbeck J, Trendelenburg MF, Stadler J, Franke WW (1976) Experimental disintegration of the nuclear envelope. Evidence for pore-connecting fibrils. *The Journal of cell biology* **69**: 1-18
- Schirmer EC, Florens L, Guan T, Yates JR, 3rd, Gerace L (2003) Nuclear membrane proteins with potential disease links found by subtractive proteomics. *Science (New York, NY)* **301**: 1380-1382
- Schirmer EC, Guan T, Gerace L (2001) Involvement of the lamin rod domain in heterotypic lamin interactions important for nuclear organization. *The Journal of cell biology* **153**: 479-489

- Schmidt M, Tschodrich-Rotter M, Peters R, Krohne G (1994) Properties of fluorescently labeled Xenopus lamin A in vivo. *European journal of cell biology* **65**: 70-81
- Schneider S, Folprecht G, Krohne G, Oberleithner H (1995) Immunolocalization of lamins and nuclear pore complex proteins by atomic force microscopy. *Pflugers Arch* **430**: 795-801
- Senior A, Gerace L (1988) Integral membrane proteins specific to the inner nuclear membrane and associated with the nuclear lamina. *The Journal of cell biology* **107**: 2029-2036
- Sewry CA, Brown SC, Mercuri E, Bonne G, Feng L, Camici G, Morris GE, Muntoni F (2001) Skeletal muscle pathology in autosomal dominant Emery-Dreifuss muscular dystrophy with lamin A/C mutations. *Neuropathology and applied neurobiology* **27**: 281-290
- Shaklai S, Amariglio N, Rechavi G, Simon AJ (2007) Gene silencing at the nuclear periphery. *The FEBS journal* **274**: 1383-1392
- Shumaker DK, Lee KK, Tanhehco YC, Craigie R, Wilson KL (2001) LAP2 binds to BAF.DNA complexes: requirement for the LEM domain and modulation by variable regions. *The EMBO journal* **20**: 1754-1764
- Smythe C, Jenkins HE, Hutchison CJ (2000) Incorporation of the nuclear pore basket protein nup153 into nuclear pore structures is dependent upon lamina assembly: evidence from cell-free extracts of Xenopus eggs. *The EMBO journal* **19**: 3918-3931
- Spann TP, Goldman AE, Wang C, Huang S, Goldman RD (2002) Alteration of nuclear lamin organization inhibits RNA polymerase II-dependent transcription. *The Journal of cell biology* **156**: 603-608
- Spann TP, Moir RD, Goldman AE, Stick R, Goldman RD (1997) Disruption of nuclear lamin organization alters the distribution of replication factors and inhibits DNA synthesis. *The Journal of cell biology* **136**: 1201-1212
- Spector DL (2003) The dynamics of chromosome organization and gene regulation. *Annual review of biochemistry* **72**: 573-608
- Steen RL, Collas P (2001) Mistargeting of B-type lamins at the end of mitosis: implications on cell survival and regulation of lamins A/C expression. *The Journal of cell biology* **153**: 621-626
- Steen RL, Martins SB, Tasken K, Collas P (2000) Recruitment of protein phosphatase 1 to the nuclear envelope by A-kinase anchoring protein AKAP149 is a prerequisite for nuclear lamina assembly. *The Journal of cell biology* **150**: 1251-1262

- Stierle V, Couprie J, Ostlund C, Krimm I, Zinn-Justin S, Hossenlopp P, Worman HJ, Courvalin JC, Duband-Goulet I (2003) The carboxyl-terminal region common to lamins A and C contains a DNA binding domain. *Biochemistry* **42**: 4819-4828
- Stuurman N, Heins S, Aebi U (1998) Nuclear lamins: their structure, assembly, and interactions. *Journal of structural biology* **122**: 42-66
- Stuurman N, Sasse B, Fisher PA (1996) Intermediate filament protein polymerization: molecular analysis of *Drosophila* nuclear lamin head-to-tail binding. *Journal of structural biology* **117**: 1-15
- Sullivan T, Escalante-Alcalde D, Bhatt H, Anver M, Bhat N, Nagashima K, Stewart CL, Burke B (1999) Loss of A-type lamin expression compromises nuclear envelope integrity leading to muscular dystrophy. *The Journal of cell biology* **147**: 913-920
- Sylvius N, Tesson F (2006) Lamin A/C and cardiac diseases. *Current opinion in cardiology* **21**: 159-165
- Taniura H, Glass C, Gerace L (1995) A chromatin binding site in the tail domain of nuclear lamins that interacts with core histones. *The Journal of cell biology* **131**: 33-44
- Vaughan A, Alvarez-Reyes M, Bridger JM, Broers JL, Ramaekers FC, Wehnert M, Morris GE, Whitfield WGF, Hutchison CJ (2001) Both emerin and lamin C depend on lamin A for localization at the nuclear envelope. *Journal of cell science* **114**: 2577-2590
- Vecerova J, Koberna K, Malinsky J, Soutoglou E, Sullivan T, Stewart CL, Raska I, Misteli T (2004) Formation of nuclear splicing factor compartments is independent of lamins A/C. *Molecular biology of the cell* **15**: 4904-4910
- Vergnes L, Peterfy M, Bergo MO, Young SG, Reue K (2004) Lamin B1 is required for mouse development and nuclear integrity. *Proceedings of the National Academy of Sciences of the United States of America* **101**: 10428-10433
- Wadhwa R, Takano S, Kaur K, Aida S, Yaguchi T, Kaul Z, Hirano T, Taira K, Kaul SC (2005) Identification and characterization of molecular interactions between mortalin/mtHsp70 and HSP60. *The Biochemical journal* **391**: 185-190
- Walther TC, Fornerod M, Pickersgill H, Goldberg M, Allen TD, Mattaj IW (2001) The nucleoporin Nup153 is required for nuclear pore basket formation, nuclear pore complex anchoring and import of a subset of nuclear proteins. *The EMBO journal* **20**: 5703-5714
- Weber K, Plessmann U, Traub P (1989) Maturation of nuclear lamin A involves a specific carboxy-terminal trimming, which removes the polyisoprenylation site from the precursor; implications for the structure of the nuclear lamina. *FEBS letters* **257**: 411-414

- Willsie JK, Clegg JS (2002) Small heat shock protein p26 associates with nuclear lamins and HSP70 in nuclei and nuclear matrix fractions from stressed cells. *Journal of cellular biochemistry* **84**: 601-614
- Worman HJ, Courvalin JC (2005) Nuclear envelope, nuclear lamina, and inherited disease. *International review of cytology* **246**: 231-279
- Wydner KL, McNeil JA, Lin F, Worman HJ, Lawrence JB (1996) Chromosomal assignment of human nuclear envelope protein genes LMNA, LMNB1, and LBR by fluorescence in situ hybridization. *Genomics* **32**: 474-478
- Yang L, Guan T, Gerace L (1997) Lamin-binding fragment of LAP2 inhibits increase in nuclear volume during the cell cycle and progression into S phase. *The Journal of cell biology* **139**: 1077-1087
- Ye Q, Worman HJ (1994) Primary structure analysis and lamin B and DNA binding of human LBR, an integral protein of the nuclear envelope inner membrane. *The Journal of biological chemistry* **269**: 11306-11311
- Yokoyama K, Fukumoto K, Murakami T, Harada S, Hosono R, Wadhwa R, Mitsui Y, Ohkuma S (2002) Extended longevity of *Caenorhabditis elegans* by knocking in extra copies of hsp70F, a homolog of mot-2 (mortalin)/mthsp70/Grp75. *FEBS letters* **516**: 53-57
- Zeller R, Ivandic BT, Ehlermann P, Mucke O, Zugck C, Remppis A, Giannitsis E, Katus HA, Weichenhan D (2006) Large-scale mutation screening in patients with dilated or hypertrophic cardiomyopathy: a pilot study using DGGE. *Journal of molecular medicine (Berlin, Germany)* **84**: 682-691

7 Abbreviations

aa	amino acid
Acc. No.	accession number
APS	ammonium persulfate
BSA	bovine serum albumin
cDNA	complementary DNA
DAPI	4', 6-diamidin-2'-phenylindol-dihydrochloride
DCM	dilated cardiomyopathy
ddH ₂ O	double distilled water
DMEM	Dulbeccos modified Eagle Medium
DMSO	dimethylsulfoxide
DNA	deoxyribonucleic acid
DNase	deoxyribonuclease
dNTP	2'-deoxyribonucleoside
DTT	dithiothreitol
<i>E. coli</i>	<i>Escherichia coli</i>
ECFP	enhanced cyan fluorescent protein
ECL	electro-chemo luminescence
EDTA	ethylenediaminetetraacetate-disodium salt
EGFP	enhanced green fluorescent protein
EGTA	ethyleneglycoltetraacetate
EDMD	Emery-Dreifuss muscular dystrophy
ER	endoplasmatic reticulum
EYFP	enhanced yellow fluorescent protein
FCS	fetal calf serum
H2A	histone H2A
HGPS	Hutchinson-Gilford progeria syndrome
IF	immunofluorescence
INM	inner nuclear membrane
IP	immunoprecipitation

kDa	kilo Dalton
LA/C	lamin A/C
LB	“Luria Bertani”, full medium for bacteria
LB1	lamin B1
LB2	lamin B2
LBR	lamin B receptor
<i>LMNA</i>	lamin A gene
MCS	multiple cloning site
MOPS	morpholinepropanesulfonic acid
mRNA	messenger ribonucleic acid
NLS	nuclear localization sequence
NMD	nonsense mediated decay
NPC	nuclear pore complex
ONM	outer nuclear membrane
PBS	phosphate buffered salt solution
PCR	polymerase chain reaction
PFA	paraformaldehyde
PVDF	phenylmethylsulfonylfluoride
rpm	rotations per minute
RT	room temperature
RZPD	German Resource Center for Genome Research
SDS	sodium dodecyl sulphate
Tris	N, N, N-tris[hydroxymethyl]aminomethan

8 Appendix

Sample	Acc. Nr.	Protein Description	Protein score	Protein Mass	matches
1	gi 31621305	leucine-rich PPR motif-containing protein	1767	159003	40
2	gi 27436951	lamin B2	1297	67762	29
	gi 14595132	Raichu404X	218	85646	5
3	gi 27436951	lamin B2	1143	67762	26
	gi 12653415	Heat shock 70kDa protein 9 (mortalin)	1045	73967	20
	gi 14595132	Raichu404X	232	85646	6
4	gi 27436951	lamin B2	583	67762	17
	gi 14595132	Raichu404X	234	85646	8
	gi 425518	anti-colorectal carcinoma heavy chain	66	51254	3
	gi 5031753	heterogeneous nuclear ribonucleoprotein H1	55	49484	3
	gi 1710248	protein disulfide isomerase-related protein 5	49	46512	1*
5	gi 27436951	lamin B2	281	67762	14
	gi 34234	laminin-binding protein	204	31888	8
	gi 16579885	ribosomal protein L4	168	47953	8
	gi 425518	anti-colorectal carcinoma heavy chain	120	51254	5
	gi 2695641	mammary tumor-associated protein INT6	68	52443	3
	gi 21361809	RNA binding motif protein, X-linked-like 1	62	42173	1*
	gi 870743	heterogeneous nuclear ribonucleoprotein D	43	30523	3
6	gi 27436951	lamin B2	911	67762	24
	gi 28336	mutant beta-actin (beta'-actin)	200	42128	6
	gi 1706611	Elongation factor Tu, mitochondrial precursor (EF-Tu)	120	49852	3
	gi 16579885	ribosomal protein L4	66	47953	3
	gi 4506649	ribosomal protein L3 isoform a	39	46365	1*
7	gi 27436951	lamin B2	282	67762	6
	gi 4506607	ribosomal protein L18	189	21735	3
	gi 14141193	ribosomal protein S9	163	22635	6
	gi 14595132	Raichu404X	139	85646	3
	gi 13904870	ribosomal protein S5	98	23033	3
	gi 4506617	ribosomal protein L17	79	21611	2
	gi 403009	PHAPII (Putative HLA DR Associated Protein II)	79	32084	1*
	gi 23308579	inactive progesterone receptor, 23 kD	63	18971	1*
	gi 793843	ribosomal protein L29	44	17713	1*

Table 10: List of proteins identified with MALDI-TOF. (*) a single sequenced peptide is not regarded as a explicit proof for a definite identification. Protein scores greater than 78 are significant.

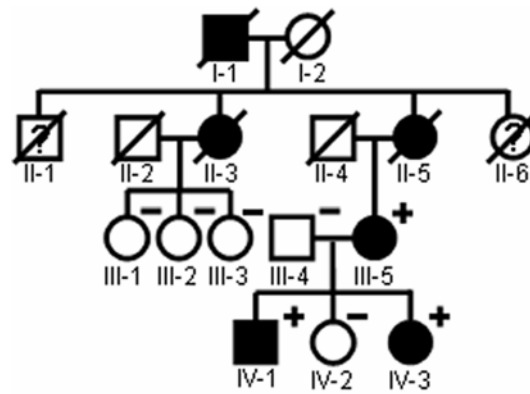


Figure 34: Pedigree of the affected family with the nonsense mutation CGA>TGA in codon 321 (pR321X) of the LMNA gene. Open and black symbols represent unaffected and affected individuals, respectively. (+) and (-) symbols indicate presence and absence of the mutation, respectively. Slanted bars denote deceased individuals. Deceased family members considered affected died of sudden cardiac death at the age of 48 (I-1), 59 (II-3) and 49 (II-5).